Multidimensional Analytical Techniques for the Characterization of Aliphatic Polyesters

by

Nadine Odette Pretorius

*Thesis presented in partial fulfillment of the requirements for the degree of **Doctor of Philosophy (Polymer Science)***

at

University of Stellenbosch

Supervisor: Prof H. Pasch

Co-supervisor: Dr J. B. McLeary   March 2013

Stellenbosch

Declaration

By submitting this thesis electronically, I declare that the entirety of the work contained therein is my own, original work, that I am the sole author thereof (save to the extent explicitly otherwise stated), that reproduction and publication thereof by Stellenbosch University will not infringe any third party rights and that I have not previously in its entirety or in part submitted it for obtaining any qualification.

_____   March 2013

Nadine Odette Pretorius

Stellenbosch

Abstract

Complex polymers are defined by their distributive properties with respect to molecular weight, chemical composition, functionality and molecular topology. As a result, polymer properties are very frequently determined not only by one of these entities but by the correlation of two or more distributions. Aliphatic polyesters are industrially implemented in high performance coatings, paints and varnishes. However, it is typically difficult to correlate the resulting properties with the synthesis parameters as these polymers vary in reactivity and application properties. Copolyester synthesis by direct polyesterification is often assumed to produce randomized products due to the mechanisms involved in stepwise polymerization. The formation of cyclic products by intramolecular reactions of hydroxyl (OH) and carboxylic (COOH) functional groups, side-reactions such as transesterification, alcoholysis, and ester-ester interchange allow even further randomization, enabling a highly complex system. Therefore, in addition to molecular weight distribution, polyesters exhibit chemical composition, functionality type as well as branching distributions, classifying them as complex polymeric systems. The different methods of polymer chromatography in combination with sophisticated spectrometry techniques are useful tools for enabling the full description of the molecular heterogeneity of these complex polyesters. The present study entails method development of different modes of chromatography and mass spectrometry along with their combination, to facilitate the analysis of the various distributions of two model polyester systems, phthalic and maleic anhydride, respectively, in combination with propylene glycol. Gradient HPLC analysis enabled an oligomeric separation based on chemical composition of the respective anhydride/propylene glycol samples. Its off-line coupling to MALDI-TOF MS and ESI-QTOF MS revealed the presence of several distributions of varying endgroup functionality type and molecular weight distributions at different intervals throughout the polymerization. In addition, online gradient HPLC x size exclusion chromatography (2D-LC) was conducted to obtain the dual chemical composition-molecular weight (CCD-MWD) distribution. The combination of the different coupling techniques provided the opportunity to a more in-depth analysis of the structure-property relationships.

Opsomming

Komplekse polimere word gedefinieer deur hul verdelings eienskappe ten opsigte van molekulêre massa, chemiese samestelling, funksionaliteit en molekulêre topologie. Gevolglik, word hul eienskappe dikwels bepaal deur nie net een van hierdie entiteite nie, maar 'n korrelasie van twee of meer verdelings. Alifatiese poliësters word industrieel geïmplimenteer in hoë werkverrigting bestrykings, verwe en politoere, dog is dit tipies moeilik om die uiteinde eienskappe met die verwante sintese parameters te korrelleer, aangesien die polimere varieer in reaktiwiteit en toepassingseienskappe. Ko-poliëster sintese vanaf direkte poliësterivering word dikwels aanvaar om willekeurige produkte op te lewer as gevolg van die meganismes wat betrokke is tydens trapgroei polimerisasie. Die produsering van sikliese produkte weens intra-molekulêre reaksies van hidroksiel(OH) en karboksiel (COOH) verwante funksionele groepe, newereaksies soos transverestering, alkoholise en ester-ester verwisseling, het verdere ewekansigmaking tot gevolg wat 'n hoog gekomplekseerde sisteem tot gevolg het.   Benewens die molekulere massa verdeling, vertoon poliësters dus chemiese samestelling, funksionaliteit tipe so wel as vertakkings verdeling wat hul as komplekse polimeer sisteme klassifiseer. Die verskillende metodes van polimeer chromatografie in kombinasie met gesofistikeerde spektrometriese tegnieke dien as nuttige bronne vir die volledige beskrywing wat betref die molekulêre heterogeniteit van komplekse poliesters. Die huidige studie stel metode ontwikkeling van verskillende modus van chromatografie, massa spektrometrie sowel as hul aaneenvoeging bekend, om die die verskillende verdelings van twee model poliester sisteme, ftaal- en maleïensuuranhidried onderskeidelik in kombinasie met propileenglikol, suksesvol te analiseer. Gradiënt hoë-druk vloeistof chromatografie (HPLC) analise het 'n oligomeriese skeiding, gebaseer op die chemiese samestelling van die verskeie anhidried /propileenglikol monsters, opgelewer. Die nie-gekoppelde skakeling met matriks-assisteerde-laser/desorpsie-ionisasie tyd-van-vlug (MALDI-TOF) en elektron-sproei-ionisasie kwadrupool-tyd-van-vlug (ESI-QTOF) massa spektrometrie het die teenwoordigheid van verskeie verdelings van varieërende endgroep funksionaliteit tipe en molekulêre verdelings by verskillende intervalle tydens die polimerisasie aan die lig gebring. Gekoppelde skakeling van gradient HPLC en grootte uitsluitings chromatografie is ook uitgevoer om die tweedelige chemiese samestelling-molekulere massa verdeling te bepaal. Aaneenvoeging van die verskeie skakelings tegnieke het die geleentheid gebied om 'n deeglike studie van die struktuur-eienskappe verhoudinge suksesvol uit te voer.

Table of Contents

Table of Contents

List Figures

List of Figures

List Figures

List Figures

List Figures

List of Tables

List of Tables

List of Schemes

List of Schemes

List of Abbreviations

2D	Two Dimensional
2D-LC	Two Dimensional Liquid Chromatography
ACN	Acetonitrile
C18	Carbon 18
CCD	Chemical Composition Distribution
CID	Collision Induced Dissociation
CN	Cyano
Da	Dalton
ELSD	Evaporative Light Scattering Detector
ESI	Electrospray Ionization
FT-ICR	Fourier Transform Ion Cyclotron Resonance
FTIR	Fourier Transform Infrared
GC	Gas Chromatography
Hex	Hexane
HPLC	High Performance Liquid Chromatography
I.D.	Inside Diameter
IT	Ion Trap
LAC	Liquid Adsorption Chromatography
LALLS	Low Angle Laser Light Scattering
LC	Liquid Chromatography
LC-CC	Chromatography at Critical Conditions
LC-CAP	Liquid Chromatography at Critical Adsorption Point
LC-PEAT	Liquid Chromatography at Point of Exclusion-Adsorption Transition

List of Abbreviations

MA	Maleic Anhydride
MALDI	Matrix-Assisted Laser Desorption/Ionization
MALLS	Multiple Angle Laser Light Scattering
MS	Mass Spectrometry
MWD	Molecular Weight Distribution
m/z	mass/charge
NMR	Nuclear Magnetic Resonance
PA	Phthalic Anhydride
PG	Propylene Glycol
RI	Refractive Index
SEC	Size Exclusion Chromatography
TOF	Time of Flight
THF	Tetrahydrofuran
UV	Ultraviolet
QTOF	Quadropole Time of Flight

List of Symbols

C_m	Concentration of solute in mobile phase
C_s	Concentration of solute in stationary phase
d	Drift region
E_{kin}	Kinetic energy
ε	Energy of interaction
ε_c	Critical energy of adsorption
ΔG	Gibbs free energy difference
ΔH	Change in interaction enthalpy
i	incrementing index
K_{ads}	Adsorption distribution coefficient
K_d	Distribution coefficient
K_{el}	Electrostatic distribution coefficient
K_{LAC}	Contribution of adsorption to distribution coefficient
K_{SEC}	Contribution of size exclusion to distribution coefficient
m	Mass of the ion
M_i	Molecular weight
$\overline{M}_n$	Number average molecular weight
$\overline{M}_w$	Weight average molecular weight
N_i	Number of molecules
q	Unit charge
R	Gas constant
ΔS	Change in conformational entropy
T	Temperature
t	Time of flight
V	Fixed potential

List of Symbols

v	Velocity
V_0	Interstitial volume
V_p	Pore and stationary phase volume
V_R	Retention volume
V_{STAT}	Volume of the stationary phase
z	Charge state

Part I. Introduction and Aims

1. Introduction

The basis for the extensive industrial application of aliphatic polyester resins are the different physical and mechanical properties of the final products brought about by the implementation of various combinations of different acids and glycols and their molar ratios that provide products with a large variety of final applications. Essentially, these resins are varied mixtures of molecules differing in molecular weight, chemical composition and degree of branching. Considerable work has been reported on the synthesis, characterization, curing behaviour and properties of aliphatic polyester resins[1-8]. Commercial resins typically consist of prepolymers obtained by polycondensation of unsaturated and saturated diacids or anhydrides with diols. Resins can be compounded with fillers and/or glass fibers and for most of the applications, they are diluted with one or several vinyl monomers for example styrene or methyl methacrylate, which are capable of free radical copolymerization with the unsaturated bonds on the polymer chains to be cured in the presence of free-radical initiators to yield the desired thermosets[9, 10]. A specific application of aliphatic polyester resins involves implementation of multi-vesiculated particles[11] in coatings and/or paint formulations to replace the more commonly used TiO_2 as opacifier due to availability and cost demands. These particles are in turn based on unsaturated polyesters of maleic anhydride, phthalic anhydride and 1,2-propylene glycol allowing a composition that would ideally resemble the structure illustrated in scheme 1.
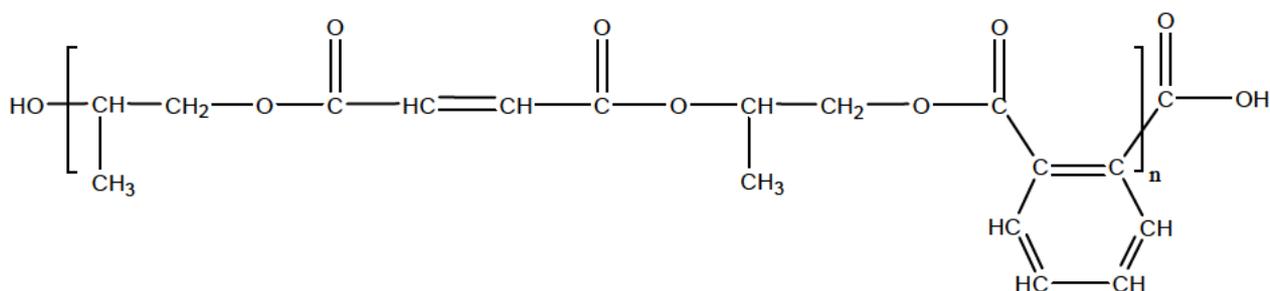
Scheme 1. Ideal proposed copolyester structure

The challenge lies in the fact that these polyester particles vary in reactivity and application properties and thus lead to difficulty in correlating the properties with the synthesis parameters. The polycondensation mechanism and kinetics of maleic anhydride, phthalic anhydride and 1,2-propylene glycol have been extensively investigated and well documented[12-16]. In all instances, the focus was on the main esterification reaction along with the occurrence of isomerization, double bond saturation and transesterification as side reactions. The presence of the unsaturated maleic anhydride as reagent allows the distribution of double bonds in the polyester chain which undergoes cis-trans isomerization[17-22].In addition, a percentage of these bonds undergoes saturation through a nucleophilic attack by the hydroxyl group of the diol (Ordelt reaction)[23]. This naturally brings about the opportunity for branching to occur. Importantly, the availability of double bonds present in the residues to enable curing has been extensively researched as the final products will show properties related to the cross-linking process[7, 24-26]. Transesterification reactions lead to the

Introduction and Aims

formation of cyclic products by intra-molecular and/or intermolecular reactions of the OH and COOH groups via back-biting and chain-end reactions. The end result is a system with an extremely complex chemical heterogeneity; and since heterogeneity influences polymer properties, it is important to have methods or techniques available to determine these characteristics.

In reality, classical analytical and physiochemical values such as the content of the hydroxyl number and acid number are all average values. Consequently, these techniques are often unable to describe the molecular weight distributions, follow the course of polycondensation, distinguish differences between individual samples, explain the differences in their properties and the relationship between the composition of the starting resins and properties of the cured materials based on them[27]. Different techniques such as polarography[2, 28, 29], infrared[12, 30], ebullioscopy[2] and bromine number determination[5] have been used for structural characterization of several types of aliphatic polyester resins. Parker et al[4] studied the differences in physical properties and found them to be due to different arrangement of the molecules along the chain as well as differences in the chemical composition[5]. Cherian et al[9] showcased the effect of choice and proportions of reactants on the final mechanical, thermal and physical properties of the aliphatic polyester resin consisting of maleic anhydride (MA), phthalic anhydride (PA) and various glycols. The authors also investigated the effect of sequence addition of reactants by NMR as well as characterizing the physical and mechanical properties of the obtained cured resin[10]. The use of ^{1}H and ^{13}C NMR analysis to study the structural characterization of the product of maleic anhydride, phthalic anhydride and aliphatic glycols[31, 32] in combination with physical properties[33], modeling simulations[34, 35] as well as SEC[14, 36] proved to be well established methods of understanding the polyesterification mechanism, the side reactions involved and their related properties.

Due to the complicated molecular and chemical nature of the aliphatic polyester resins, characterization by means of liquid chromatography has, however, been less frequent. Podzimek et al.[27, 37] summarized the application and suitability of HPLC and SEC for the analysis of synthetic resins specifically. The obtained chromatograms clearly showed the difficulties found in the attempts to separate the molecules according to molecular weight, molecular weight distribution, functionality type and functionality type distribution. The analysis of several samples was demonstrated via the use of SEC-MALLS and reversed phase HPLC. Other studies utilizing SEC and HPLC for a variety of aliphatic polyesters have also been published[31, 37, 38]. Ahjopalo et al.[39] conducted MALDI-TOF MS in order to obtain information regarding the oligomer and endgroup composition of saturated polyesters by studying the reactivity of various diols and diacids as well as reaction conditions. Importantly, they found that PA has a high tendency to form cyclic dimers and that PA containing polymers also have a high probability for transesterification and thus larger cyclic compounds could be present. Thus the combination of analytical characterization and molecular modeling has proved to be successful in studying the structure property-relationship in polymeric materials. While previous studies have either investigated the respective diol and diacids systems of interest, in the current study with other combinations of diols and diacids or with each other, investigations lacked the in-depth details concerning each system individually, particularly in the presence of excess concentration of diol participating in the synthesis.

Introduction and Aims

2. Aims

The current dissertation entails the investigation of two polyester batches based on model phthalic anhydride-1,2-propylene glycol and maleic anhydride-1,2-propylene glycol, respectively, which serve as building blocks for the more complex industrial aliphatic resin variety. In both instances, the goal was to obtain polyesters ranging between 10^2 and 10^4Da in molecular weight whereby kinetic samples were removed at varying stages of the polyesterification reaction. In order to follow the course of the polycondensation reactions in each of the polyester batches and compare the evolution of their distributions with regards to molecular weight, chemical composition and functionality type, different liquid chromatography techniques had to be developed. Size exclusion chromatography and gradient HPLC conditions first had to be optimized in order to achieve successful separations, before their subsequent on-line coupling could determine the link between the dual functionality type-molecular weight distributions. Secondly, soft-ionization mass spectrometry techniques were employed to serve as core methods to determine the extent of chemical composition, identify the functionality-type distributions as well as assist in assigning structural conformations. Suitable sample preparation and analysis conditions had to be established in MALDI-TOF MS and ESI-QTOF MS for the bulk sample investigation. In serving as selective detectors, their off-line coupling with the aforementioned LC techniques had to be conducted effectively, to facilitate the identification of the narrowly dispersed fractions obtained from the chromatographic separations. Only through the hyphenation of these sophisticated polymer characterization techniques, information on the molecular heterogeneity of these model polyester prepolymers, showing a complex variety of possible distributions, could be obtained.

3. Layout of dissertation

Part I. Introduction and Aims

A brief introduction to concepts relevant to the study, including the aims and outline of the dissertation are presented.

Part II. Historical and Theoretical Background

A concise discussion of the historical background and theory related to the synthesis mechanisms and analytical techniques significant to the study.

Part III. Results and Discussion

The following part is divided into the following four sections:

Section 1. contains a brief overview of the approach taken in order to achieve the characterization of the polyesters of interest.

Section 2. entails the method development of the different LC techniques employed during the study. The results of the optimized one dimensional analysis are presented first, followed by the subsequent coupling of the different modes in order to achieve dual functionality relationships. The SEC, gradient HPLC and

Introduction and Aims

comprehensive 2D-LC chromatograms and contour plots are presented along with detailed discussions concerning each of the polyester batches.

In Section 3 the MALDI-TOF MS analyses of the kinetic bulk samples are presented. Complimentary molecular weight and molecular weight distribution investigations are discussed. Various endgroup functionality combinations are proposed for both polyester batches. ESI-QTOF MS analyses in both positive and negative modes of the final sample in the respective batches are given.

Section 4 discusses the results concerning the hyphenation of gradient HPLC and MS techniques. The MALDI-TOF and ESI MS results of the homogeneous fractions obtained from gradient HPLC of the final samples highlight the differences in chemical composition between the PA-PG and MA-PG batches. Reasons relevant to the driving force behind the variation in separation efficiency found during the LC analysis are presented. Structural conformation assignments additional to those made in the previous section complete the discussion.

Part IV. Experimental

The experimental part contains the synthesis and analysis conditions, as well as instrument parameters for all the techniques used. A detailed list including stationary phases, mobile phases, calibration standards and matrices are also presented.

Part V. Summary and Conclusions

A summary of the main conclusions presented in the preceding results and discussion section is presented along with the compilation of the proposed structures assigned during the investigation.

Part VI. Bibliographic References

All the bibliographic references relevant to the current dissertation are given here.

Part II. Historical and Theoretical Background

1. Polymer Synthesis

1.1 Overview

Polymers vary in structure by being linear, branched or cross-linked in three-dimensional networks, and some have less common shapes resembling combs, stars or ladders. Homopolymers consist of only one type of repeating unit, whereas copolymers are made up of two or more different monomer units that can be arranged in either random or alternating sequences. The classification of polymers can be done in several ways which include the source of the product (whether it be naturally occurring, synthetically made or by the chemical modification of natural macromolecules), the chemical structure (olefin, polyamide, etc.), polymer texture during use (rubbery or glassy) and the area of application (adhesive, fiber etc.). During the early years of the application of polymers in industry, Carothers[2, 40] importantly made the distinction of classifying macromolecules into *addition* and *condensation* polymers. Due to the immense advancement in technology since then, a more useful distinction is based rather on polymerization mechanisms, than the polymeric structures. It is well known that the physicochemical properties and biological behavior of polymeric systems depend on the micro-structural characteristics of their macromolecular chains that are constructed during the polymerization process by any of the established mechanisms of reaction[41]. A particular polymerization method, mechanism and process will yield a polymer with molecular architecture and set of physical properties that differ from those obtained by another polymerization method, mechanism and process. Polymer formation involves either chain- or step-growth reactions. In chain polymerization, once a chain is initiated, monomer molecules add in rapid succession to the reactive endgroup of the growing chain until it terminates and become non-reactive. The most common mechanisms of chain polymerization are anionic, cationic and radical. Of the three, free radical polymerization dominates in industry; it has been widely used to produce synthetic materials. In turn, step-growth polymers are produced by the stepwise intermolecular reaction of functional groups of monomers. Monomer units can react with each other or with chains of any size to from dimers, trimers etc. to eventually give a higher molecular weight polymer. The polymer molecules grow over the course of the whole reaction as the functional group on the end of a monomer is assumed to have the same reactivity as that on a polymer chain of any size. When this polymerization process is accompanied by the elimination of small molecules, the process is called polycondensation. In the current dissertation the focus will be on aliphatic polyesters prepared via polycondensation polymerization.

1.2 Polyesterification

The first saturated synthetic polyesters date back to 1847 when Berzelius reacted glycerol with tartaric acid[42, 43]. Soon after Berthelot[44] reacted glycerol with camphoric acid, while Lorenzo[45] used ethylene glycol and succinic acid to produce what were believed to be cyclic or macrocyclic esters. The first linear synthetic step-growth polymer, Nylon 6,6 and the basic principles of condensation polymerization stem from the ground-breaking work done by Carothers who envisioned that large molecules could be synthesized by the direct addition of diols and diacids to form polyesters and diamines and diacids to form polyamides[46-48]. The

Historical and Theoretical Background

polyesterification process can be carried out in the presence of an added catalyst but the carboxylic acid can in itself also act as a catalyst[18]. At present, the commercial use of basic step-growth polymers is immense and still rising steadily. Due to the fact that unlike polyolefins and other vinyl polymers where catalyst and process changes can lead to different variations of monomer linkages with subsequent mechanical and physical property changes, significant variation in the properties of the achieved polymers require the incorporation of new monomers into the polymer backbone. Thus, progress continues to be made along many fronts of polycondensation.

$$n\,\text{HO}-\text{A}-\text{COOH} \rightleftharpoons \left[\!\!\text{A}-\overset{\overset{\displaystyle O}{\|}}{\text{C}}-\text{O}\!\!\right]_n + (n\text{-}1)\,\text{H}_2\text{O}$$
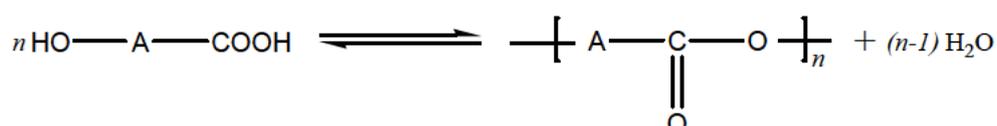
Scheme 2. Direct esterification from one compound

$$n\,\text{HOOC}-\text{A}-\text{COOH} + n\,\text{HO}-\text{G}-\text{OH} \rightleftharpoons \left[\!\!\overset{\overset{\displaystyle O}{\|}}{\text{C}}-\text{A}-\overset{\overset{\displaystyle O}{\|}}{\text{C}}-\text{OGO}\!\!\right]_n + n\,\text{H}_2\text{O}$$
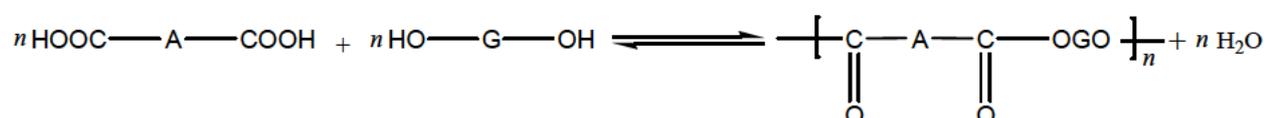
Scheme 3. Direct esterification from two compounds or more (in the case of copolymers)

The kinetics of polycondensation reactions and the requirements for successful step-growth polymerization are well documented and discussed in literature[49-51]. For the majority of the engineering resin applications of step-growth polymers, the applications, the development and commercialization of new step-growth monomers and polymers are challenging tasks.

1.3 Aliphatic polyesters

Aliphatic polyesters and their subsequent resins have widespread use in industry due to their low cost, ease of processing and combination with reinforcements, rapid cure with minimized volatile products, excellent dimensional stability and a variety of grades available. Commercial resins typically consist of prepolymers obtained by polycondensation of unsaturated and saturated diacids and their anhydrides with glycolic compounds at 150-280 °C, generally at atmospheric pressure. The resins can be compounded with fillers and/or glass fibers and for most of the applications they are diluted with one or several vinyl monomers for example styrene or methyl methacrylate, which are capable of free radical copolymerization with the unsaturated bonds on the polymer chains. These are to be cured in the presence of free-radical initiators to yield the desired thermosets[10, 52]. To enable the radical copolymerization it is thus essential that one of the dicarboxylic acids must contain a double bond and is commonly introduced as maleic anhydride or maleic/ fumaric acid. A variety of saturated acids is used, but phthalic anhydride is the most common. Ethylene, diethylene, and propylene glycols are the most frequently used glycols. Polyesters of this type are conveniently prepared with a molecular weight of approximately 800 to 2000Da, which generally represent some 6 to 15 repeating units. Considerable work has been reported on the synthesis, characterization, curing behavior and properties of numerous types of aliphatic polyester resins[53-55].

Historical and Theoretical Background

The mechanism and kinetics of the polycondensation between maleic anhydride, phthalic anhydride and 1,2-propylene glycol specifically, have been extensively investigated and well documented[12-16]. Initially polyesterification kinetics of dicarboxylic acids and diols was investigated by Flory[3]. The reactions are generally equilibrium controlled and the continuous removal of the produced water is necessary to obtain high conversions. The presence of the unsaturated carboxylic maleic anhydride and/or its respective acid leads to a complex reaction mechanism as it allows for several side reactions such as isomerization, double bond saturation and transesterification to take place in conjunction with the main polyesterification reaction. The side reactions in turn, limit the main reaction from achieving high degrees of polymerization. The main esterification actually involves two steps: the monoester formation (Scheme 3) and the polycondensation reaction (Scheme 4).
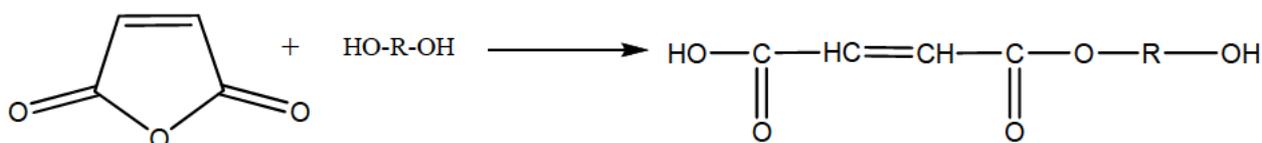
Scheme 4. Monoester formation

The monoester formation is a very fast exothermic reaction (ΔH = -40 kJ·mol^{-1}) and takes place in the temperature range from 60°C to 130°C while the polycondensation occurs above 160°C. Phthalic type resins for example, require 15 hours at 190°C to attain satisfactory molecular weights[15]. At these temperature values, the loss of glycol along with the water is prevented either by fractionating condenser systems or by the addition of acid catalysts to promote the formation of volatile ethers which are then lost as by-products. The reaction order increases due to the change of the physical properties of the liquid phase during the reaction and by the shift of the monomer-dimer equilibrium during the esterification reaction[22].
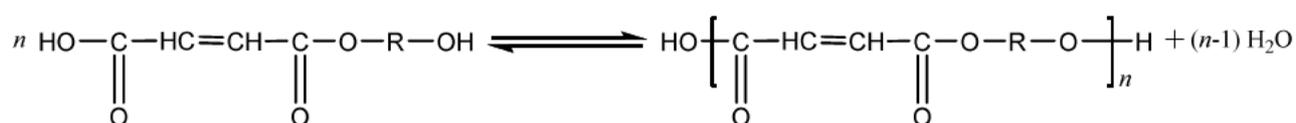
Scheme 5. Polycondensation from monoester

The first and most important side reaction typically occurs when the reaction temperature rises above 180°C when the maleate distribution of double bonds undergoes cis-trans isomerization[28]. It has been shown that the percentage of isomerization increases when a more sterically hindered glycol is used or when an aromatic diacid is included in the esterification[12, 34]. Although the rate of isomerization increases with increasing reaction temperature, the total percentage of isomerization occurring over a range of temperatures is not affected. For polyesters of an average molecular weight ranging between 1000 to 3000Da more than 90% of the double bonds along the chains underwent isomerization[31, 56]. The more planar trans-fumarate isomer is subject to less steric hindrance and displays reactivity of almost 20 times higher than that of the maleate reaction products in the subsequent copolymerization reaction with styrene[43, 57]. This phenomenon is of fundamental importance for optimum resin formation and the related physical characteristics[5].
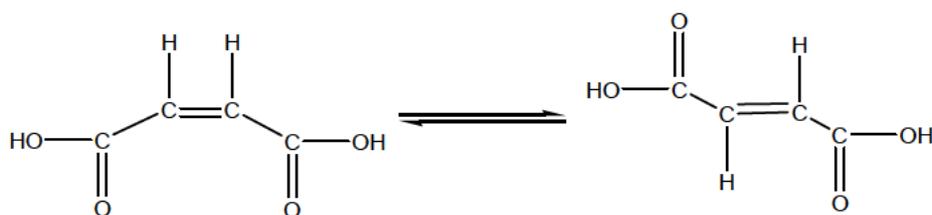
Scheme 6. Cis-trans isomerization

The second side reaction is closely related to the reactivity of the maleate-fumarate groups present, as a percentage of these bonds undergoes saturation through a nucleophilic attack by the hydroxyl group of the diol (Ordelt reaction)[21-23]. This naturally brings about the opportunity for branching (short chain and long chain branching) to occur as well as a deviation in reactant stoichiometry. Importantly the availability of double bonds present in the residues to enable curing has been extensively researched as the final products will show properties related to the cross-linking process[7, 24, 26, 58]. Paci[31] found the degree of glycol addition to the olefinic bonds along the unsaturated polyester chain to vary between 15-20%. The extent of the Ordelt reaction depends on reaction temperature, the concentration and nature of the diols and acids employed. It should be noted that saturation may also proceed via the hydroxyl group of the monoester itself, although Piras et al[59] showed that a reactive system using a diol consisting of more than two carbon atoms entailed diol-induced saturation only. Due to the fact that the destruction of unsaturation is favored by higher initial temperatures and thermal polymerization of maleic anhydride double bonds can also occur at elevated temperatures, an optimum temperature for polyester production needs to be established[5].
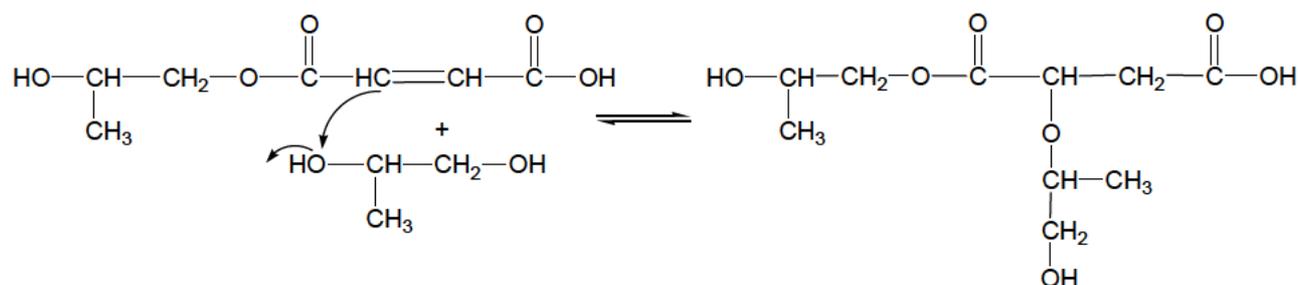
Scheme 7. Double bond saturation

Transesterification is the last type of side reaction involved at high temperatures of the polyesterification. The process involves alcoholysis or acidolysis of the polyester chains by the hydroxyl or carboxyl groups of monomer and /or polymer chains. These reactions lead to the formation of cyclic products by intra-molecular and/or intermolecular reactions of the OH and COOH groups via back-biting and chain-end reactions[39, 60].
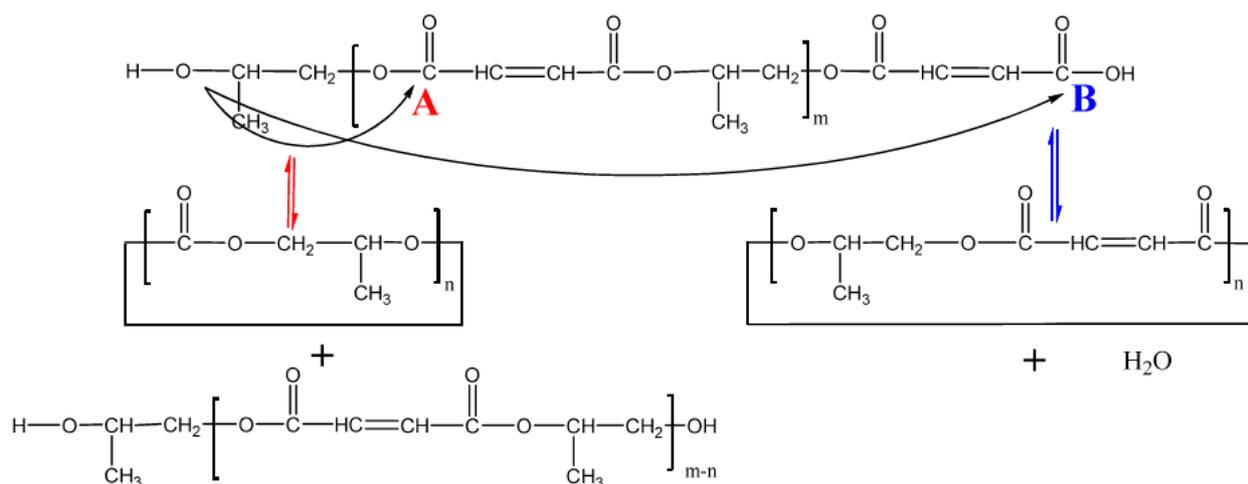
Scheme 8. Formation of cyclic structures via intra-molecular transesterification reactions (A) back-biting and (B) chain end-end reactions
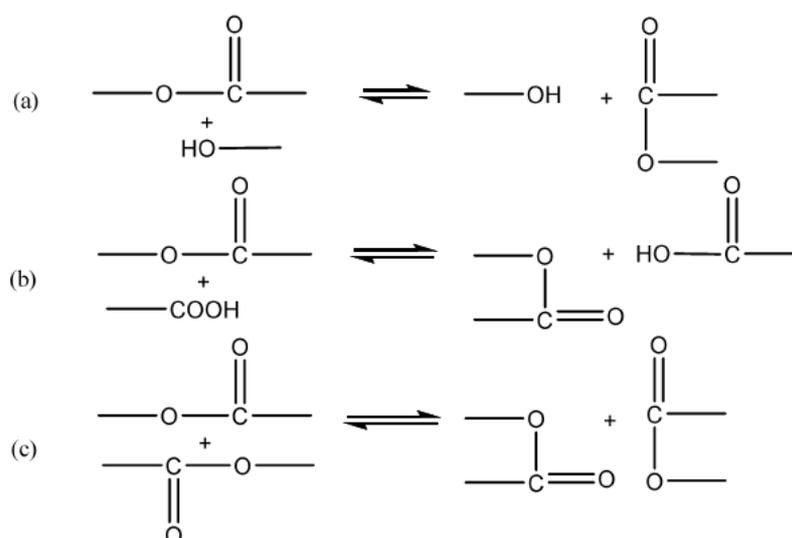
Scheme 9. Further randomization via (a) alcoholysis, (b) acidolysis and (c) ester-ester interchange

These ester interchange, ester alcoholysis and acidolysis within the same or different compounds, would redistribute molecular weight and functional endgroups of the polyester molecules, resulting in a statistical distribution of macromolecular units and chain ends[61, 62]. The end result is a system with an extremely high chemical heterogeneity; and since this heterogeneity influences polymer properties it is important to have methods available to determine these characteristics.

2. Liquid Chromatography of Complex Polymers

2.1 Introduction

In any chemical or bio-processing industry, the need to separate and purify a product from a complex mixture is a necessary and important step in the production line. For a better understanding of tailor-made products and their structure in the polymer industry, specialised analytical methods are required. Chromatography comprises a broad range of physical methods that facilitate the separation of complex mixtures with great precision by being able to purify almost any soluble or volatile substance if the correct adsorbent material, carrier fluid and operating conditions are employed. The variety of unique separation challenges that synthetic polymers present, are met by the use of liquid chromatography (LC) which has been established as a powerful tool for the molecular characterization of complex polymers that feature several simultaneous distributions in molecular characteristics such as molecular weight, chain architecture, chemical composition and functionality[63-67]. The extent of the application of LC in polymer characterization goes from the simple verification of the purity of a compound to the quantitative determination of several compounds in a given mixture. In itself, the term *liquid chromatography* comprises a selection of separation techniques that have a single denominator namely liquid for a mobile phase, which allow greater solvating capabilities and more scope for selectivity optimization as compared to for example gas chromatography. Separations are achieved by the appropriate combination of the separation mode, stationary phase type and mobile phase composition. It is, therefore, extremely important to understand the complex relationship between these terms.

2.2 Basic liquid chromatographic separation principles for neutral macromolecules

Any given chromatographic system comprises two phases: a stationary phase and a mobile phase. In HPLC, a solute mixture is introduced into the system via the mobile phase which sweeps the components over and through the stationary phase, each of which is selectively retained to a different degree in the system due to various attraction forces. The stationary phase generally consists of a porous packing material inside a stainless steel column, while the mobile phase can be a single solvent or a composition of thermodynamically "poor" and "good" solvents. It is important to note that references to "good" or "poor" solvents stand for the solvent strength and are not necessarily parallel to the thermodynamic quality of the solvent[68]. In other words, a good solvent keeps polymers in the mobile phase more strongly and vice versa. The affinity of each of these analyte components for one phase over the other will govern its separation from the other compounds, since each one of them has a specific equilibrium constant and will exhibit a different migration rate. The end result is the elution from the stationary phase at specific retention times. The interactions between the solute mixture and the two phases give rise to different modes of separation which can be applied to the analysis of a large variety of sample types containing non-polar, moderately or strongly polar and ionic compounds, either as simple species or high-molecular weight synthetic polymers. For liquid chromatography of uncharged synthetic macromolecules, the most commonly applied separation mechanisms are steric exclusion, adsorption, partition and phase separation (solubility). The application of

ion-exchange, ion-inclusion and ion-exclusion for the separation of charged polymeric species is outside the scope of this dissertation and will not be discussed here.

Retention of polymeric macromolecules can be expressed by means of a thermodynamic coefficient which defines the affinity of a molecule for the two phases. The distribution coefficient K_d is related to the Gibbs free energy difference as follows:

Since
$$\Delta G = \Delta H - T\Delta S = -RT \ln K_d$$

Then
$$K_d = \frac{C_s}{C_m} = \exp\left(\frac{-\Delta G}{RT}\right) = \exp\left(\frac{\Delta S}{R} - \frac{\Delta H}{RT}\right) \tag{1}$$

Where C_s and C_m are the solute concentrations in the stationary and mobile phase, respectively, and ΔG, ΔS and ΔH are the changes of Gibbs free energy, entropy and enthalpy related to the transfer of the solute from mobile into stationary phase, respectively. The term R is the gas constant and T the temperature.

STERIC EXCLUSION

Depending on the size of the macromolecules, they can partially penetrate into the pores of the porous material and undergo interactions with the active sites of the stationary phase located mainly inside the pores. The change in Gibbs free energy may be related to two different effects that could take place. Firstly, the pores are limited in size therefore the molecules cannot attain all possible conformations, leading to the decrease in conformational entropy ΔS. Secondly, the interactions with the pore walls result in the change in enthalpy ΔH. This implies that the magnitude of entropic and enthalpic effects will define the mode of separation[69]. This is illustrated in the case of *classical* steric exclusion, where the retention volume is expressed as:

$$V_R = V_0 + V_p K_d \tag{2}$$

With V_0 as the interstitial volume in the inter-particle space, V_p as the pore and stationary phase volume. Thus from equation (1) K_d and the retention is dependent on both the entropic and enthalpic terms. When a thermodynamically good solvent for the macromolecules is used which ideally also suppresses enthalpic interactions to ensure that separation is exclusively governed by the conformational changes (entropic exclusion) of the molecules, then ΔH effectively becomes 0.

$$K_{SEC} = \exp\left(\frac{\Delta S}{R}\right) \tag{3}$$

This chromatographic mode is known as size exclusion chromatography (SEC). Casassa[70, 71] showed that SEC is related to changes of conformational entropy of macromolecules entering the stationary phase within the LC column. For large molecules which are totally excluded from the pores (total exclusion) $K_{SEC} = 0$ and for small molecules, which can completely enter the pores (total permeation), $K_{SEC} = 1$. Accordingly, the separation range is $0 < K_{SEC} < 1$ and retention decreases with increasing molecular weight. The retention volume for ideal SEC equals

Historical and Theoretical Background

$$V_R = V_0 + V_p K_{SEC} \tag{4}$$

However, if enthalpic effects due to electrostatic or adsorptive interactions of the macromolecules and the pore walls have to be taken into account, the distribution coefficient K_{Excl} of real SEC is:

$$K_{Excl} = \exp\left(\frac{\Delta S}{R} - \frac{\Delta H}{RT}\right) = \exp\left(\frac{\Delta S}{R}\right)\exp\left(\frac{-\Delta H}{RT}\right) = K_{SEC} K_{el} \tag{5}$$

In which case, the retention volume would be a function of K_{SEC} and K_{el}. Similarly, if electrostatic or adsorptive interactions occur at the outer surface of the stationary phase, an additional term $V_{stat}K_{LAC}$ has to be included. The extent of exclusion and entropy loss depends on the size of both the macromolecules and pores and the accessibility of the pores.

ADSORPTION

Subsequently, when the separation is governed by adsorptive interactions between the macromolecules and the stationary phase, an ideal case for liquid adsorption chromatography (LAC) may be defined. This phenomenon occurs when the thermodynamic quality of the mobile phase is decreased by either the addition of a thermodynamically poor solvent or a change in the analysis temperature. Conformational changes are assumed to become negligible ($\Delta S = 0$) and in ideal LAC the distribution coefficient is determined solely by enthalpic effects:

$$K_{LAC} = \exp\left(\frac{-\Delta H}{RT}\right) \tag{6}$$

In the current case scenario, the pore size of the stationary phase plays an even more important role. If small enough, the separation takes place only on the outer surface as the pores are not accessible to the macromolecules. Thus $K_{SEC} = 0$ and the retention volume is a function of the inter-particle volume and the volume of the stationary phase (V_{stat}):

$$V_R = V_0 + V_{stat} K_{LAC} \tag{7}$$

When accessibility of the pores of the stationary phase is limitless ($K_{SEC} = 1$), the pore volume V_p adds to the inter-particle volume:

$$V_R = V_0 + V_{stat} K_{LAC} + V_p \tag{8}$$

In reality, however, only a fraction of the pores is accessible in LAC and, therefore, the distribution coefficient is again a function of both ΔH and ΔS which is similar to real SEC:

$$K_{ads} = \exp\left(\frac{\Delta S}{R} - \frac{\Delta H}{RT}\right) \tag{9}$$

In turn, the retention volume now is a function of enthalpic interactions at the surface of the stationary phase, possible enthalpic interactions inside the pores (K_{el}), as well as entropic effects due to the limited dimensions of the pores. This gives a definition for V_R in real LAC which is formally similar to that of real SEC:

$$V_R = V_0 + V_p(K_{SEC}K_{el}) + V_{stat}K_{LAC} \tag{10}$$

This indicates that in fact, the retention behaviour of macromolecules responds to both enthalpic and entropic interactions, and only the predominance of one of these determines the mode of operation. With regard to complex polymers, these effects become profoundly complicated as molecules of different composition experience various extents of both interaction types.

CRITICAL POINT OF ADSORPTION

This specific separation condition is a unique situation referred to as the point of enthalpy-entropy compensation. It has been established that in the size-exclusion mode of LC entropic interactions are predominant and $T\Delta S > \Delta H$, while in LAC separation the reverse is true, $\Delta H > T\Delta S$ and the separation is governed by enthalpic interactions. Although the chemical composition and architecture of a polymer species affect the extent of its adsorption and therefore its retention, (via the continuous or stepwise adjustment of the eluent strength of the mobile phase) the effect of its molecular weight can be successfully suppressed. Due to the fact that both modes are affected by the polymer molecule size and the pore size of the stationary phase, a value of energy of interaction, ε, was defined, which characterizes the particular interactions of a monomer unit and the stationary phase and is a function of the chemical composition of the monomer unit, the mobile phase composition and the temperature. According to the theory of adsorption at porous adsorbents, a finite critical energy of adsorption ε_c exists where the macromolecule starts to adsorb at the stationary phase. It implies that at $\varepsilon > \varepsilon_0$ the macromolecules are adsorbed, and in turn at $\varepsilon < \varepsilon_0$ it remains unabsorbed. The transition between the two separation mechanisms takes place at $\varepsilon = \varepsilon_0$ and is termed "critical point of adsorption" or liquid chromatography at "critical conditions" (LC-CC) which relates to a situation, where the adsorption forces are exactly compensated by the entropy losses $T\Delta S = \Delta H$[72-74]. Accordingly, at the critical point of adsorption the Gibbs free energy is constant ($\Delta G = 0$) and the distribution coefficient is $K_d = 1$, irrespective of the molecular weight of the macromolecules[75, 76]. The critical point of adsorption is extremely sensitive towards temperature and mobile phase composition and exists in a narrow range between SEC and LAC. The relation of the LC-CC mode to that of SEC and liquid adsorption chromatography (LAC) is usually illustrated by the schematic representation shown in Figure 1.
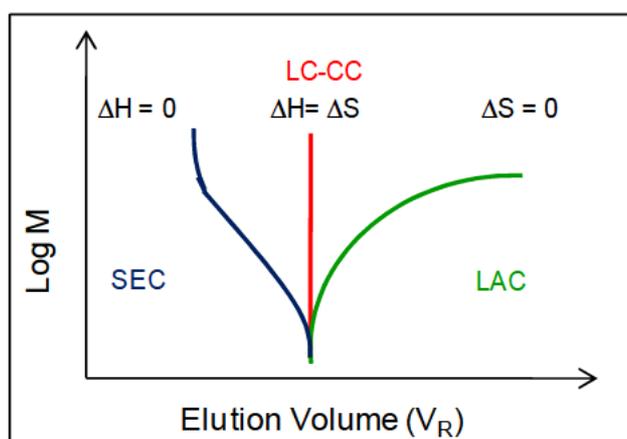
Figure 1. A schematic representation of the different chromatographic modes found in liquid chromatography brought about by change in the eluent composition or analysis temperature

Historical and Theoretical Background

During this specific mode of isocratic LC, retention is independent of molecular weight and solely influenced by the chemical composition or functionality of the molecules. Studies based on this concept started in the 1970s when Tennikov et al[77] and Belenkii et al[78] showcased the change in transition from one mode to another by altering the temperature or the mobile phase composition. The concept of "chromatographic invisibility" was developed by Entelis et al[75] as a method for the determination of the functionality type distribution of telechelic oligomers and polymers. Soon after, this interesting feature was widely utilized in the characterization of block copolymers and their functionality[64, 74, 79, 80]. Several other experimental studies have made use of LC at the critical point of adsorption, although not without controversy whether such a precise co-elution condition exists[74, 81-83]. The technique is generally known as LC at the critical condition (LC-CC), however other terminologies do exist such as LC at the point of exclusion-adsorption transition (LC-PEAT) or LC at the critical adsorption point (LC-CAP). Berek and co-workers[80, 84, 85] further distinguished the method based on the solvent strength of the injection sample solvent relative to the mobile phase; LC at the critical adsorption point (LC-CAP), LC under limiting conditions of adsorption (LC-LCA) and LC under limiting conditions of desorption (LC-LCD). The use of LC-CC for the characterization of complex polymers is a well investigated area of polymer chromatography research, however, beyond the scope of the current dissertation and therefore the reader is referred to the following literature for interest[74, 80, 86-90].

2.3 Size exclusion chromatography

SEC is the most commonly applied LC technique for separation based on the hydrodynamic volume ("effective" molecular size) of molecules in solution and the extent to which they are excluded from the porous particles of the stationary phase[91-98]. In essence, it has completely replaced previous tedious fractionation methods used for the determination of the molecular weight and the molecular weight distribution of synthetic macromolecules[99, 100]. Its popularity in molecular characterization of polymers stems from the wide applicability, high speed, ease of use and low sample consumption. As an entropy driven separation technique, is it often assumed that SEC does not involve any enthalpic interaction. This implies that the stationary phase must be inert and that the mobile phase serves solely as a carrier for the solute mixture, as all interactions between the solute molecules and the stationary phase need to be prohibited. Modern SEC employs small rigid, polymeric or silica-based beads of controlled pore size with numerous types of phases commercially available[101, 102]. The subsequent mobile phases can be organic, organic/aqueous or aqueous[103] but more importantly they should be good solvents for the polymer under investigation and be compatible with the stationary phase and the properties of the detector of choice[104-106]. Furthermore, the choice of column type, its pore size and pore size distribution, the mobile phase and temperature must be carefully selected to achieve high precision and reproducible separation.

The mobile phase is pumped continuously through the column, the porous packing is wetted and the dilute solution mixture of macromolecules is moved over and through the stationary phase. The separation of the macromolecules differing in hydrodynamic volume is affected by the degree of retention in the pores. The fundamental aspects of the mechanism have been established by Casassa et al[70, 71, 107-109], Giddings[110] and Yau et al[111, 112]. The smaller molecules are retained to a greater degree than their larger counterparts as their smaller hydrodynamic volume allow them to diffuse in and out of the pores. The larger size molecules are excluded from the particles and travel more in the interstitial volume between them, thereby eluting first due

to their shorter flow paths. The determining factor enabling effective separation is the nature of the pore size distribution present in the selected column. For any given solute mixture, the retention can be presented graphically by molecular size vs. retention volume, V_R as shown in Figure 2.
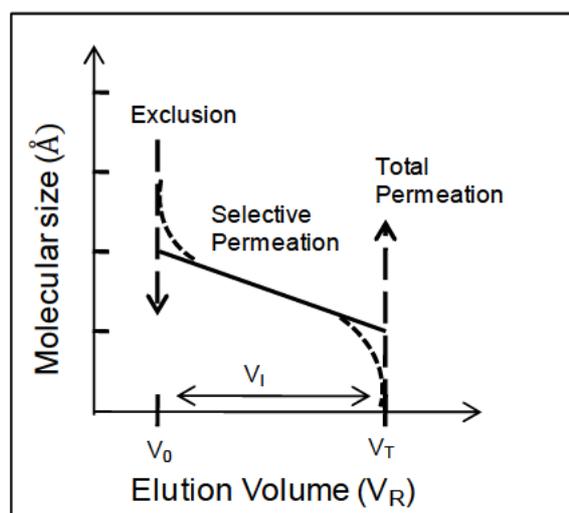
Figure 2. An example of a typical calibration curve obtained in SEC analysis, indicating the effective separation range of a given stationary phase[94]. For SEC VT = V0 + VI, VR = V0 (1 − K) + KVT and 0 ≤ K ≤ 1

The linear portion of the curve is the fractionation range and represents the useful SEC separation range for the column. The deviations at the ends represent the exclusion limit where the larger macromolecules cannot access the pores and are completely excluded, and the permeation limit where the smaller macromolecules all have equal access to the pores and are eluted together, typically close to the dead volume of the column, V_0. Consequently, the pore size and pore size distribution of the stationary phase should be comparable to the size(s) of the macromolecules' mixture in solution. At times this requires a serial coupling of columns, each with a different molecular range or a single column having various pore size distributions. The molecular weight (MW) and molecular weight distribution (MWD) of polymer molecules can be obtained using a calibration curve that transfers the retention time or volume to the logarithm of the molecular weight[65, 97, 113, 114], or by using (on-line) molecular weight sensitive detectors such as light scattering, viscometry, NMR (off-line), MALDI-TOF MS and ESI-MS(on-line and/or off-line). In the first instance, calibration with standards of similar structural properties and known molecular weights is required to obtain molecular weight information. For monodisperse samples the situation is straightforward, but for polydisperse samples no absolute value exists and therefore statistical functions must be employed to describe the distribution of different absolute molecular weight species around an average value. The molecular weight averages and distributions are given by the principal relationships defined in terms of number-average molecular weight ($\overline{M}_n$) and weight-average molecular weight ($\overline{M}_w$)[115, 116].

$$\overline{M}_n = \frac{\sum_i N_i M_i}{\sum_i N_i} \tag{11}$$

$$\overline{M}_w = \frac{\sum_i N_i M_i^2}{\sum_i N_i M_i} \tag{12}$$

Where N_i is the number of molecules having a molecular weight M_i and i is an incrementing index over all molecular weights present. The dispersity of a sample is described by the ratio of $\overline{M}_w/\overline{M}_n$ with monodisperse polymers having dispersity of 1.0. The various averages are typically calculated from the digitized peak profile by manual construction, or preferably by software-based procedures.

In SEC analysis, the most common detector is a differential refractometer, however, spectrophotometers operating at fixed wavelengths, are also used as alternative or auxiliary detectors. Due to the complex nature of polymer molecules or systems, SEC has however an intrinsic limitation in that it cannot distinguish between heterogeneity in composition, chain architecture, microstructure and functionality. In the case of a copolymer or a blend, each eluting fraction can represent a number of different types of molecules, varying in each of the abovementioned distributions but having the same hydrodynamic volume. In order to address this problem several selective detection techniques have been combined with SEC. Although very useful information on the heterogeneity of a sample can be obtained, this type of methodology still does not determine the compositional distributions. The success of coupling SEC to several detectors is dependent on the fact that the number of detectors should at least equal the number of different chemical components under investigation and that each detector should respond differently to those components. Hyphenated techniques involving SEC have been covered extensively in literature[95, 117, 118].

2.4 Interaction-based liquid chromatography (LAC)

Liquid adsorption chromatography (LAC) utilizes the differences in molecular interactions between solute molecules and the mobile phase and more importantly, their surface adsorption onto the stationary phase[64, 66, 119]. Although, the process is predominantly enthalpy-driven, small entropic effects are inevitably present in LC systems dealing with macromolecules. Still, the general assumption is that LAC is the more suitable technique over SEC for the characterization of chemically heterogeneous polymers and the many aspects involved were discussed in the early studies by Glöckner[69, 120-124]. The behaviour of polymer macromolecules is inherently different from small molecules due to the fact that their adsorption is dependent on the affinity of their repeating units towards the stationary phase, illustrated very simplistically in Figure 3. The macromolecule-stationary phase interaction is controlled by either adsorption-desorption phenomena where once adsorbed, a molecule can suddenly detach if they acquire enough activation energy to rearrange or break the chemical/physical bonding, and/or diffusion controlled sorption-desorption kinetics; where the changes are gradual due to their diffusion in and out of the porous particles[65]. Consequently the combination of adsorption, partition and phase separation/solubility effects are employed to facilitate different degrees of retention for the heterogeneous species present in polymeric samples, their differences in migration rates and the selectivity of their separation.

Historical and Theoretical Background
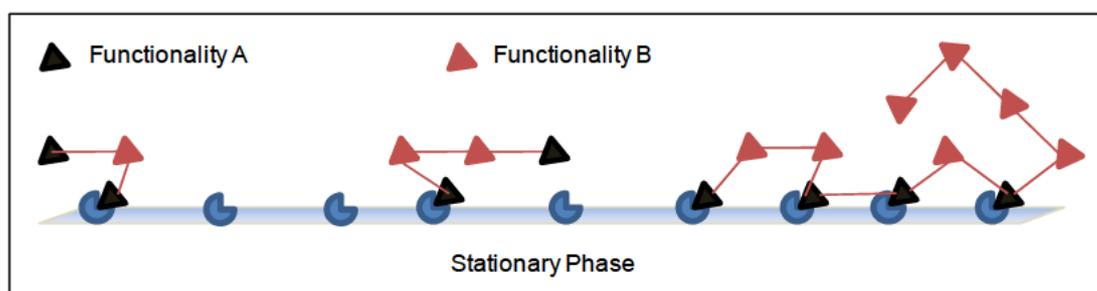
Figure 3. A simplified illustration of the adsorption of macromolecules due to the affinity of their repeating unit towards the stationary phase

Eluent strength has proven to be a pivotal factor in adsorption due to conformational entropy losses of macromolecules on the inner or outer surface of packing particles and column walls. As a rule, the retention factor in isocratic conditions increases exponentially with increasing molecular weight of polymers and the retention time for large molecules might be too long for practical use. This behaviour is explained by an empirical relationship known as Martin's rule[125, 126]. Due to multiple attachment higher molecular weight species would be strongly retained and desorption would require a stronger eluent. In order to achieve the desired separation, the mobile phase composition can be altered. This is often achieved by gradient elution chromatography[127-130]. The stepwise adjustment of increasing eluent strength allows the change in elution behaviour of different sample components. Gradients can also be achieved by changing the ionic strength, the pH composition of the eluent, changing the flow rate or temperature, yet changing the eluent composition remains the most popular application.

Gradient elution chromatography of polymers received attention as early as the 1970s[131] but most of the pioneering work was conducted by Glöckner[69]. Since then other groups have successfully applied the technique for the investigation of a variety of polymer blends, statistical and graft copolymers[132-137]. In principle, it allows the separation based on chemical composition of heterogeneous polymer systems. Typically, the polymer solution mixture is injected in a weak eluent and the molecules are retained at the column inlet due to their limited solubility[41]. The starting eluent is often a non-solvent causing precipitation of the polymer molecules. The eluent and solvent strengths are subsequently increased and the molecules are gradually dissolved, desorbed and start eluting. Although the elution profile is known to be dependent on both the chemical composition and the molecular weight, the contribution of the latter can be controlled by the extent of which dissolution takes place. Either critical conditions (as discussed previously) will arise or the polymer molecules can elute at different elution times due to differences in solubility based on the chemical composition of the backbone, functional groups, architecture[138] etc. Several investigations of statistical and graft copolymers in gradient LC illustrated a separation independent of molecular weight[139-143]. This situation is beneficial in the instances where gradient LC is combined with SEC as a second separating technique. As the sample capacity is higher than in SEC, the obtained fractions can be forwarded directly to SEC for further separation according to molecular weight. When the precipitation-redissolution gradient LC is employed, the partition mechanism can be enforced[144-146]. Philipsen conducted a detailed study of several oligomers and low molecular weight polymer utilizing the precipitation-redissolution technique[68, 147].

The solvent gradient HPLC fractionation of synthetic polymers works well, but it has a few drawbacks in that it is difficult to include useful detection methods for the characterization of polymers such as DRI, light

scattering and viscometry due to the background signal drift[148]. Characterization of the molecules having continuous distributions in various molecular characteristics, require the determination of these distribution curves quantitatively with accuracy and reproducibility. The background signal drift can be avoided by alternatively using changes in temperature to control the retention. The temperature dependency of the retention factor k' has been widely used to study the thermodynamics involved in the LC separation process, but it is not a popular variable due to the limited possible range of temperature variation which is in turn curbed by the freezing and boiling of mobile phase and/or precipitation of the polymeric solutes. More details regarding suitable detector systems will be given in section 2.6.

2.5 Hyphenation of LC separation techniques: 2D chromatography

A very efficient approach to analyzing the molecular heterogeneity of complex polymers is by combining different mechanisms of their chromatographic separations with each other or with a selective detector. As complex polymers feature simultaneous distributions (functionality type, chemical composition and/or molecular weight) that are mutually dependent, a two-dimensional separation is required to characterize each distribution independently. Two-dimensional liquid chromatography (2D-LC) systems have been used for many years to separate and characterize synthetic polymers, bio-molecules and complex mixtures[118, 149-151]. Erni and Frei[152] were the first to explore the on-line approach, which is currently referred to as "comprehensive" 2D-LC. Work done by several research groups has contributed greatly to the development of 2D-LC[64, 153-156]. A typical experimental configuration of 2D-LC in polymer analysis has incorporated LC-CC as the first dimension to separate in terms of the molecular characteristics (composition or functionality). The chemically homogeneous fractions are then subsequently transferred to SEC as the second dimension to separate according to molecular weight[65, 157, 158]. SEC has been a preferred choice for the second dimension separation since it is a universal technique to separate polymers according to molecular weight. The SEC retention can be greatly affected by molecular characteristics other than molecular weight, but once homogeneity of the sample is achieved a more meaningful correlation with molecular weight can be made. Furthermore, the development of new types of columns allows SEC separation to be carried out within minutes[159].

"Comprehensive" 2D-LC setup

In a comprehensive 2D-LC setup, a multiple port (8 as used in the current study) switching valve equipped with two loops is used in a symmetrical configuration. While one loop is being filled with the first dimension eluate, the fraction that has previously been collected in the second loop is analysed in the second dimension. The collection time of each fraction in the first dimension separation has to be equal or longer than the analysis time in the second dimension separation. As a consequence, the analysis time in the second dimension and the loop volume together determine the (maximum) flow rate for the first dimension separation. The total analysis time is essentially the product of the analysis time of the second dimension separation and the number of fractions collected from the first dimension separation. To limit the total analysis time and to conserve the chromatographic separation (resolution) efficiency obtained in the first dimension, it is very important that the second dimension separation be kept fast. In order to obtain a truly comprehensive coupled separation, the flow rate of the first dimension separation cannot be very high.

Figure 4 shows a typical "comprehensive" two dimensional chromatographic system with its individual analytical components.
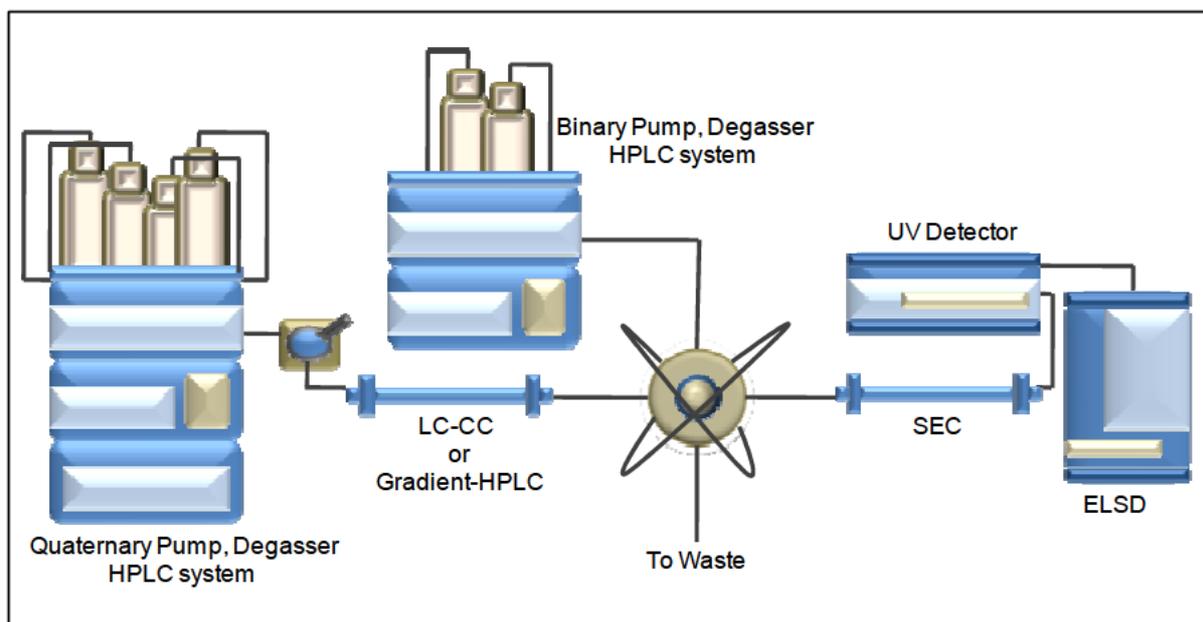
Figure 4. A schematic of a typical online 2D-chromatography system; The first dimension represents separation with regard to chemical composition, while the second dimension involves separation with regard to hydrodynamic volume (an adaptation)[65]

Furthermore, it illustrates how fractions collected from the first dimension, after separation with regard to chemical composition, are transferred to the second dimension to undergo SEC analysis for separation based on hydrodynamic volume. The increased demand for chromatographic materials that are able to achieve fast, reproducible and well-resolved separations of large quantities of structure analogues is a challenge. The chromatographic triangle represents the most important criteria in chromatography, namely resolution, speed and loadibility[154, 160, 161]. Optimizing any of these parameters could come at the expense of others. A fast separation, for example, may result in bad resolution and loadability, and *vice versa*. Variable parameters are column dimensions (length, inner diameter), mobile phase (type and flow rate), column temperature (starting temperature, temperature program) and stationary phase (type, particle size, pore size, phase volume ratio).

2.6 Detection systems

One key component of any HPLC system, regardless of the type of technique or mode of operation is the detection method as it ideally allows the required verification, identification and (if possible) quantitative determination of the various species separated from a solute mixture, thereby providing information on the character of the macromolecules under investigation[162-164]. The on-line units employed to monitor the effluent from the column in real time and present an electrical analogue or digital signal to specialized software, tend to be the most sophisticated and expensive component of the system. Features which play an important role in the choice of detection are selectivity, specificity, sensitivity, stability and linearity. At times is it also desirable that the method of detection is not destructive towards the sample, especially in the case of multiple-detection systems. Generally, detectors can be divided into being concentration or molecular weight sensitive. Furthermore, concentration based detectors can be selective or universal as illustrated in Table 1.

Historical and Theoretical Background

Table 1: The classification of different detectors based on sensitivity

	Concentration sensitive	Molar mass sensitive
Selective detectors	**Universal detectors**	
Ultraviolet (UV) detector	Refractive Index (RI) detector	Viscometer detectors: single capillary, differential
Infrared detector (FTIR)	Evaporative light scattering detector (ELSD)	Light scattering detectors: LALLS, MALLS
NMR	Density detector	Mass spectrometers as detectors: MALDI-TOF MS, ESI-MS
Fluorescence detector	Conductivity detector	
Electrochemical detector		

The field of detectors for HPLC has been well reviewed in literature[65, 165-167]. Selective detectors give different responses depending on the molecular structure of the sample under investigation, while universal detectors show a similar response for most compounds. In both instances, some detectors are favoured over others in its application for polymer characterization.

Due to continuing advances in technology and the increasing demand of characterizing novel complex polymer systems, it has become common practice to utilize the coupling of selective with universal detectors or concentration with molecular weight sensitive units[118, 168-170]. With the use of on-line coupled molecular weight sensitive detectors such as light-scattering detectors (LALLS and MALLS)[171-174] and viscometers[95, 175-177], one can determine branching, molecular size and conformation as a function of molecular weight in a single analysis. Moreover, their use in conjunction with a concentration detector has greatly improved accuracy of HPLC/SEC measurements. Consequently, the precision of analysis actually worsens due to additivity of variances related to each component. Another well-known combination of detectors include that of spectroscopic detection such as UV with concentration sensitive RI for the determination of compositional heterogeneity of oligomers and various copolymers[178-180]. An alternative for copolymers that lack a chromophore is RI and density detection[181]. In isocratic mobile phases, RI detection is invaluable but due to changes of the refractive indices brought about by mobile phase composition changes it has major limitations in gradient elution HPLC. The alternative detector of choice would then be ELSD[158, 181-183]. NMR has proven to be a powerful spectroscopic technique for the characterization of polymeric systems. Its application as on-line detection method in LC has been published by several authors[87, 184-188] and is becoming increasingly popular. However, it still has several drawbacks which include high costs of the specially designed LC probe, lack of sensitivity due to the low sample concentration used in LC as well as required optimized pulse

Historical and Theoretical Background

sequences in order to suppress solvent signals[189]. Some of these issues can be overcome with off-line coupling methodology, which allows the fractionation and collection of several more homogenous components of a sample and consequently entail more absolute results[190]. The advantages of off-line coupling have greatly increased the application of e.g. LC-FTIR, as the possibility of solvent adsorption is diminished[154, 191]. Probably the biggest advancement in the characterization of heterogeneous polymeric materials is the use of mass spectrometry for absolute molecular weight and chemical composition analysis. Off-line and on-line approaches of MALDI-TOF MS and ESI-MS as specific detectors respectively can provide full structural information as well as the nature of endgroups present in heterogeneous polymeric systems[192-197] after selective LC separations.

3. Mass Spectrometry of Complex Polymers

3.1 General aspects

The classical definition of mass spectrometry is the study of the formation, separation, detection and interpretation of ions generated from ionization or fragmentation, in the gas phase[198, 199]. The obtained spectra typically entail the graphical presentation of the ion abundance versus the mass-to-charge ratio (m/z) of the separated ions, enabling the rapid determination of structural information and its relation to the molecular weight of a particular compound or molecule. The various components of a typical mass spectrometer are illustrated in Figure 5.

Sample preparation

Sample Introduction
Direct probe/infusion
GC
HPLC

Rough, Turbomolecular, Diffusion or Cryo pumps

Vacuum System

Ionization source
Electron Impact (EI)
Chemical Ionization (CI)
Atmospheric Pressure
Chemical Ionization (APCI)
Electrospray Ionization (ESI)
Matrix Assisted Laser
Desorption/Ionization (MALDI)
Fast Atom Bombardment (FAB)

Mass Analyzer
Electrostatic (ESA)
Magnet (B)
Time-of-flight (TOF)
Quadropole (Q)
Ion Traps (2D and 2D IT)
Ion-Cyclotron
Resonance (ICR)
Orbit

Detector
Electron Multiplier
Photo multiplier
Faraday Cup
Array Detectors
Multichannel Plate

Computer

Figure 5. A simplified flowchart of the basic components of a mass spectrometer. In principle, any combination of source and analyzer can be made based on the analysis requirements[199]

The application of mass spectrometry as a characterization technique for polymeric compounds was restricted for many decades due to the inability of successfully ionizing molecules of a larger size and low volatility into the gas phase. The methods used were based on chemical or thermal degradation such as pyrolysis which preceded the actual mass spectrometry procedure. The biggest limitation was that such an approach only revealed information regarding the constituting monomers and average chemical composition but nothing on the actual polymer distribution of a compound. Very importantly, the biggest demand in science and industry remains to have the ability to determine the different structural distributions present in a macromolecule for the optimization and development of well-designed compounds. The advent of 'soft-ionization' techniques in the 1980s effectively removed these shackles and has since proven to be a powerful additional toolset for the structural investigation of synthetic complex polymers[197, 200-204]. Matrix-assisted laser desorption/ionization (MALDI) and electrospray ionization (ESI) mass spectrometry in particular, has revolutionized the analysis of large molecules as the essential steps of ionization and transfer to the gas phase with very little or no fragmentation could be achieved[193, 205, 206]. Given that the detector efficiency is independent of molecular weight, absolute molecular weight and molecular weight distributions can be obtained in a single measurement, requiring very little time. The only calibration required is that of the

mass scale. The obtained mass spectra of the intact ions represent the constituent oligomers of the polymer. Furthermore, if need be, the amount of energy bombardment can be manipulated to induce specific patterns of fragmentation to further aid in identification of chemical functionality. In general, an MS instrument consists of four essential components which include the sample input, the ion source, a mass analyzer and last but not least the ion detection recording device connected to designated software to enable instrument control, data manipulation and output. Numerous commercial instrument models are available, utilizing a range of different components.

3.2 Matrix-assisted laser desorption/ionization time-of-flight (MALDI-TOF) MS

The importance of the invention of MALDI-TOF MS was acknowledged by awarding the Nobel price to Koichi Tanaka[207] in 2002. Karas and Hillenkamp made invaluable contributions by establishing that the laser ionization efficiency is significantly improved with the inclusion of a matrix[208]. As a 'soft-ionization' technique, MALDI is renowned for the transfer of high molecular weight polymer ions without any fragmentation, with the critical role of the matrix distinguishing the method from its peers. The success of the technique is dependent on several parameters which, in addition to the proper matrix selection, include sample preparation and the selectivity of the mass analyzer. The general experimental procedure involves the deposition of a matrix-polymer solution onto a target plate which is allowed to crystallize before being subjected to pulses from a laser beam and desorbed under high vacuum. The majority of commercially available instruments are equipped with a N_2 laser having a frequency which falls in the UV region (337nm)[199]. The role of the matrix is several-fold. Not only does it in principle isolate the macromolecules from each other, but it absorbs most of the energy and most importantly assists in the formation of the protonated or cationized species by subsequently donating the charge to the polymeric molecules. Additionally a salt can be added to the solution by acting as an additional cationizing agent. Consequently, the final protonated or cationized products are separated in the mass analyzer. Several investigations have been conducted into the exact mechanism of ionization, with the latest account given by Batoy et al[206].
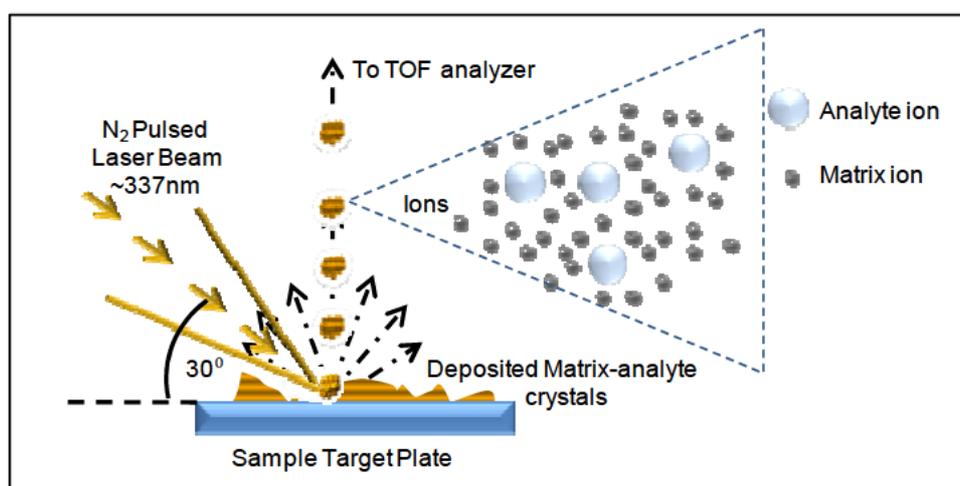
Figure 6. The matrix-assisted laser desorption/ionization process (an adaptation)[209]

Historical and Theoretical Background

Importance of the matrix

One of the biggest challenges is to select the most suitable matrix for the polymer under investigation. The most common matrices include nicotinic acid, benzoic acid and cinnamic acid ((E)-3-phenylprop-2-enoic acid) derivatives, dithranol and azobenzoic acid derivatives. They all have two structural features in common; a group which acts as a source of an acidic proton and the fact that they absorb around 337nm (the N_2 laser wavelength). Different polymer-matrix combinations have been investigated and are well documented[210]. It was also shown that with various isomers of specific matrices such as DHB (2,5-dihydroxybenzoic acid), different results can be obtained[206, 211]. Moreover, the ratio of matrix material to polymer sample concentration can be varied, ranging from 10:1 to 10 000:1 and in the case of high molecular weight polymers, the higher ratios of matrix to polymer are recommended[212]. Supplementary properties of the matrix should include similar solubility character to that of the polymer molecules in a specific solvent, co-crystallization with the polymeric molecules and once ionized should show no ionic interference with the sample. The addition of the matrix is dependent on the sample preparation method and can therefore be added before, during or after deposition of the polymer sample solution. Studies have shown that both the order and method of deposition can influence final results with respect to ionization efficiency and the observed polymer distribution[213, 214].

Sample preparation and deposition method

The matrix and polymer mixture solution preparation can be achieved in various approaches. The most popular is the 'dried droplet' which entails deposition of the selected matrix and polymer solution either together in a single droplet or successively to form a combined layer. The disadvantage, however, is that the rings of crystals being formed after evaporation are not homogeneous and so-called 'hotspots' are found which can produce intense signals. The effect is negligible for structural repeating unit or endgroup identification but with regards to molecular weight and molecular weight distribution analysis large discrepancies can be found. The heterogeneity of the matrix/polymer-crystal layer can be related to capillary flow[215] or diffusion effects causing the segregation, the extent of which can be decreased by changing the solvent used for sample preparation. Attempts to overcome this problem lead to solvent-free sample preparation[216-219], as well as spray-methods[220, 221]. Care should, however, be taken with electrospray deposition, since the molecular weight distributions can change at higher voltages due to fragmentation.

Time- of- flight (TOF) mass analyzer

Generally speaking the mass analyzer is the entity of the mass spectrometer that separates the ionized species according to the mass/charge ratio. The mass resolution ($R = M/\Delta M$) and its dependence on the mass is determined by the type of analyzer employed. In mass spectrometry, numerous types of analyzers are available which include the classic magnetic sector with single and double focusing, quadropole analyzer, time-of-flight (TOF), Fourier transform ion cyclotron resonance (FT-ICR) and ion-trap (IT). MALDI is known to be efficiently compatible with TOF mass spectrometers which measure the flight time of ions with an equivalent kinetic energy over a constant distance[222]. The TOF process is perhaps the simplest of the mass analyzer technologies. A schematic of the basic components of a linear TOF is illustrated in Figure 7.
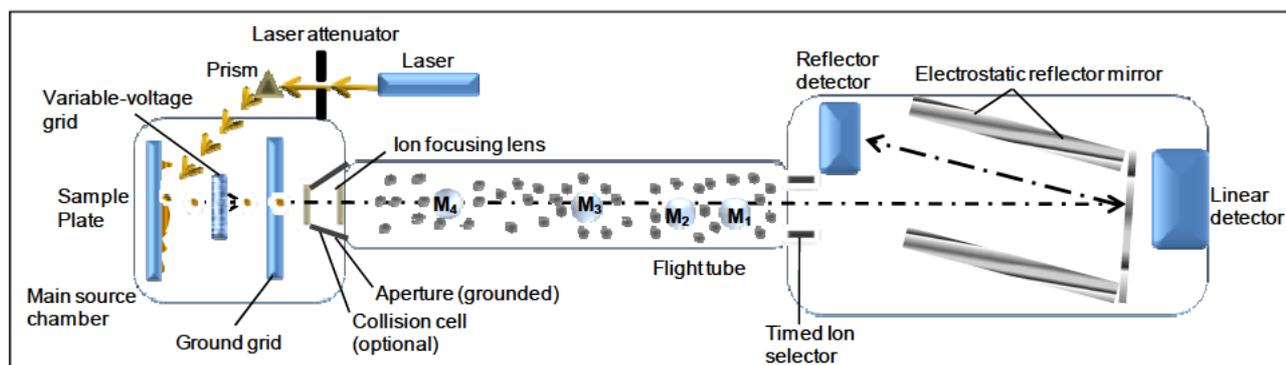
Figure 7. The TOF mass spectrometer (an adaptation)[223]

Arriving from the ion source, ions are gathered in a short source region under a fixed potential (V) and accelerated into a drift region with no electric field. Ideally these packets of mono-energetic ions will all enter the drift regions with the same kinetic energy:

$$E_{kin} = zqV = \tfrac{1}{2}mv^2 \qquad (13)$$

Where m is the mass of the ion, v the velocity, z indicates the charge state and q the unit charge. If an ion with a velocity of v is allowed to fly for the distance of the drift region d, the time of flight can be determined by:

$$t = \frac{d}{v} \qquad (14)$$

The combination of the equations above give:

$$t = \left(\frac{d}{\sqrt{(2V)}}\right)\left(\sqrt{\left(\frac{m}{zq}\right)}\right) \qquad (15)$$

illustrating that the lower mass ions will obtain a greater velocity than the higher mass ions and will thus traverse the distance of the drift region in a shorter amount of time. Within a time range of tens to hundreds of microseconds, the mass selected ion packages arrive in succession at the detector situated at the end of the drift region. By measuring the time it takes for the ions to reach the detector, the m/z of the ions can be determined.

TOF offers several improvements over scanning analyzers due to the fact that the majority of the ions that are injected are detected, therefore, sensitivity is increased and the mass range is limited only by the detector's ability to convert the ion's arrival time into a measurable signal. The differences in flight times are relatively small (ns to ms) so fast detection is required. A pulsing technique which is often used in Q-TOF instruments involves the application of a perpendicular pulse to the already continuous ion beam. Although the pulses are rapid, the formed ions consist over a significant spatial and velocity spread, resulting in loss of separation efficiency and less accurate mass determinations. Loss of resolution and broadening effects are compensated for by utilizing the reflectron mode[207, 222], which has electrostatic ion mirrors and doubles the effective path length. At the end of the linear flight distance, the ions enter the mirrors, sending them down a second flight path towards the detector. The ions reflect differently depending on their incoming energies. For example, those with larger energies penetrate the reflectron more deeply and essentially exhibit longer flight

Historical and Theoretical Background

paths; thus arriving at the detector at a similar time to the ions of less energy. The second development allowing improvement of resolution is the delayed extraction technique, used to compensate for the spatial spread. Ions are extracted using a high voltage pulse after a predetermined time delay, allowing the dependence of ion flight time on initial velocity to be corrected for.

Advantages of MALDI

The application of MALDI-TOF MS as characterization technique for polymers does not come without a few drawbacks, although most issues are related to the properties of the polymer sample under investigation. Certain classes of polymer materials have limited scope due to a lack of availability of suitable matrices, cationizing agents and/or solvent systems for sample preparation. A given matrix may perform well for one type of polymer but could exhibit undesirable chemically and photo-chemically induced reactions in another. Coupling to a TOF mass analyzer, in principle allows the technique to be unlimited in mass range, yet inherent upper mass limits may occur due to inefficient sample conditions. Although polymers with molecular weights of up to 70 000Da have been recorded[224], successful analysis has proven to be related to the polydispersity of the sample. Narrowly dispersed samples have a much higher accuracy and reproducibility rate. Reduced instrumental detection sensitivity for higher-mass ions can also occur. Regardless, with the advantages of strong mass resolution, the extent of mass range that can be covered, the speed of cycles or scans generated as well as high sensitivity, it is not surprising that instruments such as MALDI-TOF and Q-TOF are extensively used for high-throughput analysis of samples of various origin. MALDI-TOF in specific offers a fast, sensitive and accurate means of molecular weight and molecular weight distributions. Although multiple charging, non-covalent- and matrix-adducts can occur, the generation of mostly single charged ions makes the spectra easily interpretable.

3.3 Electrospray ionization (ESI) MS

Complementary to MALDI-TOF MS, ESI-MS is the other 'soft-ionization' technique successfully employed for the ionization of polymer molecules without fragmentation[225-227]. The main difference is that the process involves the transformation of analyte molecules or ions in solution into the desired gas phase through either solvent or ion evaporation. The analyte solution is introduced into the source chamber via a hypodermic needle, either by direct infusion or as eluent from a LC chromatograph. Due to the fact that the ion formation involves extensive evaporation, typical solvents for ESI are prepared by mixing water with volatile organic compounds (e.g. methanol, acetonitrile). The liquid stream is dispersed into an electrospray of charged droplets due to the large electrostatic potential difference (2- 4kV) that exists between the needle inlet and the cylindrical surrounding counter-electrode walls. To decrease the initial droplet size, compounds that increase the conductivity (e.g. acetic acid) are customarily added to the solution. Depending on the applied potentials, positively or negatively charged droplets are formed.
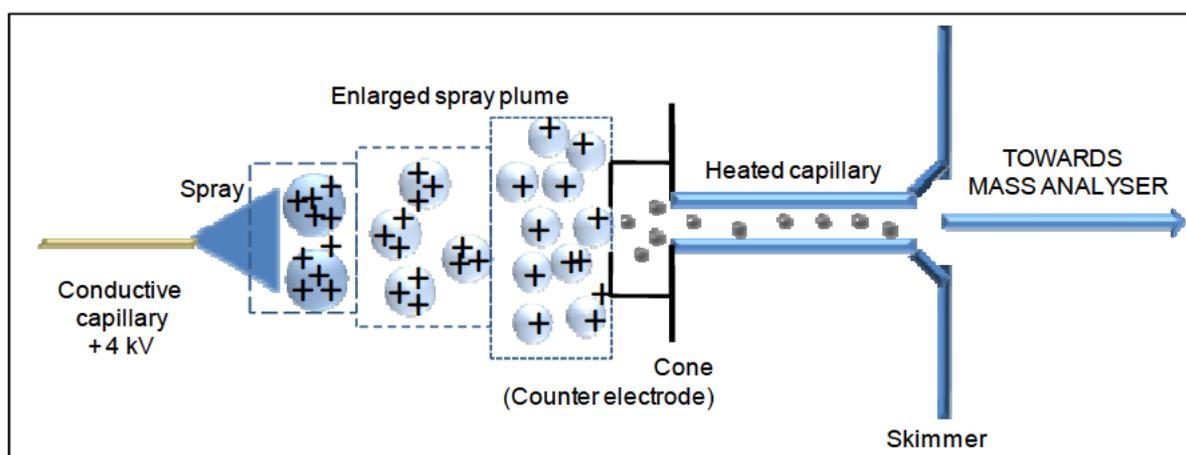
Figure 8. The characteristic components and occurrence at the source during electrospray ionization (an adaptation)[228]

Solvent evaporation takes place resulting in the shrinkage of the droplets as they enter a heated transfer capillary. Consequently, the surface charge density increases up to the point where the droplet size reaches 90% of its "Rayleigh" limit, the droplet deforms and the surface tension cannot compensate for the 'Coulombic' repulsion. The droplets disintegrate, continuously forming smaller sizes until virtually no solvent molecules are present any longer, only the protonated or deprotonated analyte molecules. Additionally, ions can be evaporated directly from charged droplets as well as via collisions with neutral molecules in the source region as they are accelerated through a nozzle, a skimmer and the ion optics toward the mass analyzer. Ideally the obtained spectra are relatively simple and consist primarily of quasi-molecular ions created by the addition of a proton $[M + H]^+$ or of another cation such as a sodium ion $[M + Na]^+$ or the removal of a proton, $[M-H]^-$. It is, however, not difficult to imagine that due to the continuous modifications of the gas-phase ions in the atmospheric and ion-sampling regions of the mass spectrometer, multiple-charged ions $[M + nH]^{n+}$ are also produced.

Given that the size of the molecular weight range for ESI is considerably lower than that of MALDI, the presence of multiply charged species effectively broadens the scope. In turn, it also complicates the obtained spectra and makes structure elucidation much more difficult. This partially explains why ESI-MS is a much more established method for the characterization of biological macromolecules than for synthetic polymers. The overlapping of multiply charged oligomer ions hinders the determination of the average molecular weight for high molecular weight polymers[202] especially in the case of samples having mixtures of polymers, copolymers or differing average molecular weights. The majority of research on ESI of polymers also focuses on polymer compounds consisting of relatively low molecular weights, typically less than 10 000Da[205, 229], thereby predominantly showcasing singly or doubly charged species and avoiding problems related to spectral congestion associated with higher charge states. Another issue is the more stringent solvent requirements compared to other mass spectrometry. Only polymer samples that are soluble in electrospray compatible solvents such as water, methanol, acetonitrile and/or their combinations are amendable to ESI analysis.

Nevertheless, ESI has several advantages over MALDI which include the absence of peaks associated with a matrix. Even more importantly is the fact that samples are introduced in solution, which makes on-line coupling to classical separation techniques such as SEC and HPLC possible. It also consists of more readily

Historical and Theoretical Background

available instrumentation for collision-induced dissociation (CID) studies. Although a variety of analyzer types can be utilized in ESI such as quadropole, ion trap and Fourier transform ion cyclotron resonance (FT-ICR) instruments, TOF is the preferred choice for polymer analysis. Their upper molecular weight range[193, 230] as well as the relatively high resolution, proves to be vital advantages, especially in the case of copolymer analysis where the number of different product grows exponentially with molecular weight.

3.4 The use of MALDI-TOF and ESI mass spectrometry as method of detection

Keeping in mind that the characterization of a given polymeric material entails investigating the chemical composition and sequencing of the repeating units, the degree of polymerization, endgroups present as well as the architecture of the macromolecule chains, one realizes the extent of the impact mass spectrometry has made in polymer analysis. Of the numerous techniques available, only MS has the capability of determining all these characteristics for individual chains using absolute molecular weight information. For the past 20 years, two-dimensional analysis and hyphenated techniques have been dominated by the principle of coupling two different chromatographic techniques for the simultaneous investigation of molecular weight and chemical heterogeneity. However, the continuous development and application of contemporary mass spectrometry has lead to employing MALDI-TOF and ESI-MS as proxy for the molecular weight dimension analysis as it allows simultaneous access to molecular weight distribution and structural information. The union of chromatography and mass spectrometry is ideal as the shortcomings of both techniques can be overcome. Developments in the LC-MS research area are well documented[194, 197, 231].

The biggest disadvantage of both MALDI-TOF and ESI-MS in the analysis of complex polymers is that the results obtained are largely dependent on the dispersity of the sample. This is due to the fact that the sensitivity of mass spectrometry varies with molecular weight and chemical composition which causes severe discrimination in ionization, transmission and detection towards higher molecular weight species[205, 230, 232-234]. The practical solution to overcome this is problem is the pre-fractionation of the disperse sample via separation methods such as the different modes of liquid chromatography. In principle, all LC modes in polymer analysis can be interfaced with MS although SEC coupled with mass spectrometry has proven to be the most popular. In this instance, the disperse sample is separated into several fractions exhibiting a more narrow molecular weight distribution during the SEC part of the analysis. The fractions show an improved result when subsequently characterized by MALDI-TOF or ESI-MS. As mass spectrometry technique, MALDI-TOF enjoys preference over ESI-MS due to the upper molecular weight range limitation as mentioned previously. Furthermore, these mass-measured fractions can be utilized as absolute calibration points (i.e. log *M* vs retention volume) for the LC chromatogram and the absolute molecular weight distribution averages can be calculated with the aid of established SEC software programs. This in turn overcomes the inherent problem of SEC with regards to the availability of well-characterized calibration standards for a specific polymer type as the synthetic polymer can now be characterized using an absolute method based on the investigated polymer itself. Consequently, structural information is obtained from the mass spectra which include monomer type (s) present, calculated from the repeating unit mass increment as well as the combined endgroup mass after extrapolation to zero monomers and subtraction of the cation mass. Due to the ease of implementation, the coupling of LC-MS is performed on-line, the advantage being that the fast-scanning mass analyzer from the mass spectrometer allows the recording of several mass spectra every second so that numerous mass spectra can be produced during a chromatographic run. This

Historical and Theoretical Background

implies that from the chromatography separation based on a specific feature, whether it is molecular weight, chemical composition or functionality type, valuable qualitative information from a concentration detector is collected and fractions of sufficiently low dispersity are available for further qualitative and quantitative MS analysis. Although on-line investigations have been published[194, 235], the vast majority of LC-MALDI-TOF MS uses off-line methodologies even though it suffers from reproducibility issues[213]. Similar to the LC-FTIR technique, commercial interfaces are available for LC-MALDI-TOF MS consisting of targets that are pre-coated with matrix[236]. ESI-MS is by far the popular choice for on-line MS analysis, yet due to their optimum flow rates which are in the order of magnitude 30μl/ min, the use of conventional scale LC stationary phases requires post column splitting[237]. Several examples of LC-MS techniques dedicated to investigate several types of polymer systems can be found in literature. Functionality type distributions and endgroup type variations for aliphatic resins[230, 238], cyclic formation[233] and the chemical composition of copolymers[236, 239] were all successfully determined by LC-ESI-MS and LC-MALDI-TOF-MS; showcasing contemporary mass spectrometry's unique ability to serve as a powerful additional characterization technique of synthetic complex polymer materials.

Part III. Results and Discussion

1. Overview of the Characterization of Aliphatic Polyesters

In the following section, the results obtained from the analyses conducted to satisfy the aims of the current dissertation are compiled. The discussion is subdivided into the respective chromatographic and spectrometric characterization techniques which include the method development and optimization in each case to enable the investigation of the extent of heterogeneity for two inherently different model polyester batches. Different modes of liquid chromatography and their combination were employed to obtain compositional information regarding the molecular weight, the molecular weight distribution, the chemical composition and the chemical composition distribution. Concomitantly, MALDI-TOF and ESI mass spectrometry analyses allowed the elucidation of structural information on the polyester chains following the off-line coupling methodologies with the respective chromatography techniques. For the purpose of our investigations model polyesters of phthalic anhydride and maleic anhydride with 1,2-propylene glycol (PA-PG and MA-PG) were synthesized respectively in the case where the glycol was added in 30% molar excess relative to the anhydride. The proposed structures for the two different batches are given in Figure 9.
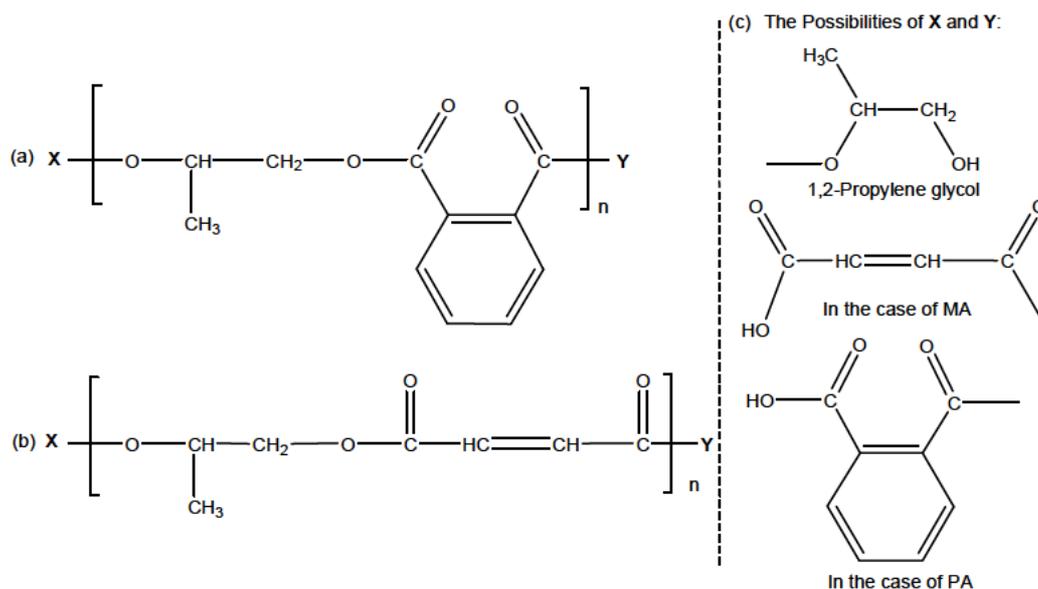
Figure 9. *Proposed structures in the polyester preparation where (a) and (b) refer to the repeating unit of polyesters PA-PG, MA-PG and (c) to the different possible endgroup combinations*

The samples were prepared and provided by Freeworld Coatings Research Centre and the details are discussed in the related Part IV: Experimental. Attempts were made to follow the course of the polycondensation reaction in terms of molecular weight and molecular weight distribution by removing samples at pre-determined values of water formation (in ml). The targeted molecular weight of the final products for both anhydride types were typical of prepolymers used in resin applications, ranging between 10^2 and 10^4Da. All samples were used as received.

Results and Discussion

2. Method Development of Liquid Chromatography Techniques

2.1 Size exclusion chromatography of PA-PG and MA-PG based polyesters

Considering the limitations found in SEC for the characterization of complex polymeric materials, it remains the traditional first step of liquid chromatography as it importantly provides a distribution of the material based on calibrations established through the use of homogeneous standards when employing RI, UV and/or ELS detectors. As the properties of the final polymeric product are largely influenced by the molecular weight and the molecular weight distribution, the technique plays a fundamental role in distinguishing differences between individual samples as well as diverse polymer systems. SEC analysis on the polyester samples from the respective PA-PG and MA-PG batches were conducted in THF using polystyrene as calibration standards, the results of which are summarized in Tables 2 and 3. The sample range of each polyester type represents the different oligomeric species aimed for, which in turn was established through calculations based on the volume of water produced throughout the polyesterification reaction. The theoretical values for the corresponding molecular weights are given in comparison to the experimental values for each oligomer type. The calculated values were based on the most basic ideal structure of HO-[PA-PG]$_n$-H where [PA-PG]$_1$ constitutes a monomer unit of n=1 degree of oligomerization for the phthalic anhydride system. The repeat unit has a value of 206Da, whereby the endgroups of –OH and –H constitutes the rest of 18Da. Subsequently, the same methodology was used for the MA-PG system, where the most basic ideal structure was HO-[MA-PG]$_n$-H with a repeat unit value of 156Da. Despite the fact that the $\bar{M}_n$ values obtained from SEC corresponded well to the theoretical calculations for the samples at the beginning stages of the polycondensation, as the reaction proceeds an increasing deviation was found, especially in the case of the $\bar{M}_w$ calculations and the subsequent polydispersity values reported by the analysis software.

Table 2. Theoretical calculations vs SEC results for the molecular weight determination of the PA- PG (30% more PG by mole) polyester samples. Polystyrene standards were used for the SEC calibration. The calculated values are based on the most basic ideal structure of HO-[PA-PG]$_n$-H at n degrees of oligomerization

Sample	n values for HO-[PA-PG]$_n$-H	$\bar{M}_n$ (calc.) (g/mol)	$\bar{M}_n$ (SEC) (g/mol)	$\bar{M}_w$ (SEC) (g/mol)	Dispersity index
s23	1	224	135	216	1.60
s24	2	430	184	464	2.52
s25	3	636	283	837	2.96
s26	4	842	553	1470	2.65
s27	7	1460	530	1450	2.75
s28	8	1666	569	1520	2.67

Results and Discussion

Table 3. Theoretical calculations vs SEC results for the molecular weight determination of the MA- PG (30% more PG by mole) polyester samples. Polystyrene standards were used for the SEC calibration. The calculated values are based on the most basic ideal structure of HO-[MA-PG]n-H at n degrees of oligomerization

Sample	n values for HO-[MA-PG]$_n$-H	$\bar{M}_{n \text{ (calc.)}}$ (g/mol)	$\bar{M}_{n \text{ (SEC)}}$ (g/mol)	$\bar{M}_{w \text{ (SEC)}}$ (g/mol)	Dispersity index
s11	1	174	180	295	1.64
s12	2	330	266	582	2.19
s13	3	486	383	897	2.34
s14	4	642	668	1470	2.20
s15	7	1110	823	1790	2.18
s16	8	1266	871	1950	2.24

The SEC chromatograms in Figure 10 show that the polyester samples are all oligomer mixtures, exhibiting fairly broad dispersities already present from the onset of the polyesterification reaction (s23 and s11), which possibly explains the large variations in the molecular weight values. Due to the fact that the stationary phase used (see Part IV. 1.2.1) is particularly suited for the SEC separation of lower molecular weight polymeric compounds, each of the bulk samples was fractionated into a number of distinct oligoester sets, despite the fact that dimers (n = 2), trimers (n = 3) etc. were specifically targeted at varying stages of the polymerization reaction.
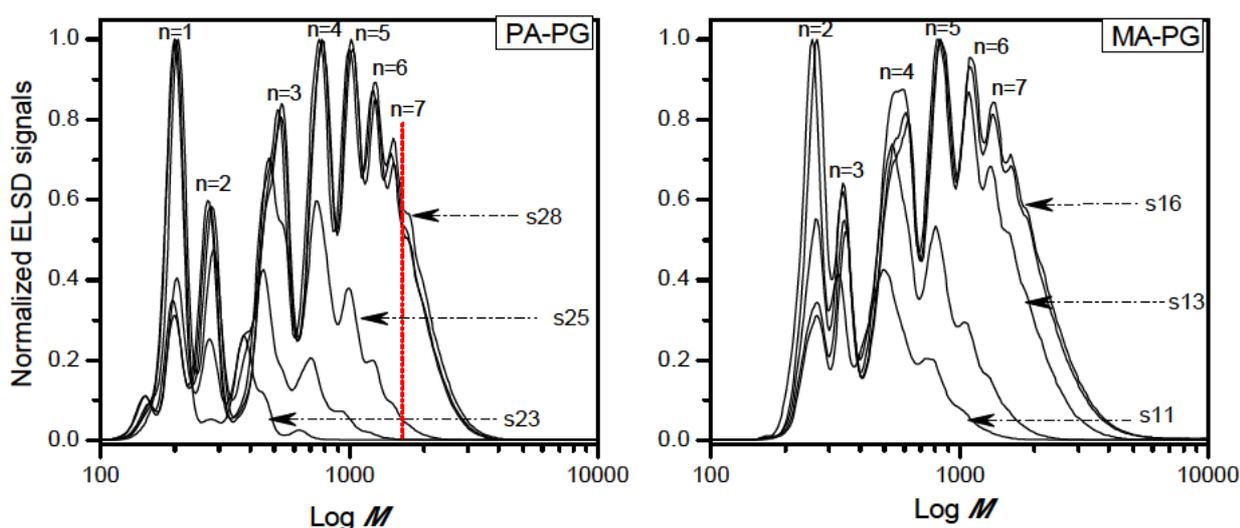
Figure 10. SEC chromatograms of the respective PA-PG and MA-PG polyester batches based on PS standard calibration. The proposed degree of polymerization for the different oligomeric species found within each sample n, is indicated above each peak distribution. In the PA-PG graph, the higher molecular weight fraction collected for mass spectrometry analysis is illustrated by the dotted red line.

Results and Discussion

From the chromatograms, the evolution of the polyester chains could easily be monitored and the molecular weights of both PA-MG and MA-PG polyesters were found to be in the range of approximately 100 to 5000g/mol and 140 to 6000g/mol, respectively. For both polyester types, the different size distributions are most likely brought about by the transesterification side reactions where the ester-ester interchange, ester acidolysis and alcoholysis are known to promote randomization of the chain length distribution (as discussed in Part II. 1.3). The extent to which these phenomena occur in conjunction with the other two major side reactions namely branching and cyclic formation can, however, not be identified with SEC as the sole characterization technique. Earlier studies conducted by Ahjopalo et al.[39] on saturated polyesters specifically, showed the use of SEC in combination with MALDI-TOF MS and GC-MS. The aim was to not only have complimentary techniques to investigate molecular weight distributions but also to determine different endgroup functionalities as well as structural differences between polyesters synthesized from various combinations of diols and diacids.

For the purpose of the current investigation, a similar approach was used by means of repetitively fractionating the eluting oligomer-separated peaks of the last sample in each polyester batch during SEC. In order to follow the elution time of each of the fractions, a UV detector at 254nm wavelength was employed. After the evaporation of the mobile phase, the concentrated fractions were dissolved in a matrix solution and subjected to MALDI-TOF MS. Figure 11 shows the mass spectrum of the unresolved higher molecular weight fraction of s28 in the PA-PG polyester set.
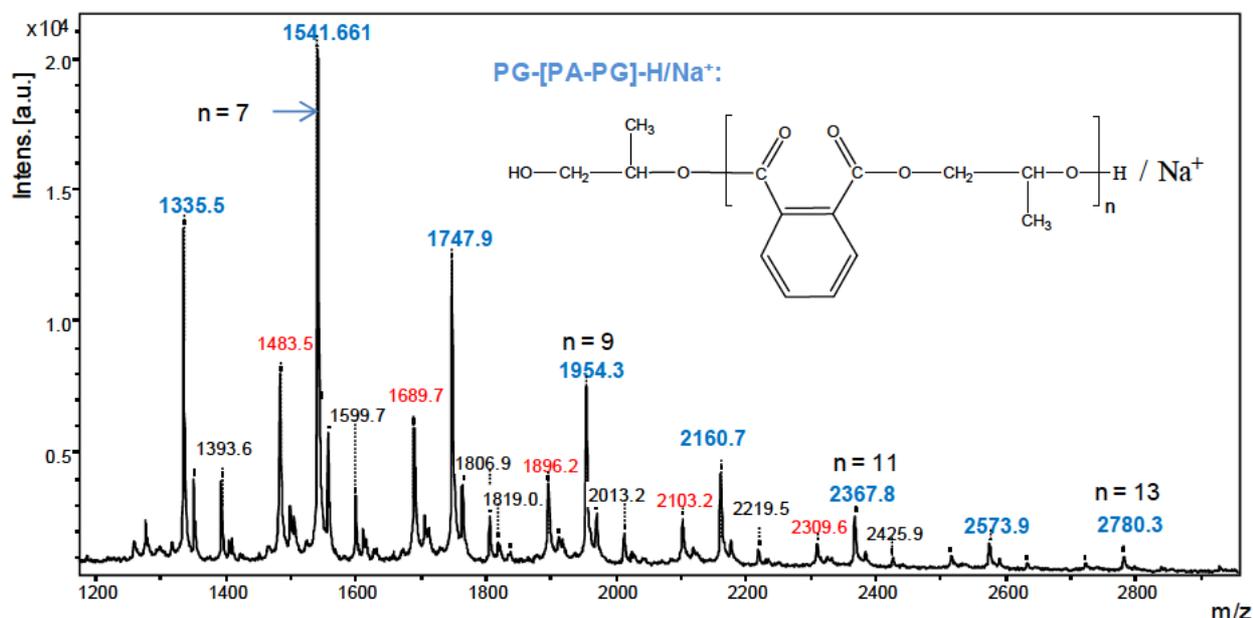
Figure 11. MALDI-TOF mass spectrum of the unresolved higher molecular weight fraction of s28 in the PA-PG polyester batch. The matrix solution used was dithranol in 1,4-dioxane (10mg/ml) and no additional cationizing agent was added. The highlighted peak distribution is related to the sodium adducts of the structure Na+/PG-[PA-PG]-H.

The peak distributions with the highest intensity suggested that ionization took place mainly via the addition of sodium ions, although potassium and proton related ions could also be found. In the mass spectrum, the oligomeric peaks showed a peak-to-peak mass increment of 206Da which corresponds to the calculated repeating unit of the PA-PG polyester. The peaks highlighted in blue in Figure 11 can be attributed to the

Results and Discussion

hypothetical structure that consists of a propylene glycol unit at the one end of the oligoester chain and a hydrogen atom at the other end. This suggests that m/z 1541.7 is due to:

$$PG\text{-}[PA\text{-}PG]_7\text{-}H + Na^+$$
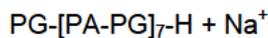
$$76.1 + 7(206.1) + 23 = 1541.8$$

Furthermore, the peaks highlighted in red and black revealed the presence of additional distributions having the same degree of polymerization or chain length yet different endgroup functionality combinations.

Considering that 30% excess mole glycol compared to the diacid was incorporated into the polycondensation at the onset of the reaction, the presence of esters having a glycol unit at one chain end is to be expected. For this specific oligomeric series, the distribution was found to continue up to m/z 2780, which relates to a degree of polymerization n = 13. This value, however, did not correspond very well with the molecular weight values indicated by the SEC chromatograms, which initially suggested that much higher molecular weight species are present. In utilizing polystyrene standards for the SEC calibration with the analysis of a different monomer and/or polymer type, considerable deviations between the relative and absolute values are to be expected. Therefore, MALDI-TOF MS is an excellent technique to compliment SEC in terms of molecular weight determination. Subsequently, mass spectrometry was also conducted on the lower molecular weight fractions of the same polyester sample. Their respective average molecular weights obtained from MALDI-TOF MS vs. their elution volumes in comparison to the styrene standard calibration values from SEC are given in Figure 12.
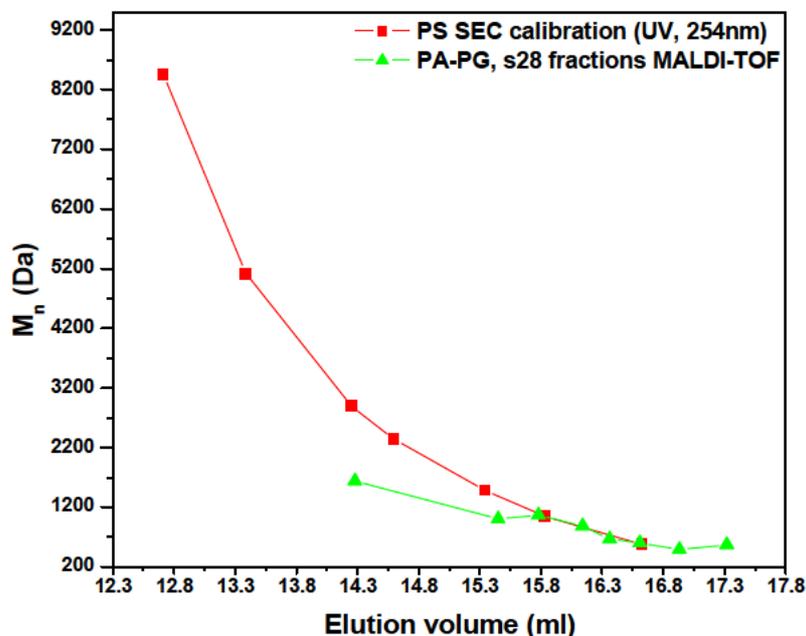
Figure 12. Average molecular weight values determined from MALDI-TOF MS of the PA-PG polyester (s28) fractions, compared to the values expected from SEC with PS calibration at a certain elution volume.

It can be seen that for the peaks fractionated from SEC where the assignment was initially denoted 1< n <7, an excellent agreement was found between average molecular weight values obtained from SEC and

34

Results and Discussion

MALDI-TOF MS. The deviation in values between the two techniques however became increasingly larger with increasing molecular weight; with the mass spectrometry illustrating that a much lower degree of polymerization was obtained. Notably, the investigations of Ahjopalo et al.[39] referred to previously found that the incorporation of phthalic anhydride and its subsequent diacid with any of the diols used in the related study lead to the formation of cyclic oligomers in addition to the linear counterparts with carboxyl and/or hydroxyl endgroups during the esterification reaction. Additionally, they indicated that ring-closure was independent of temperature variations found during the polyesterification and that back-biting occurred readily even at early stages of the reaction, leading to the formation of dimeric and trimeric cyclic structures. As SEC separations are based on conformational size (hydrodynamic volume), the cyclic structures are smaller than their corresponding linear chains of equal degree of polymerization and consequently their elution times are longer, thereby further emphasizing the limitations of SEC.

For the PG-MA series, the inclusion of double bonds in the main chain is the most important phenomenon regarding the mechanism of the polyesterification reaction. In the current study, samples were collected at temperatures above 180°C which means that monoester formation is assumed to be completed and that esterification has commenced. Importantly, maleate- to fumarate isomerization is assumed to be optimized and subsequently the fumarate bond is more reactive towards saturation through the nucleophilic attack by the hydroxyl group of the diol, leading to short- and long chain branching[57]. It would therefore be unrealistic to assume that each fraction would represent a homogeneous species regarding size. Interestingly, a discontinuity was found in the average molecular weight values obtained from the mass spectrometry for the elution volume range 15.3 to 16.3ml. Due to the fact that the MALDI-TOF MS calculations are based on the distribution with the highest peak intensity for the sample (fraction), it is proposed that the variation is as a result of a different chemical composition distribution starting to dominate with increasing molecular weight.

Following the deviation obtained in the average molecular weight determinations for the fractions between the MALDI-TOF MS analysis and the classic PS calibration from SEC, a new oligomer calibration equation was employed whereby the molecular weight calculations of each of the polyester samples were revised. By applying a polynomial equation, the relation between the absolute mass values of the oligomers found in MS to their elution volume in SEC was found. Subsequently, the average molecular weight distributions of the PA-PG and MA-PG polyester batches obtained from the different techniques are given in Table 4 and Table 5, respectively. In general, an improved correlation was found for the molecular weight values from the oligomer calibration with the theoretical calculations. Keeping in mind that the calculated values are based on an ideal structure of, for example HO-[PA-PG]$_n$-H, it should be taken into consideration that the MS showed the presence of distributions having a variety of endgroup functionality combination as well as structural differences; any of which could have contributed to a smaller or larger scale towards the oligomeric calibration function. Nevertheless, in the case of the lower molecular weight samples, the $\bar{M}_n$ and $\bar{M}_w$ values were higher than both corresponding theoretical and SEC determinations, while the exact opposite was found for the higher molecular weight samples. In addition, the two entities were also very similar in relation to each other.

Results and Discussion

Table 4. Comparison of the values obtained from the different techniques used for the molecular weight determination of the PA-PG polyester samples for the most basic ideal structure of HO-[PA-PG]$_n$-H.

Sample	n values for HO-[PA-PG]$_n$-H	$\bar{M}_{n \text{ (calc.)}}$ (g/mol)	$\bar{M}_{n \text{ (SEC)}}$ (g/mol)	$\bar{M}_{w \text{ (SEC)}}$ (g/mol)	$\bar{M}_{n \text{ (MALDI-TOF)}}$ (Da)	$\bar{M}_{w \text{ (MALDI-TOF)}}$ (Da)
s23	1	224	135	216	662	681
s24	2	430	184	464	644	666
s25	3	636	283	837	671	705
s26	4	842	553	1470	787	868
s27	7	1460	530	1450	784	865
s28	8	1666	569	1520	803	888

Table 5. Comparison of the values obtained from the different techniques used for the molecular weight determination of the MA-PG polyester samples for the most basic ideal structure of HO-[MA-PG]$_n$-H.

Sample	n values for HO-[MA-PG]$_n$-H	$\bar{M}_{n \text{ (calc.)}}$ (g/mol)	$\bar{M}_{n \text{ (SEC)}}$ (g/mol)	$\bar{M}_{w \text{ (SEC)}}$ (g/mol)	$\bar{M}_{n \text{ (MALDI-TOF)}}$ (Da)	$\bar{M}_{w \text{ (MALDI-TOF)}}$ (Da)
s11	1	174	180	295	618	631
s12	2	330	266	582	619	638
s13	3	486	383	897	650	689
s14	4	642	668	1470	770	862
s15	7	1110	823	1790	833	954
s16	8	1266	871	1950	849	977

In conclusion, the mass spectrometry clearly indicated that several peak distributions of the same repeating unit value are present but with different endgroup combinations as well as different structural conformations (shown by the red and black peak labels in Figure 11). Since it has been shown that for aliphatic polyesters conventional SEC has a tendency to overestimate $\bar{M}_n$ values and underestimate $\bar{M}_w$ values[15, 37], MALDI-TOF MS was employed to further investigate the absolute molecular weight distribution of each of the

Results and Discussion

bulk samples, differences in structural conformation and endgroup functionality of the polyester samples for both batches. The related results are presented and discussed in Part III section 3.

2.2 Interaction chromatography for the chemical composition analysis

Despite the separation limitations observed during the SEC analysis, the results provided valuable qualitative information regarding the complexity of the polyester chains produced during the various stages of the polyesterification reaction. In order to investigate the extent of the heterogeneous nature of the chemical composition distribution, several interaction LC methodologies were attempted utilizing different mobile and stationary phases of varying polarity. The initial strategy involved isocratic chromatography analysis in both normal and reversed-phase conditions, however, despite the fact that the molecular weight of the polyester chains were oligomeric in size, the different species were either too strongly retained on the stationary phase without the incentive of being sufficiently separated or were not separated at all. Figure 13 shows examples of the chromatographic conditions used during the current study in attempts to achieve separation based on composition and/or functionality. In all cases, a flow rate of 1ml/min was applied, the injection volume was 20µl, the sample concentrations varied between 5.0 to 10.0 mg/ml and analyses were conducted at 30°C, with ELS and/or UV as detectors. In order to achieve separation based on the composition of the backbone of the polyester or on the possible endgroup combinations, the polarity of the samples, their solubility in a particular mobile phase composition and their interaction with the stationary phase had to be considered.
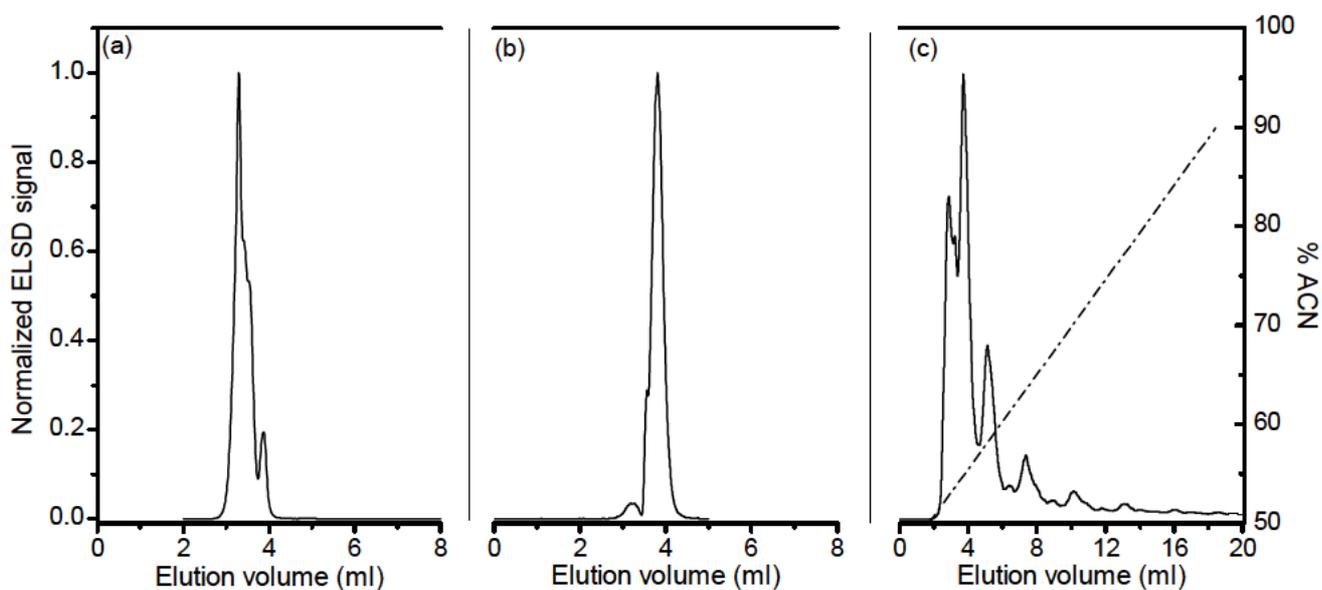
Figure 13. Examples of the various interaction LC separations achieved during the method development of the polyester samples. The chromatographic conditions were as follows: (a) For a MA-PG sample; Stationary phase: Si 100Å, 5µm, 250 x 4.6mm I.D Mobile phase: 80% THF/ 20% DCM (b) For a PA-PG sample; Stationary phase: CN 100Å 5µm, 250 x 4.6mm I.D Mobile phase: 60%THF/ 40%Hex (c) For a MA-PG sample; Stationary phase: reversed-phase C18 100Å, 5µm, 250 x 4.6mm I.D Mobile phase: linear gradient from 50%ACN/ 50% water to 90% ACN/ 10% water in 20min

The potential applicability of gradient elution chromatography for polyester resins has been documented[68, 131, 147, 240-242] and in most cases, reversed phase systems were used although the possibility of normal phase gradient HPLC has also been published[243, 244]. Importantly, the preliminary results indicated that the elution

Results and Discussion

behavior of the PA-PG polyesters differed from that of the MA-PG batch to such an extent that no one stationary-mobile phase combination could be found that would allow sufficient separation for both. Naturally, it can be argued that this phenomenon would be obvious since their chemical compositions are inherently different, yet interestingly it was also found that varying the molar ratios of diol to diacids during the polyesterification with each type of polyester requires the development of entirely separate chromatographic conditions. Subsequently, due the variable success and unsatisfactory separations obtained from isocratic mobile phase compositions, gradient HPLC analysis was conducted on the respective phthalic and maleic anhydride polyester batches. Remaining within the scope of the current dissertation, the gradient HPLC results of the respective anhydride batches with PG in 30% molar excess will be reported.

2.2.1 Gradient elution HPLC of the PA-PG oligoester batch

Following the results obtained from the preliminary tests conducted on the traditional bare silica (normal phase) and C18-grafted silica (reversed phase) stationary phases, a cyano-functionalized silica column was selected for the gradient HPLC analysis of the phthalic anhydride-propylene glycol samples. The advantage of a CN-grafted phase is that it has intermediate polarity between the aforementioned two extremes and depending on the mobile phase composition selection it can exhibit both hydrophilic and hydrophobic properties[64]. The mobile phase composition consisted of THF-hexane and although several gradient profiles were tested, the best separation was obtained in the case of the step-gradient labeled nr.8 in Table 6.

Table 6. Gradient profiles used for the optimization of the gradient elution HPLC of the polyester batches with THF-hexane as mobile phase composition.

			Gradient Profiles				
Nr.3		**Nr.4**		**Nr.8**		**Nr.14**	
Time (min)	**% THF**	**Time (min)**	**% THF**	**Time (min)**	**%THF**	**Time**	**%THF**
0	0	0	0	0	0	0	0
2	0	2	0	2	0	2	0
12	100	3	20	5	20	3	5
15	100	5	20	7	20	6	5
16	100	6	40	10	40	7	10
20	0	8	40	12	40	10	10
-	-	9	60	15	60	11	15
-	-	11	60	17	60	14	15
-	-	12	80	20	80	15	20
-	-	14	80	22	80	18	20

Results and Discussion

-	-	15	100	25	100	19	25
-	-	19	100	30	100	22	25
-	-	20	0	-	-	23	30
-	-	-	-	-	-	26	30
-	-	-	-	-	-	27	35
-	-	-	-	-	-	30	35
-	-	-	-	-	-	31	40
-	-	-	-	-	-	34	40
-	-	-	-	-	-	40	100

Initially, linear gradients were followed to monitor the elution behaviour of the polyester sample with increasing percentage THF as good solvent. With gradient profile nr.3 as example, a PA-PG sample was injected in 100% hexane, after which a linear ramp was applied until 100% THF was reached. The mobile phase was then kept constant to allow the complete elution of the adsorbed species from the stationary phase, before the system was re-equilibrated back to the starting conditions. In general, a much improved result was obtained with the linear gradient methodology as compared to the isocratic conditions as the bulk sample was fractionated into several peaks, all eluting after the dead volume of the column in LAC mode. In an attempt to further optimize the analysis, steps were introduced into the solvent composition adjustment ramp to improve the retention selectivity (gradient profile nr.4). Finally, the gradient steepness was decreased to investigate whether baseline separation could be achieved. The corresponding elution profiles of the different gradient strategies for s28, the final sample in the PA-PG batch is shown in Figure 14.

Results and Discussion
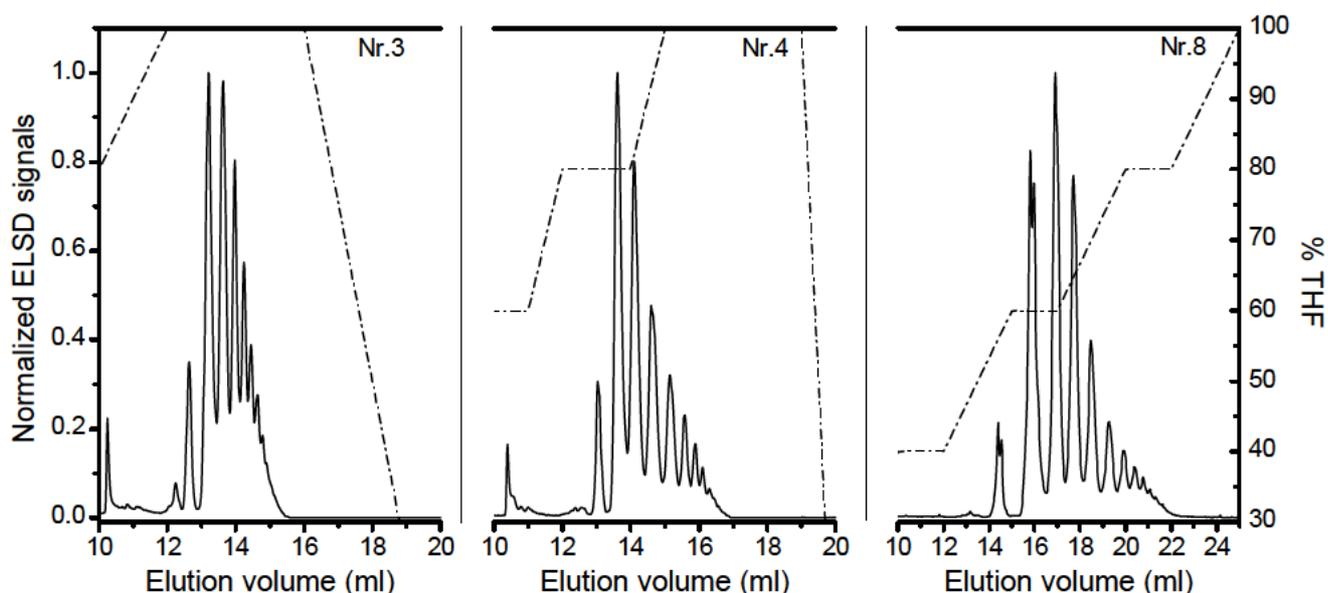
Figure 14. HPLC separations of s28 in the PA-PG batch under the different gradient elution profiles nr.3, nr.4 and nr.8 as given in Table 6. Stationary phase: CN 100Å 5μm, 250 x 4.6mm I.D Mobile phase: THF/hex, 1ml/min, 30°C.The sample concentration were 5mg/ml of which 20μl was injected

The incorporation of steps into the linear ramp had the desired effect, yet by slowing down the gradient only a small measure of selectivity was gained at the cost of longer analysis times. The early eluting peaks seemed to benefit the most from the gradient adjustment as they became more separated from each other, while at later elution volumes, the chromatogram indicated that there was still a portion of the sample distribution which was unable to separate sufficiently. The elution behaviour of sample s28 under gradient nr.8 is highlighted in Figure 15 which illustrates a magnification of the unresolved distribution as well as the occurrence of peak splitting in the early eluting peaks. Generally, the assumption would be that the separation would be governed more by the length of the oligoester backbone than by the endgroup functionality, as with increasing chain lengths the interaction with the stationary phase becomes stronger, thus leading to later retention times. Several authors have established, however, that during oligomeric separations different retention mechanisms can dominate depending on whether reversed- or normal phase LC is being conducted[245-249]. Differences in the mechanism and prediction of the retention of oligomeric species in the two phases was well summarized by P. Jandera[250]. Essentially, the study showed that in reversed-phase systems the separation selectivity is determined mainly by the size and polarity of the repeat unit unless the presence of bulky, polar and significantly different endgroups has to be taken into consideration, which in effect could have the order of elution reversed.

40

Results and Discussion
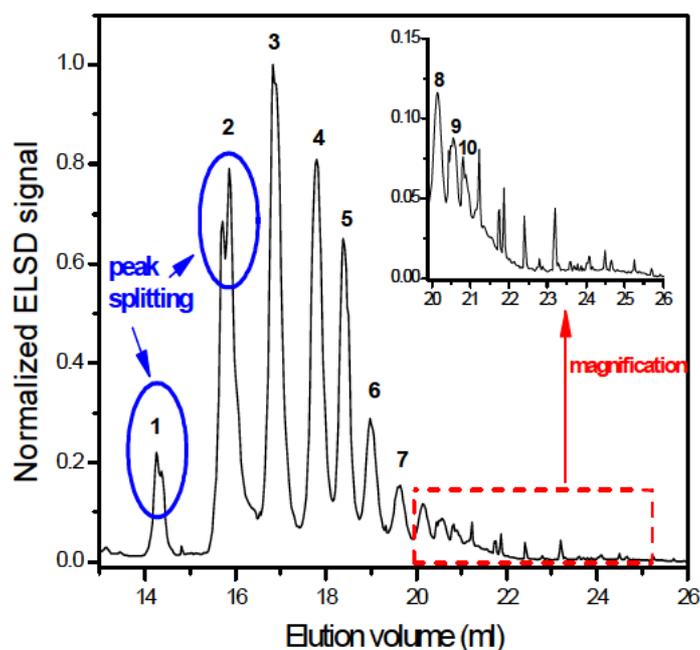
Figure 15. Gradient HPLC chromatogram of sample s28 of the PA-PG polyester, illustrating the peak splitting behaviour as well as the extent of the separation achieved with the zoomed part of the elution volume 20 to 26 ml. The gradient conditions are according to gradient profile nr.8 as given in Table 6. Stationary phase: CN 100Å 5μm, 250 x 4.6mm I.D Mobile phase: THF /Hex, 1ml/min, 30°C.

The currently employed polar-bonded CN-silica stationary phase in conjunction with THF as polar modifier for the gradient HPLC separation of the PA-PG polyester is, however, classified as a normal-phase LC system[251]. Consequently, the separation selectivity is dependent on the adsorption energy, the adsorbed area and nature of the oligomeric unit as well as the concentration and polarity of the polar solvent in the mobile phase. During the PA-PG gradient elution HPLC analysis it was found that the injected sample required at least 2 minutes of residence time on the column under non-solvent conditions to ensure sufficient alignment and/or interaction of the chains of different lengths with the active sites available on the packing material. The subsequent increasing concentration of polar solvent (THF) enabled the stepwise manner of elution of oligomers sharing similarities in chemical composition and/or endgroups, most likely via re-dissolution. The peak splitting of the early eluting peaks might suggest that separation is not exclusively with regards to molecular weight, chemical composition or functionality type distribution but rather that co-elution of chains with the same degree of oligomerization yet differences in structural conformation might occur. As the number of repeating units increases, however, the chain length distribution start to dominate meaning that these differences become increasingly negligible[252]. It was also noted that while this specific gradient profile allowed ample time for the system to be running under 100% THF conditions before re-conditioning, no later eluting species were detected after 26ml elution volume. Interestingly, sample recovery tests based on sample 28 indicated that approximately 77-80% of the injected sample mass was recovered. Five different injection volumes, ranging from 5-25μl were conducted under gradient conditions with and without the stationary phase. The obtained peak areas were integrated, compared with each other and the results were reproducible, with deviations starting to occur at injection volumes larger than 20μl, indicating along with band broadening possible overloading of the column. In order to investigate whether the remainder of the sample was irreversibly adsorbed onto the column, the same methodology was conducted as discussed by Beadoin et al[253]. By injecting a blank solution of 100% THF, the solubility-enhancing organic modifier acts

41

Results and Discussion

as a displacer to disrupt the strong interactions which occur between the repeating unit and the stationary phase and further promote dissolution of the adsorbed molecules[249]. It was found that with the pure THF injection, the trapped chains eluted from the column, which constituted the rest of the original sample concentration injected. Although baseline separation could not be achieved, gradient profile nr.8 was chosen as the best compromise to further analyze the rest of the samples in the PA-PG polyester batch. The results of samples s23, s25 and s28 in Figure 16 are representative of the different stages of the polyesterification reaction.
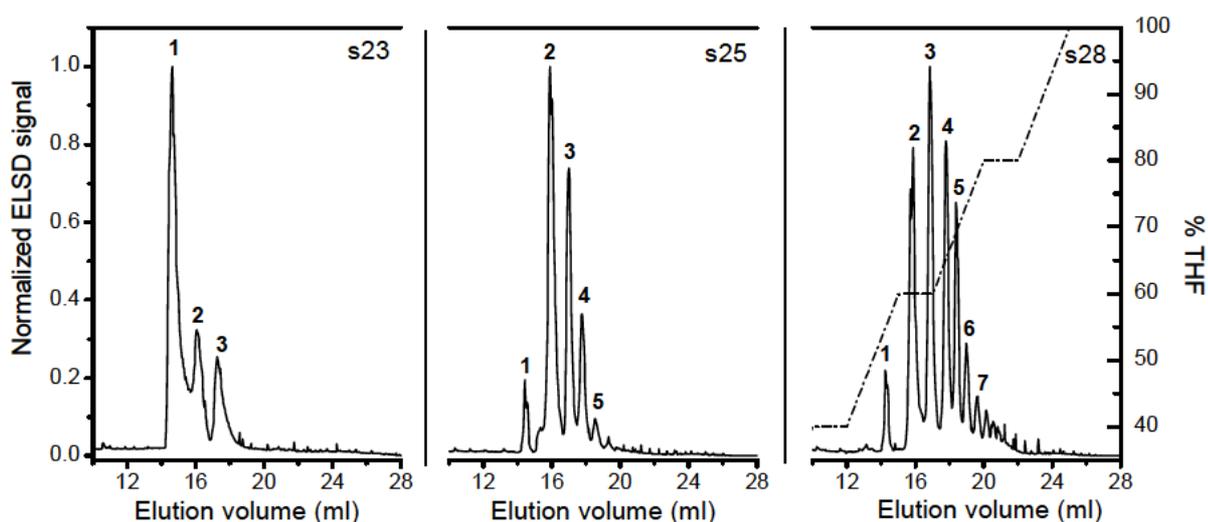
Figure 16. Gradient HPLC chromatograms for samples of the PA-PG batch illustrating the development of different species during the polyesterification reaction. Sample details are given in Table 2 and the gradient conditions are according to gradient profile nr.8 as given in Table 6. Stationary phase: CN 100Å 5μm, 250 x 4.6mm I.D Mobile phase: THF /Hex, 1ml/min, 30°C.

The three peaks found in the chromatogram of s23 appear in both of the subsequent samples, along with the addition of new distributions which indicate the possible formation of larger molecular weight oligoesters or the formation of chains consisting of increasingly different chemical compositions. More importantly, the evolution of the different species could clearly be followed and the results reflect, although again in qualitative fashion, how the complexity of the polymer increases during the esterification reaction. In addition, as to be expected from step-wise polymerization, it is clear that the species formed at the early stages of the polyesterification reaction, participate in the formation of higher species but they are never completely consumed in the process. The chromatograms show that when targeting species of higher molecular weight, the presence of the lower species is not negligible and should be accounted for in terms of the properties of the final resin product.

2.2.2 Gradient elution HPLC of the MA-PG oligoester batch

A similar methodology as in the previous section was followed to obtain optimized gradient elution conditions for the analysis of the MA-PG samples. Considering that the majority of research studies available on LC characterization of aliphatic polyesters made use of binary and ternary mobile phases consisting of water as non-solvent and acetonitrile, THF and/or methanol as good solvent combinations[31, 38, 249], their application for the purpose of the current investigation proved unsuccessful. Although reversed- phase LC mode was found to be better suited for the MA-PG samples, the resulting separations showed poor reproducibility, long

Results and Discussion

retention times and weak selectivity. Due to the more hydrophobic nature of the C18-grafted packing material compared to that of the CN-functionalized stationary phase used previously, the interaction between the oligoester and the stationary phase was increased. Even though the employment of very polar mobile phases as good solvent ensured the displacement of the chains from the stationary phase, the solubility of the maleic anhydride-propylene glycol polyesters in these solvents had to be considered which limited the choice of mobile phase compositions. Therefore, the same solvent combination as used for the PA-PG batch (THF/hexane) was investigated and the gradient profile was adjusted in order to achieve the results illustrated in Figure 17.
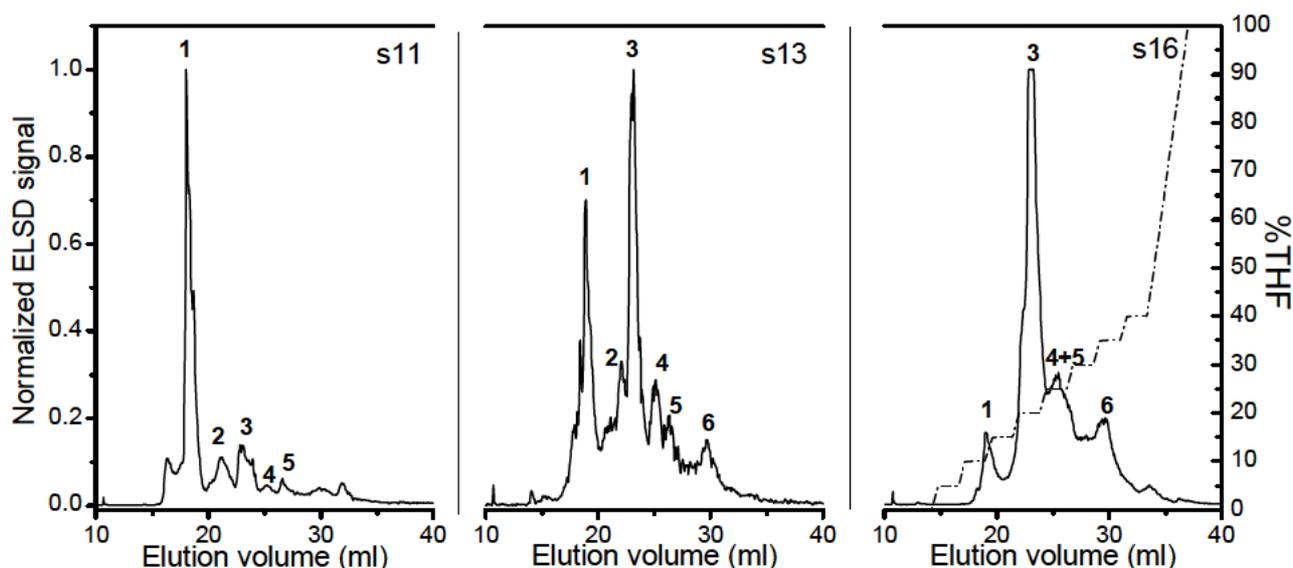
Figure 17. Gradient HPLC chromatograms for samples of the MA-PG batch illustrating the development of different species during the polyesterification reaction. Sample details are in Table 3 and the gradient conditions are in accordance to gradient profile nr.14 in Table 6. Stationary phase: C18 100Å 5μm, 250 x 4.6mm I.D Mobile phase: THF /Hex, 1ml/min, 30ᵒC.

The chromatograms of samples s11, s13 and s16 represent different stages during the MA-PG polyesterification reaction. The additional side-reactions afforded by the involvement of maleic anhydride results in a highly complex system with chains of several functionalities and/or chemical composition distributions being formed from the beginning of the reaction. This is clearly illustrated in chromatogram s11, where several peaks are present although not very well resolved. Interestingly, species 1 to 5 is also present in s13 as well as s16, yet it seems that as the molecular weight distribution presumably increases, the separation selectivity decreases. The existing differences between the chains, whether they are based on polarity, functionality or molecular weight become less defined which in turn result in the inefficient separation between peaks of the different sample constituents. The gradient elution separation remained far from ideal since in the current mobile phase-stationary phase combination the solvent-solute interaction is more likely to dominate over the solute-stationary phase interaction. This was supported by the sample recovery investigations which showed that a much higher percentage, 95% of the sample is being eluted from the column during gradient profile nr.14 (Table 4). In contrast to the PA-PG results, the chromatograms for all three samples taken at various stages of the esterification reaction spanned over approximately the same elution volume, suggesting that the principle of separation is not as well defined and that the elution behaviour is influenced by several factors. Moreover, it shed light on the differences obtained between the

43

Results and Discussion

two polyester batches in terms of heterogeneity and the additional complexity of the MA-PG model over that of the PA-PG system in that achieving efficient separation proved to be more challenging.

2.3 Hyphenation of the LC-separation techniques: On-line 2D chromatography of the final samples of the respective PA-PG and MA-PG model polyester batches

Given that both SEC and interaction LC techniques employed for the investigation of the two inherently different polyesters indicated the existence of a multifaceted system, the need to characterize the multiple distributions independently, yet simultaneously was recognized. As a result, instead of using a single separation method, the different modes of chromatography were combined in order to determine the different aspects of the molecular heterogeneity contained in the final polyester product. The following section entails the "comprehensive" two-dimensional chromatography analysis of the last samples in the PA-PG (s28) and MA-PG (s16) batches in order to investigate the relationship between the chemical composition and molecular weight distributions via the on-line coupling of the gradient elution HPLC with SEC. For each of the samples, the optimized gradient elution HPLC conditions obtained in the previous section were used as the first dimension separation in order to obtain isolated, more homogenous fractions ideally based on their chemical composition which were then transferred to the second dimension where SEC permitted the separation of each by hydrodynamic volume.

For the first dimension separation, the CN 100Å (5µm, 250 x 4.6mm I.D) stationary phase was used for s28 in the PA-PG batch, while the C18 100Å (5µm, 250 x 4.6mm I.D) was employed as the stationary phase for s16 in the MA-PG batch. For both samples, the mobile phase composition was THF/Hex and the analysis temperature 30°C. In addition, the sample concentration was kept at 5mg/ml, while the injection volume was increased to 100µl. Several variations of sample concentrations and injection volumes were tested, with the aforementioned values allowing the best reproducibility. The second dimension SEC separation was conducted on a PL-Rapide L (100 x 10mm I.D.) stationary phase and the flow rate was set to 4ml/min. ELSD detection was used. To facilitate the best possible automated coupling system, the second dimension analysis time and loop volume had to be taken into account to recalculate the flow rate in the first dimension. Therefore, in order to fill one 100µl loop in the time required to complete the SEC analysis of a single fraction, the flow rate had to be decreased to 0.05ml/min. Consequently, the gradient profiles of nr.8 and 14 had to be re-calculated so that the mobile phase changes could be adjusted to the lower flow rate, which in turn led to much longer analysis times. The 2D contour plots of s28 (**A**) and s16 (**B**) are presented in Figure 18, with each plot showing the separation based on chemical composition vs. the separation based on hydrodynamic volume. The first 2D separation in each plot is the linear color distribution while the second is the logarithmic response, the difference being a marked increase in intensity whereby species of smaller concentration can be detected. The colour scale bar on the right hand side indicates the signal intensity, which is related to the concentration of chains present at a specific elution volume.

The 2D results illustrated several dissimilarities between the samples. The most important was the clear contrast in separation efficiency occurring during the gradient HPLC dimension. For the PA-PG sample s28 in plot **A**, several entities could be distinguished, each of which proved to have a concurrent molecular weight dependence. As the oligoesters comprising distinct chemical composition distributions experience

44

Results and Discussion

different molecular interactions with the stationary phase, once they are transferred to the SEC second dimension, they appear to elute at increasingly shorter times, thus having an increase in molecular weight distribution. Furthermore, a clear indication of overlapping effects of size and functionality can be seen as co-elution of species with similar molecular weights in the SEC dimension, yet different chemical composition in the LAC dimension, is illustrated.
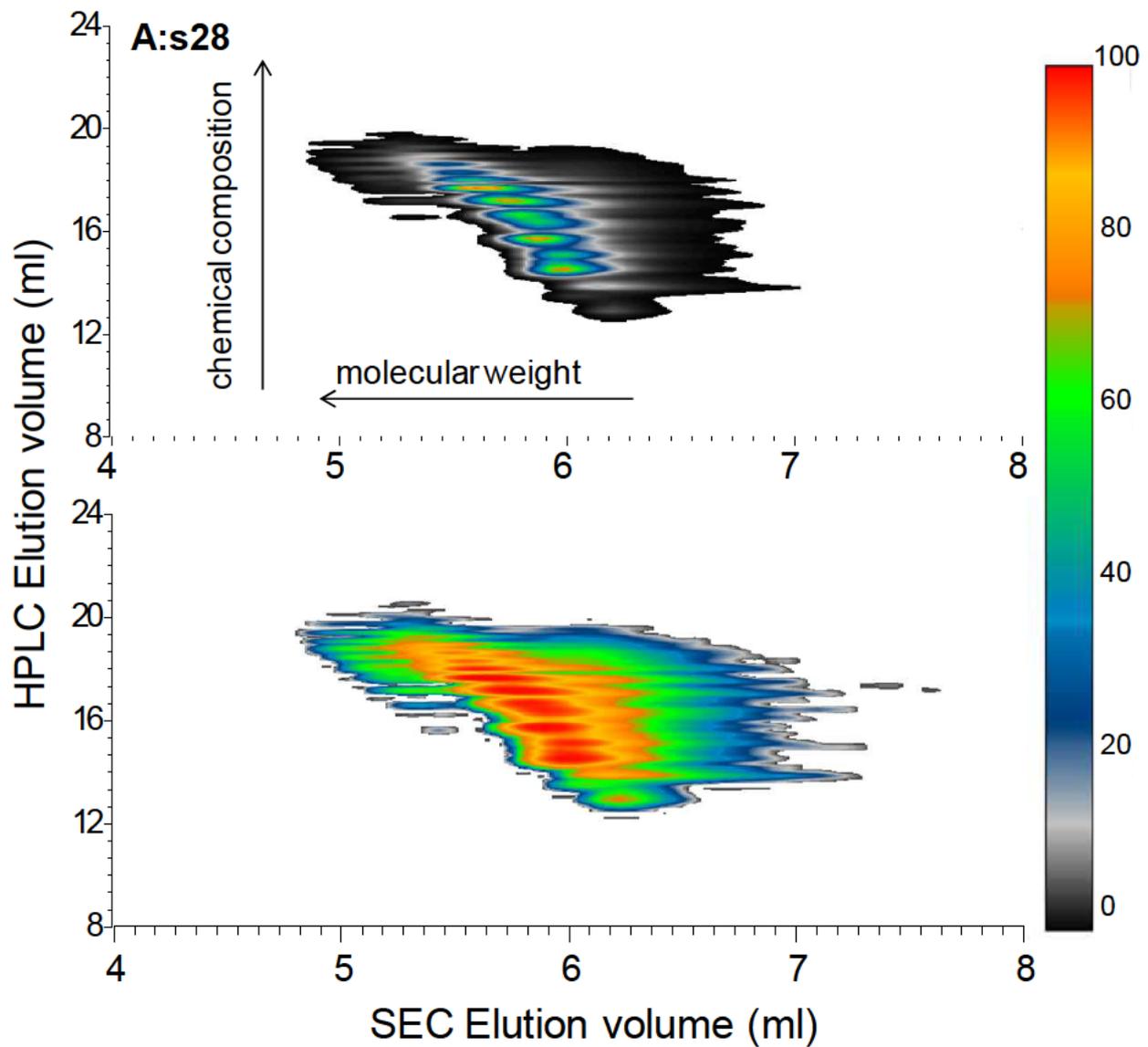
Results and Discussion
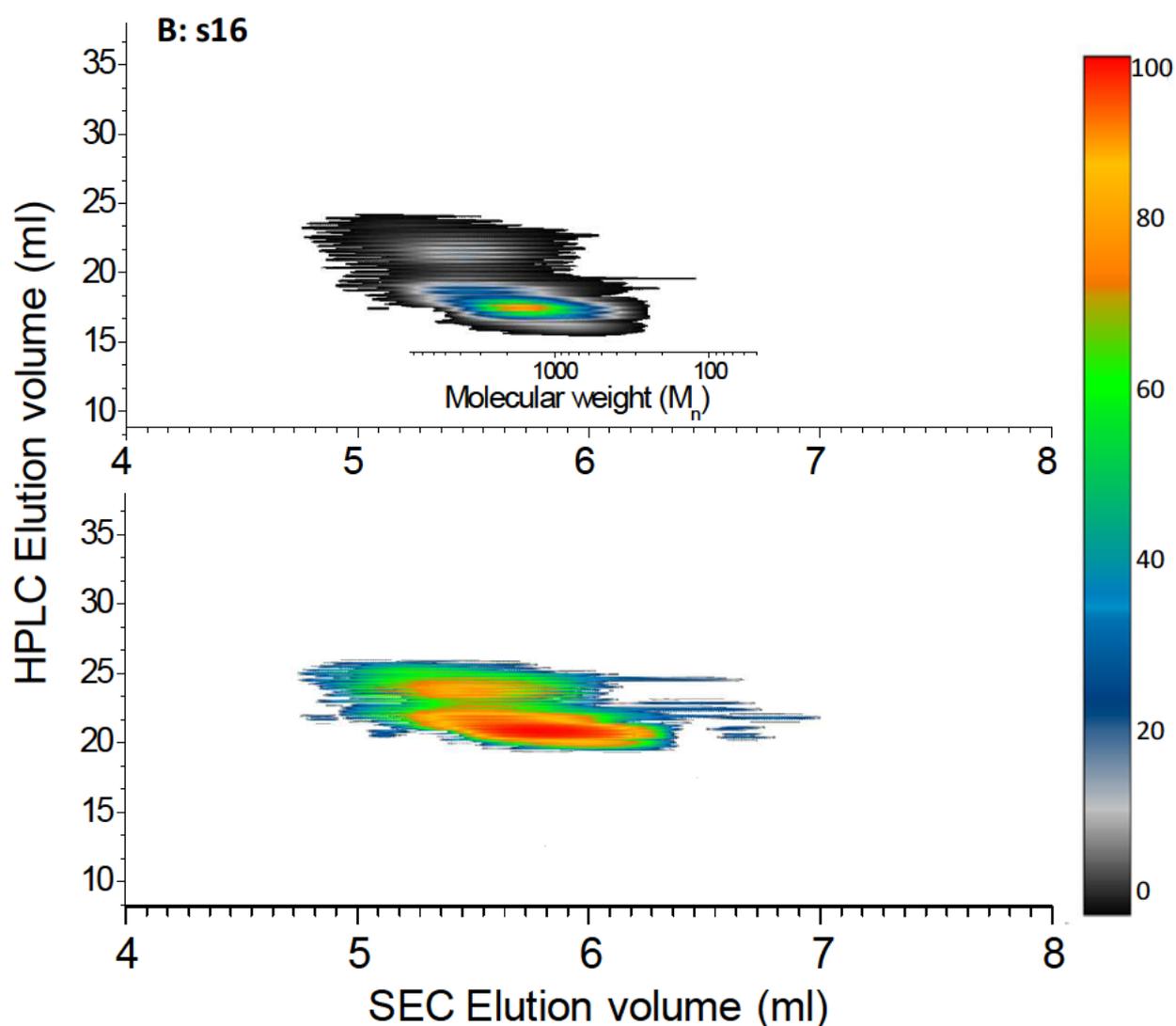
Figure 18. (A) 2D contour plot of sample s28 in the PA-PG batch. (B) 2D contour plot of sample s16 in the MA-PG batch. Much higher plot intensities are found in the logarithmic colour presentation.

The elution behaviour strongly points towards the gradient HPLC conditions enforcing a separation where the different peaks or species are eluting in the order of increasing chemical composition and perhaps increasing degree of oligomerization. The lack of separation found in contour plot **B** of sample s16 in the MA-PG batch serves as confirmation that the employed gradient conditions fell short in producing a sufficient separation based on chemical composition. Considering the diverse reactions taking place during MA-PG synthesis, the possibility of a large number of randomized, poorly defined distributions does exist. If so, finding optimized HPLC conditions to successfully conduct a separation based on an isolated parameter is an extremely difficult task. Based on the signal intensity values, the MA-PG sample roughly identified two large entities having slightly different molecular weight distributions in the second dimension. Of the two, only one had considerable concentration, indicating that the bulk fraction of the sample remained unresolved. Upon closer investigation, both appeared to consist of smaller fractions having seemingly similar elution behaviour to their neighboring peaks in the first dimension. Although not as pronounced as in the PA-PG

Results and Discussion

sample, the elution profile, therefore, does indicate that the sample was somewhat separated by slight differences in chemical composition.

One similarity found between the two polyesters was that, the second dimension elution volumes appeared to be quite similar. In accordance to standard procedure, an attempt was made to conduct a second dimension calibration based on polystyrene standards. However, both polyesters proved to be more favorable towards the lower molecular weight end, which was in close proximity to the permeation limits of the stationary phase, making a sensible calibration difficult. For this reason, in 2D-LC, quantification of synthetic materials which are oligomeric in size continues to be a challenge. The PL-Rapide L (100 x 10mm I.D.) was specifically selected as stationary phase, as it is has a suitable particle size and pore range required for lower molecular weight species as well as being able to deal with the high pressures experienced from high flow rates in 2D-LC. Considering that for each polyester batch, 2D-LC was conducted on the final sample in the series set, it was interesting that in each case molecular weights corresponding with starting materials could still be identified. Both polyester samples appeared to have molecular weight ranging between 100 and 3000 g/mol in the second dimension, which corresponded well with the SEC analysis conducted previously on the bulk samples.

Following the success of sample s28, the other two samples, s23 and s25 from the PA-PG batch shown earlier in Figure 16, were also analyzed. The resulting contour plots given in Figure 19 made it possible to follow the two-dimensional evolution of the PA-PG batch at different stages of the synthesis reaction. For the purpose of having a visual confirmation of the different distributions present in each of the samples, the contour plot of sample s28 is also included. Sample s23 indicated that the three peaks identified at the beginning stages of the polyesterification in section 2.2.1, were essentially lower species having different chemical composition distributions, yet similar molecular weight. The contour plot resembled the one-dimensional analysis in that peak **1** had the highest concentration, followed by much smaller concentrations of peak **2** and **3**. Changes in the sample composition distribution with esterification became evident in sample s25, where in addition to a clear shift in molecular weight towards slightly higher values for all the peaks, the presence of additional peaks could also be seen.

Results and Discussion
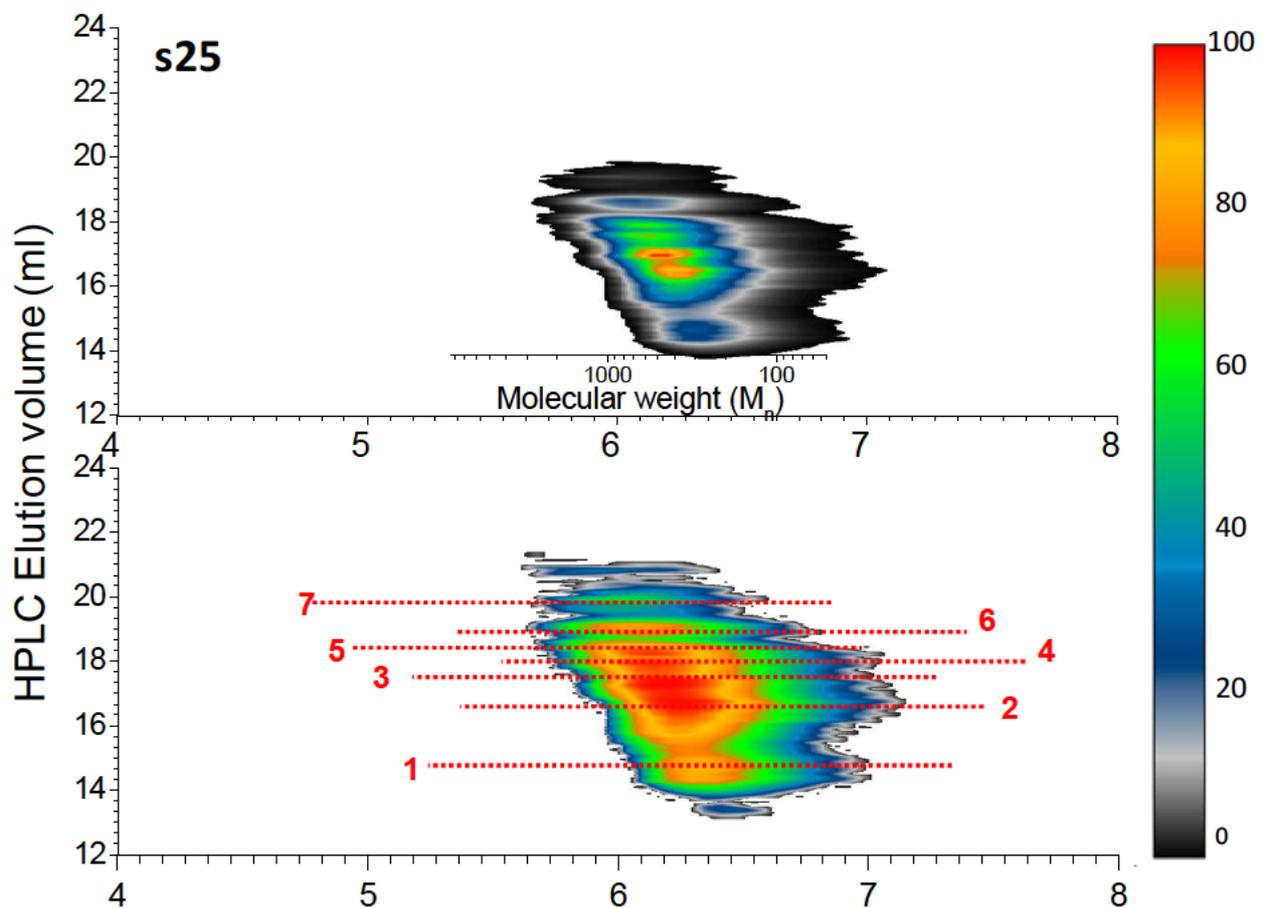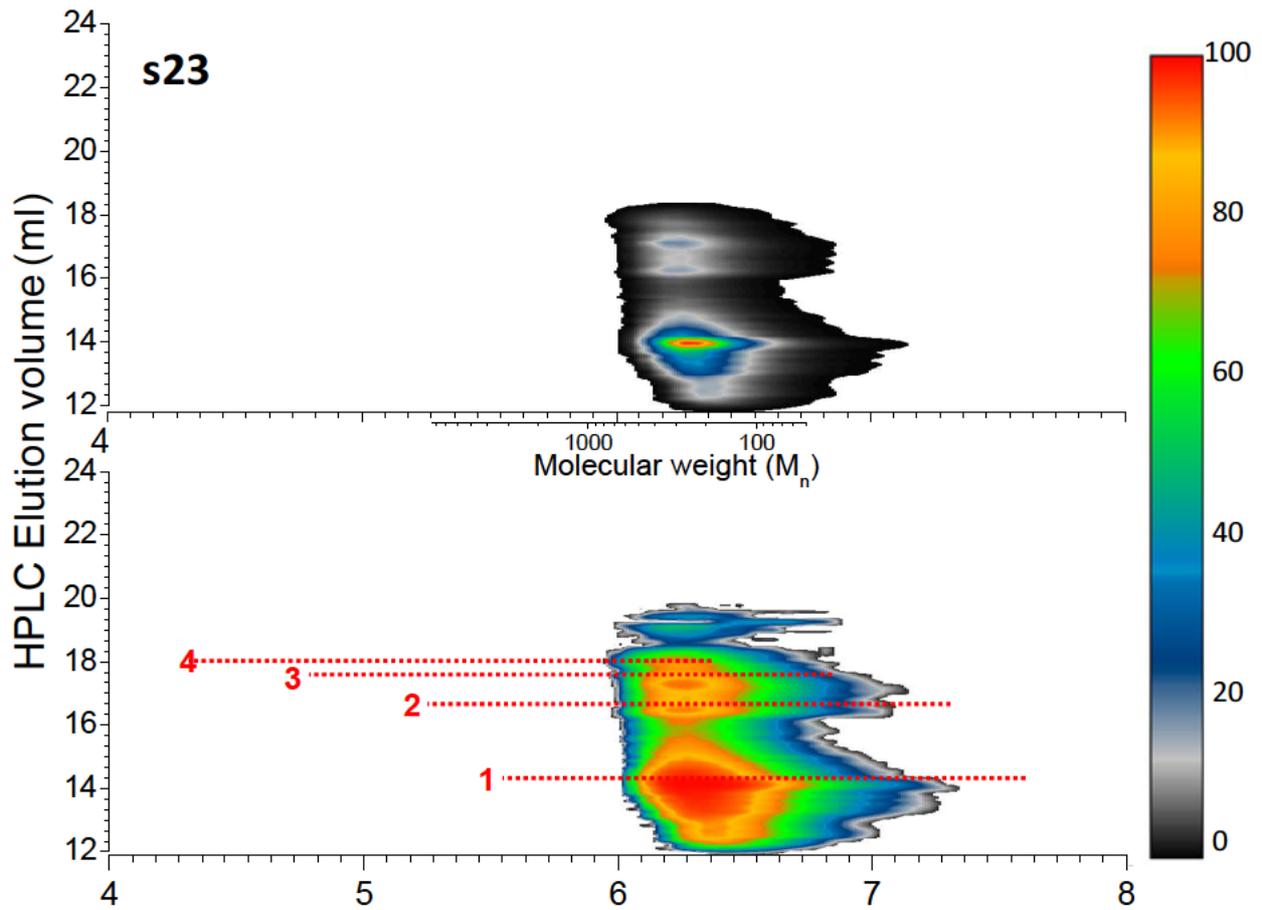
Results and Discussion
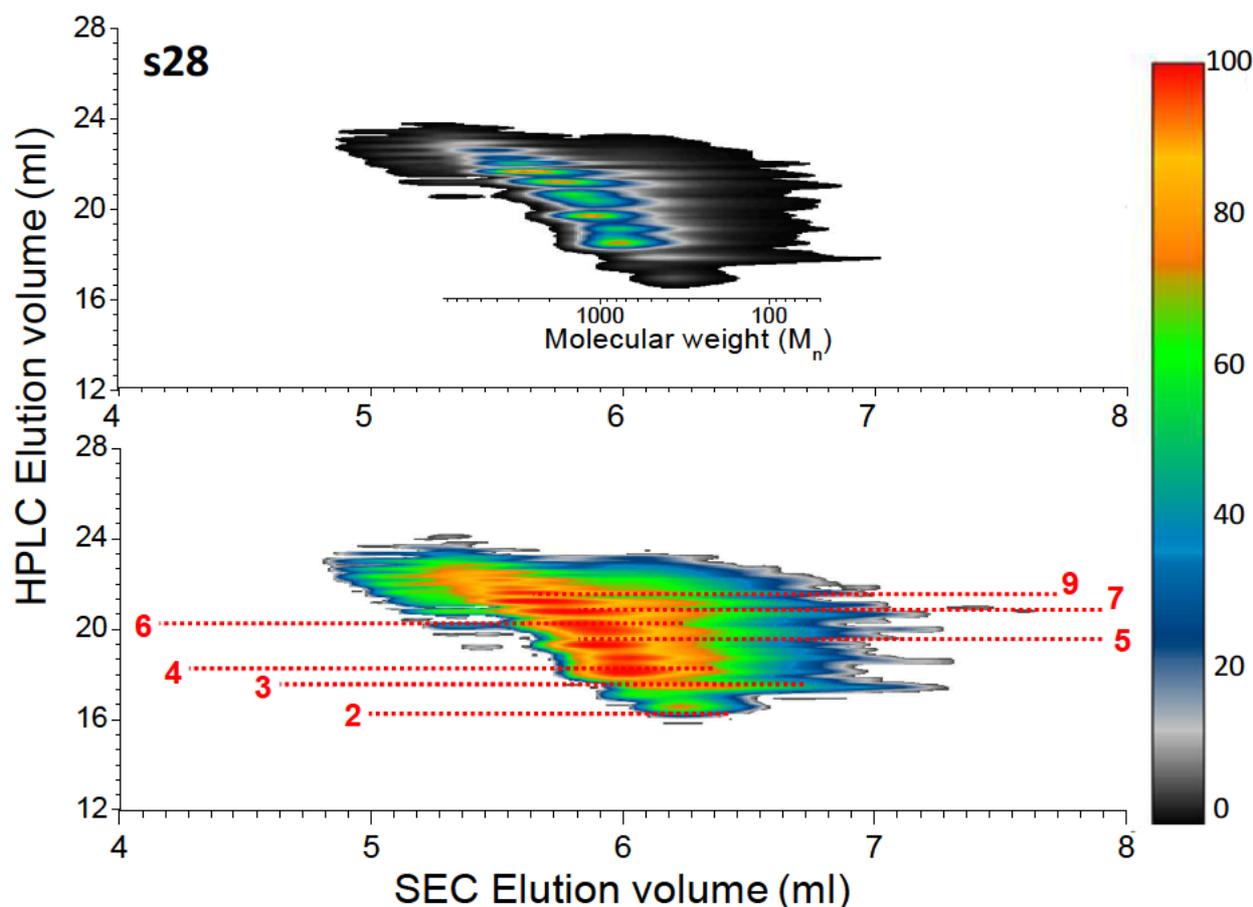
Figure 19. 2D contour plots of sample s23, s25 and s28 in the PA-PG batch. The numbers shown are peaks associated with the one dimensional gradient HPLC analysis conducted previously (section 2.2.1). In all cases the sample concentration was 5mg/ml, with an injection volume of 100µl at a flow rate of 0.05ml/min

These events were repeated, effectively producing the array of chemical composition distribution in relation with molecular weight obtained in the contour plot of sample s28. More importantly, the splitting pattern exhibited for peaks **2** to **4** in the contour plots of samples s25 and s28 are further evidence in support of the peak splitting theory discussed previously for the one dimensional analysis. These particular peaks indicate the formation of species sharing similarities in chemical composition distributions with regards to chain lengths but might be different in structural conformation. Furthermore, the peak numbers **1** to **9** in all three two-dimensional contour plots correlate well with the peak separations found in both the original one-dimensional investigations. Consequently, the 2D-LC of the three samples representing different stages of the PA-PG polyesterification reaction confirms that with increasing degree of polymerization, the chemical composition distribution escalate. Essentially, the hyphenation of the two LC techniques provided verification that the driving force behind the HPLC separation was based on chemical composition with increasing molecular weight distribution. It also emphasized the difference in complexity between the PA-PG and MA-PG polyester batches suggested by the results obtained in the individual analyses. The characterization of the phthalic anhydride batch by means of LC was significantly more successful over that of the maleic anhydride based polyester.

Results and Discussion

3. Method Development of Mass Spectrometry Techniques

3.1 MALDI-TOF MS of the PA-PG and MA-PG based polyesters

Over the past two decades the application of mass spectrometry for polymer characterization has experienced tremendous growth due to its versatility, relative ease of operation and the wealth of information that can be acquired in the process[192, 198, 200-202]. For MALDI-TOF MS in specific, numerous examples exist in literature involving the technique either as a core investigative method or as compliment to more traditional analytical approaches such as NMR, SEC and HPLC. In review, MALDI-TOF MS has the added advantage of, besides providing information regarding molecular weight distribution; it also facilitates the determination of repeat units, endgroup information of homo-, copolymers and synthetic blends. Furthermore, it can be employed to distinguish between linear and cyclic counterparts[254, 255] as well as assist in in-depth studies regarding reaction mechanisms, kinetics and degradation[197, 231, 256, 257]. These principles form the foundation behind employing MALDI-TOF MS as complimentary characterization technique for the polyester samples currently under investigation. Due to the influential role that several variables play during MALDI-TOF analysis, method development is critical to ensure optimized, reproducible results. Although the experiment would be dominated by the strategy of sample preparation, the core importance lies in the choice of solvents, matrix and the need for additional cationizing agents. Several reports are available on the characterization of polyesters and derived materials, indicating that a variety of matrix-solvent-cationizing agent combinations are possible in order to complete successful analyses[193, 233, 258-260]. To avoid inhomogeneous co-crystallization of the matrix, sample material and salt during sample deposition before analysis, the polarity of the matrix should closely match that of the sample under investigation[261] to ensure that solubility of both components in a selected solvent is equally matched[262]. In the present study, several combinations of matrices, with and/or without the addition of cationizing agents were attempted, which effectively lead to different sample preparation conditions for the PA-PG and MA-PG polyesters to facilitate optimized results. For the phthalic anhydride based polyesters, the samples were dissolved in THF (4mg/ml) while the matrix (dithranol) was dissolved in dioxane (10mg/ml). The addition of a cationizing agent was deemed to be unnecessary as ionization appeared to occur readily for these particular polyester samples. The sample preparation procedure for the maleic anhydride-propylene glycol polyesters differed in the sense that even in the absence of a matrix the oligomers appeared to experience sufficient ionization to be able to move down the TOF tube. Yet to ensure enough stability for the ions to be detected, a cationizing agent (LiCl) was added to the droplet mixture. The abovementioned variations were carried out in order to obtain spectra that did not consist of too many overlapping adduct ions which in turn would lead to complications in terms of making sensible assignments. For the preparation of each polyester type, the two solutions were combined and deposited onto the sample target plate via the "dried droplet" method. Positive ion spectra were obtained for all the polyesters.

A similar approach was taken as in the SEC analysis by attempting to investigate the molecular weight characteristics of each of the kinetic samples within a batch, how the spectra and m/z values obtained compare from sample to sample and their relation to the SEC results found previously. In both PA-PG and MA-PG batches a clear increase in molecular weight was found for the kinetic samples given in Tables 2 and

Results and Discussion

3 (Part III. section 2.1). The MALDI-TOF mass spectrometry of samples s23 to s28 of the PA-PG polyester batch is shown in Figure 20. Even though there was a discrepancy in the values obtained from the two different analysis techniques, the evolution of molecular weight and molecular weight distribution from sample to sample corresponded well to the SEC results obtained earlier. As expected from condensation polymers, highly dispersed, fairly unsymmetrical oligomer distributions were found, increasing steadily from the first (s23) to the last sample (s28).
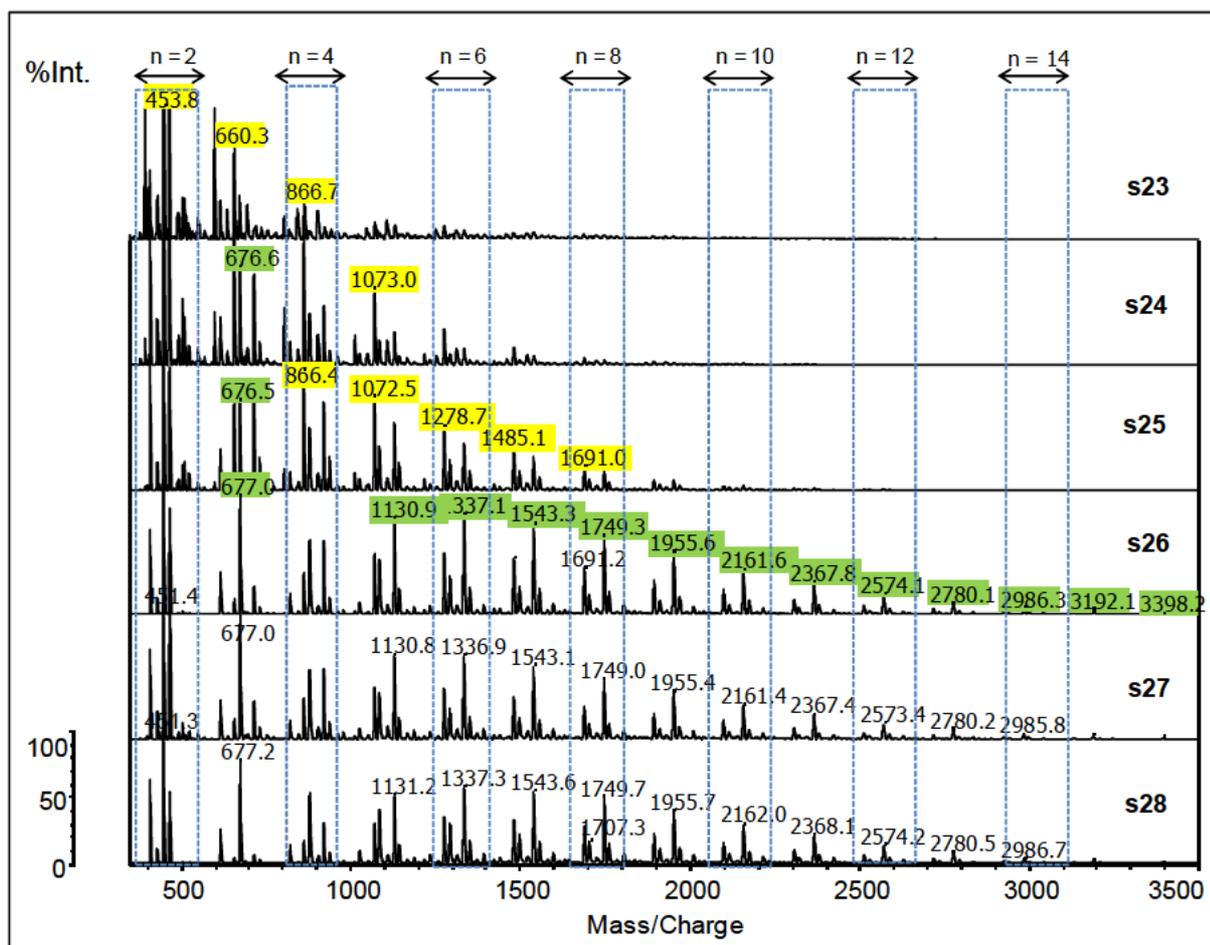
Figure 20. MALDI-TOF spectra of the kinetic samples s23 to s28 in the PA-PG batch, illustrating the development of molecular weight distribution of the oligoester species during the polyesterification reaction. The peak distributions marked yellow corresponds to Na+ adducts while the green is indicative of K+ related adducts of the same structure

The mass range below m/z 350 was dominated by matrix, starting material and metal-ion related peaks and above 3500 m/z peaks were absent. Another similarity to the SEC results was that the molecular weight distributions of the last three samples, s26 to s28 were found to be practically the same. The mass difference between adjacent peaks having similar cationization properties was approximately 206Da, which corresponds to the expectant repeating unit based on the proposed structure in Figure 9 (Part III. section 1). Following the deduction of the cation and the repeat unit mass n, structural elucidation was made from the combined terminal group mass calculation. The highest intensity peak in all the samples throughout the series was found at around m/z 453 which is due to the sodium cationized oligomer having the proposed structure of HO-[PA-PG]$_n$-H, where n = 2. The linear structure was present throughout the polyesterification reaction, reaching a value of up to at least n = 14 in sample s28, which corresponds to m/z 2514. In the last

Results and Discussion

sample s28, the intensity of this particular peak has decreased significantly with the simultaneous increase in the intensity of peaks representing other oligomeric species consisting potassium ionized adducts as well as different structural features. In being the most basic linear identity to be produced during the esterification reaction between the phthalic diacid and propylene diol present in the reaction mixture, the HO-[PA-PG]$_n$-H structure was expected and utilized in the subsequent assignment of the other possible endgroup combinations. A few samples from the PA-PG batch series were selected and a magnified part of the spectra in the range of m/z 580 to 1000 is presented in Figure 21.
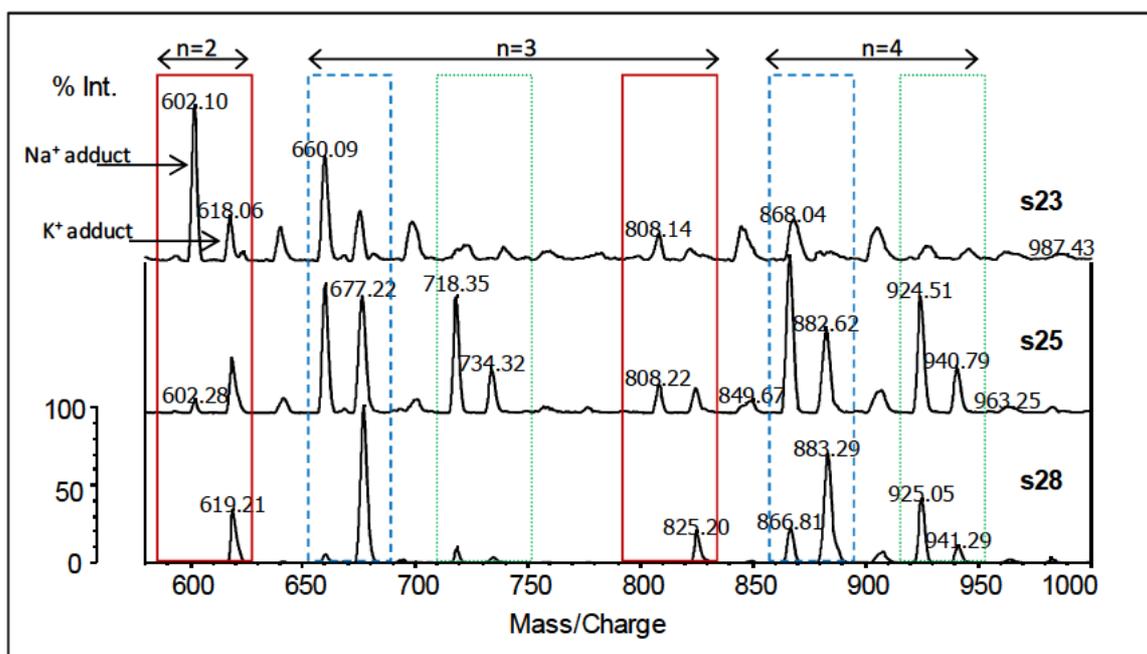
Figure 21. Magnified spectra in the range m/z 580 to 1000 of samples s23, s25 and s28. The differently formatted boxes indicate the different endgroup structures found: A. (—) HO-[PA-PG-]n-PA, B. (---) HO-[PA-PG]n-H and C. (…..) PG-[PA-PG]n-H. Cyclics of structures B and C were also found corresponding to m/z 640 and m/z 698

Two other linear structures corresponding to HO-[PA-PG]$_n$-PA and PG-[PA-PG]$_n$-H were identified. In addition, both a sodium and potassium adduct having a mass difference of 16Da was obtained for each structure. Interestingly, for the earlier samples, the intensity of the sodium adducts seem to dominate over that of the potassium counterparts but the trend appears to be the exact opposite for the later samples of higher molecular weight. Keeping in mind that no external cationizing agent was added during the sample preparation, it suggests that the higher oligomers could either have a preferred adduct formation during ionization with potassium over sodium or that due to their higher mass they have higher ion stability and therefore arrive at the detector in higher abundance. Based on peak intensity, the PG-[PA-PG]$_n$-H associated peaks dominate throughout the distribution of every sample and over the whole series. This agrees with the fact that the diol was added in 30% mole excess to the diacid. Furthermore, peaks at m/z 640 and m/z 689 indicated that cyclic products of [PA-PG]$_n$ and (PG-[PA-PG]$_n$) respectively can also be distinguished from their linear counterparts. An important feature in the PA-PG series is the decreasing intensity of the peaks related to the cyclic structures. At the start of the esterification reaction, these structures seemed to have equal importance compared to their linear counterparts but as the conversion of the polyesterification reaction increases, they account for a much smaller percentage of the structural heterogeneity present in the

Results and Discussion

polyester. A summary of all the proposed structures found along with their mass/charge values are given in Table 7.

Table 7. Proposed structures for the PA-PG polyester samples deduced from MALDI-TOF MS analysis. The m/z values correspond to the Na+ related adducts.

Chemical structure	Abbreviation	m/z$_{(exp)}$ values for n		
		2	**3**	**4**
A.	**HO-[PA-PG]$_n$-PA**	602	808	1014
B.	**HO-[PA-PG]$_n$-H**	453	660	866
C.	**PG-[PA-PG]$_n$-H**	512	718	924
D.	**cyclic of** **[PA-PG]$_n$**	434	640	847
E.	**cyclic of** **PG-[PA-PG]$_n$**	492	698	904
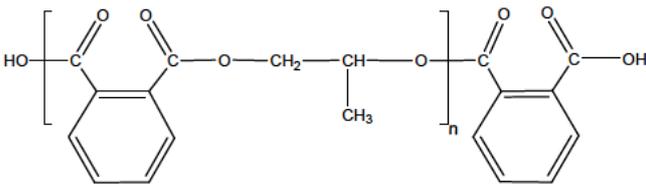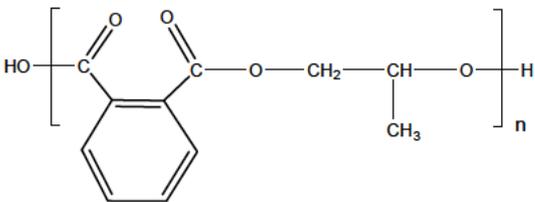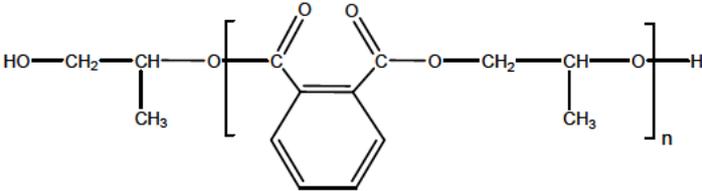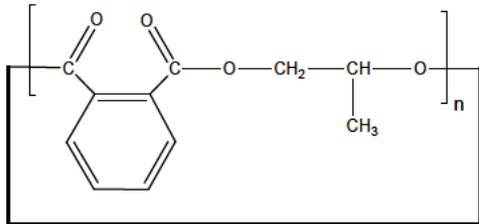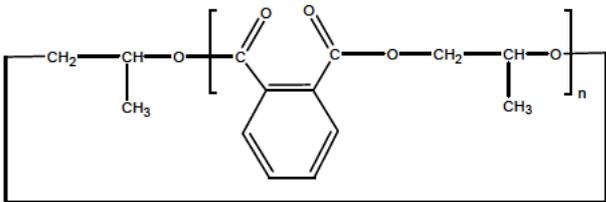
53

Results and Discussion

In general, the mass spectra of the MA-PG polyesters showed peaks of much less intensity that gave values of only up to m/z 2000. From the overlays of sample s11 to s16 compiled in Figure 22, the highest intensity peak was at m/z 239 which corresponds to the lithium cationized linear structure of PG-[MA-PG]$_n$-H where n = 1. Although, the absence of matrix molecules essentially led to extremely low ionization efficiency and thus weak resolution, it was the more positive trade-off as the MA-PG samples showed extensive matrix-adduct formation following its inclusion during the sample preparation procedure. In previous studies, Puglisi et al. found that different polymers could generate very different signal intensities, even though they exhibited similar molecular weight distributions and they theorized that the endgroups are a primary parameter in determining ionization efficiency[263]. Due to the excess diol during the polyesterification of both types of polyesters, the endgroup combinations produced should ideally be similar, thus any difference in ionization efficiency should be more closely related to the properties of the diacids in each case. It is, therefore, likely that higher molecular weight species are present in a similar fashion as in the previous batch.
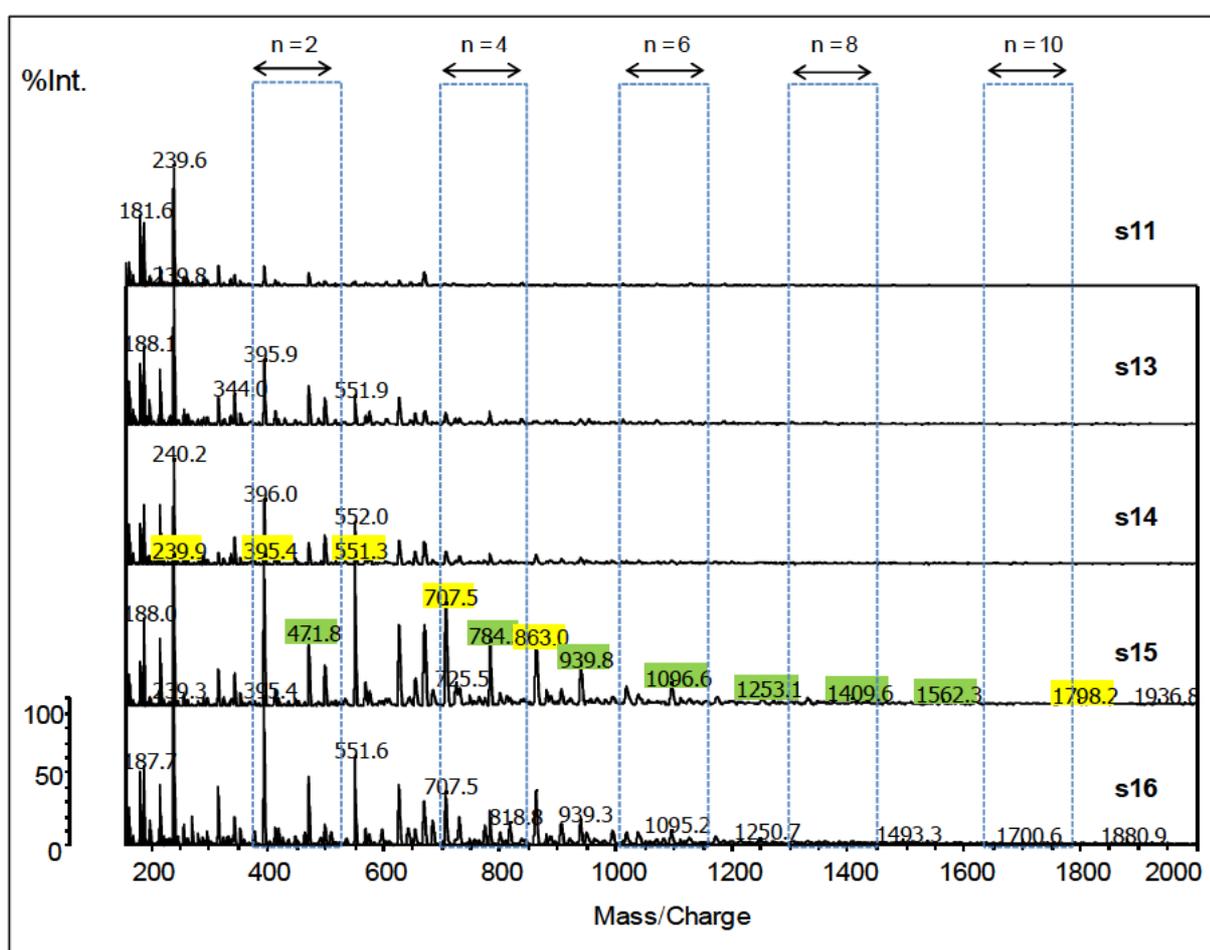

Figure 22. *MALDI-TOF spectra of the kinetic samples s11 to s16 in the MA-PG batch, illustrating the development of molecular weight distribution of the oligoester species during the polyesterification reaction. The distribution marked in yellow indicates the Li+ adduct of PG-[MA-PG]-H, while the green is H+ adduct of cyclic [MA-PG]n*

Although very little variation was found between the last three samples in the batch series again, the motivation behind the mass spectrometry analysis was shifted more towards chemical composition and endgroup identification, rather than molecular weight distribution trends. For most of the structures identified from the MALDI-TOF spectra, values of up to n = 5 were found. Due to the fact that LiCl was added as

Results and Discussion

cationizing agent the subsequent adducts had higher intensity than their protonated counterparts which is also accounted for at certain m/z values even though at extremely low intensities. The results of samples representing the onset, middle stages and end of the MA-PG polyesterification reaction is presented in Figure 23. Due to the 30% molar excess of propylene glycol, a second linear structure of HO-[MA-PG]$_n$-H (m/z 499 and m/z 649) was also found, along with two additional distributions which were confirmed to be the cyclics of [MA-PG]$_n$ and ([MA-PG]$_n$-MA) at m/z 471 and m/z 413 respectively.
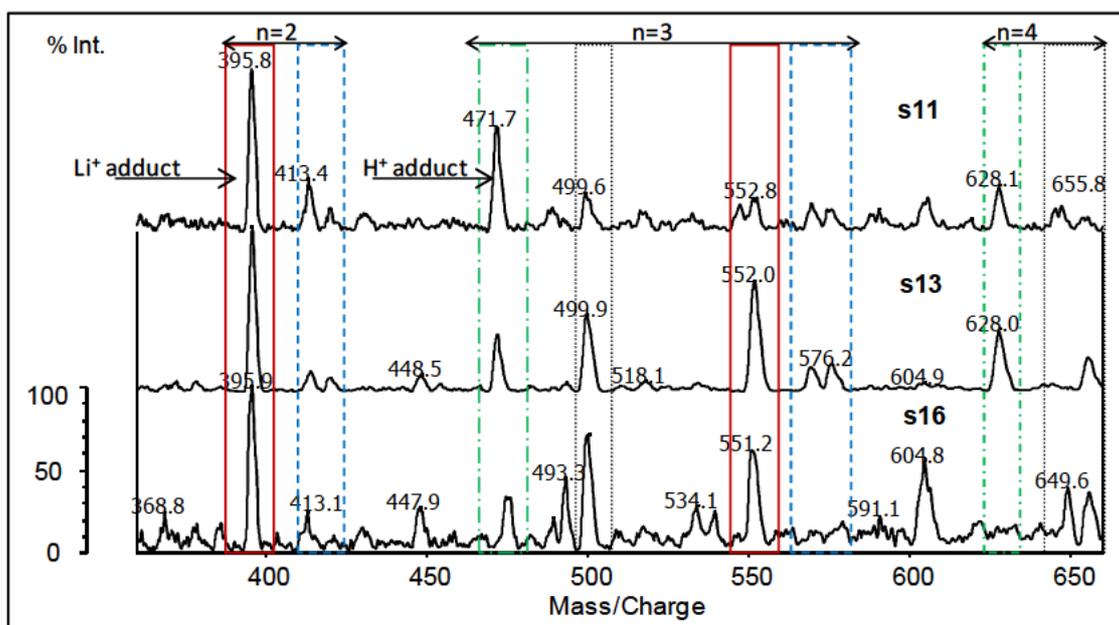
*Figure 23. Magnified spectra in the range m/z 360 to 660 of sample s11, s13 and s16. The differently formatted boxes indicate the different endgroup structures found: A. (———) PG-[MA-PG]n-H, B. (-----) the cyclic of [MA-PG]n-MA , C. (._._._.) the cyclic structure of [MA-PG]n and D. (......) HO-[MA-PG]n-H.*

Interestingly, the MA-PG series appeared to have all the identified endgroup combinations present throughout the polyesterification reaction. This suggests that transesterification as a side reaction to give cyclic structures is not confined to the early stages of the esterification reaction and lower degrees of polymerization. The proposed structures found for the polyesterification of the MA-PG polyester from the bulk sample analysis is summarized Table 7.

The overall observation made from the MALDI-TOF MS analysis is that it proved to be invaluable in identifying the possible endgroup combinations present. Similar to the SEC analysis, distinct distributions of numerous oligoesters were identified, even though very different ionization behaviour patterns were observed for the two different batches. From the PA-PG spectra several degrees of polymerization could be identified, proving to be complimentary in terms of molecular weight distribution to the SEC chromatograms shown earlier where the higher mass species could not be resolved. More importantly, the identification of cyclic structures in the PA-PG batch proved that the effect of side reactions should be considered in the case of saturated polyesters as well, particularly during the early stages of the reaction. For the MA-PG polyester only the lower molecular weight oligomers could be resolved, due to the fact that the MALDI-TOF MS results were clearly dependent on the matrix and salt employed during the sample preparation.

Results and Discussion

Table 8. Proposed structures for the MA-PG polyester samples deduced from MALDI-TOF MS analysis. The m/z values correspond to the Li+ related adducts

Chemical structure	Abbreviation	$m/z_{(exp)}$ for values n		
		2	4	6
A.	PG-[MA-PG]$_n$-H	395	708	1020
B.	cyclic of [MA-PG]$_n$-MA	417	729	1041
C.	cyclic of [MA-PG]$_n$	316	628	940
D.	HO-[MA-PG]$_n$-H	337	649	961

Based on the limitations found in terms of the different types of adduct formation and ionization efficiency between the phthalic and maleic anhydride based polyesters, ESI-MS was selected as a comparable "soft-ionization" technique to support the MALDI-TOF results in order to investigate if any additional information can be acquired.

Results and Discussion

3.2 ESI- MS of the PA-PG and MA-PG based polyesters

The biggest limitation of ESI MS as a "soft-ionization" technique with regard to polymer analysis has always been the difficulty of resolving the overlapping distributions stemming from the range of oligomeric species in high molecular weight materials in conjunction with the distributions arising from multiple charging during the ESI process. An increasing number of studies have, however, shown that besides being a complementary mass spectrometry method along-side MALDI-TOF MS, it features its own advantages that can be beneficial in overcoming the shortfalls of the latter technique[258, 264, 265]. Since the analyte is introduced into the source chamber in solution, the spectra obtained are based on total sample representation, the peak distributions observed accurately reflect the true mass distribution of ions and the abundances are accurately represented by the peak heights or areas. Considering the improved sensitivity in the lower molecular weight ranges, information can be acquired regarding smaller oligomer sizes which normally fall in the m/z range where metal-ion and matrix associated peaks dominate in peak intensity. In terms of method development, the only issue that had to be overcome was the solubility of the polyester samples in an appropriate solvent to facilitate the analysis and ease of evaporation. The final samples in each of the polyester batches were selected and dissolved in ACN (2mg/ml), after which ESI QTOF MS in both positive and negative modes of ionization was conducted. The analysis details are summarized in the experimental section (Part IV.) The strategy behind acquiring data in both modes of ionization was to examine whether the positive mode results correlated with the previous mass spectrometry results obtained from MALDI-TOF and to acquire additional information on the samples via the negative mode as certain functional groups have a greater affinity for de-protonation rather than protonation or cationization.

The ESI-QTOF MS spectrum for sample s28 in the PA-PG polyester batch acquired from positive mode ionization is presented in Figure 24. Due to the fact that masses were scanned from 200 to 2000 amu, only values for the repeating unit distributions up to n = 9 for each of the oligomer species were found. Compared to the positive mode MALDI-TOF MS result, the current spectrum has a much higher peak distribution population, with no apparent base peak.

Results and Discussion
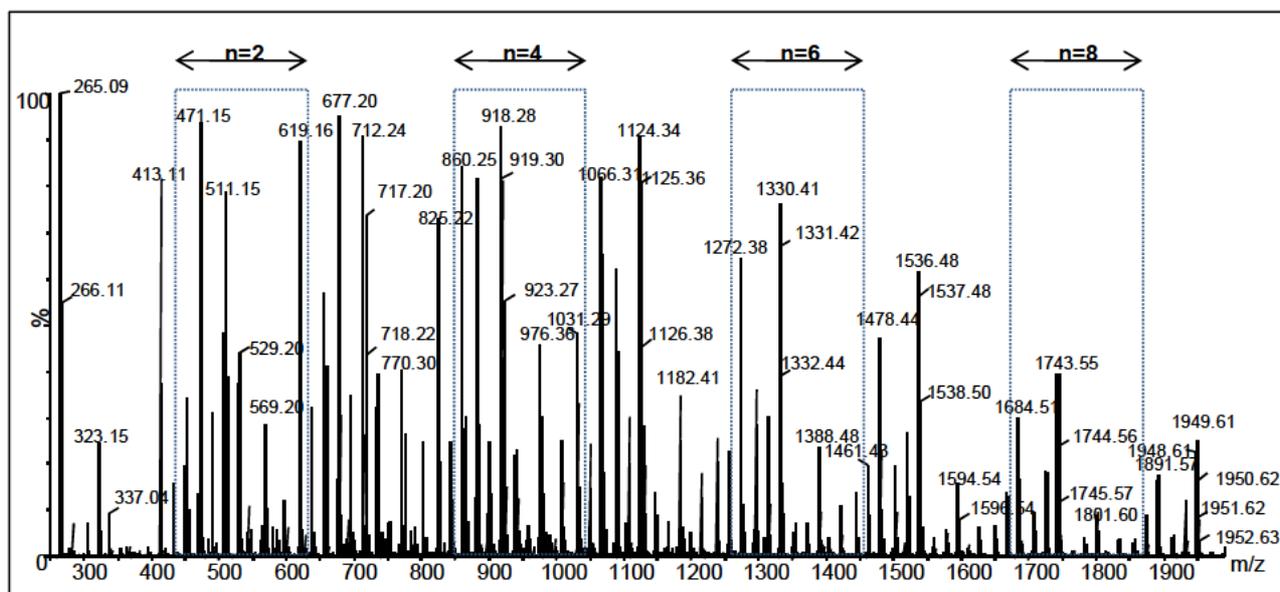
Figure 24. ESI-QTOF MS spectrum of sample s28 in the PA-PG batch with positive mode ionization. The different degrees of polyesterification are identified with series n = 1 to n = 9

Mass values obtained from the previously conducted MS analysis were used as reference to assist in identifying the molecular ions related to the expected linear and cyclic structures. To illustrate the structural assignment by designated labels, the mass range m/z 1500 to 1990 at the higher oligomeric weight region was selected and is presented in Figure 25.
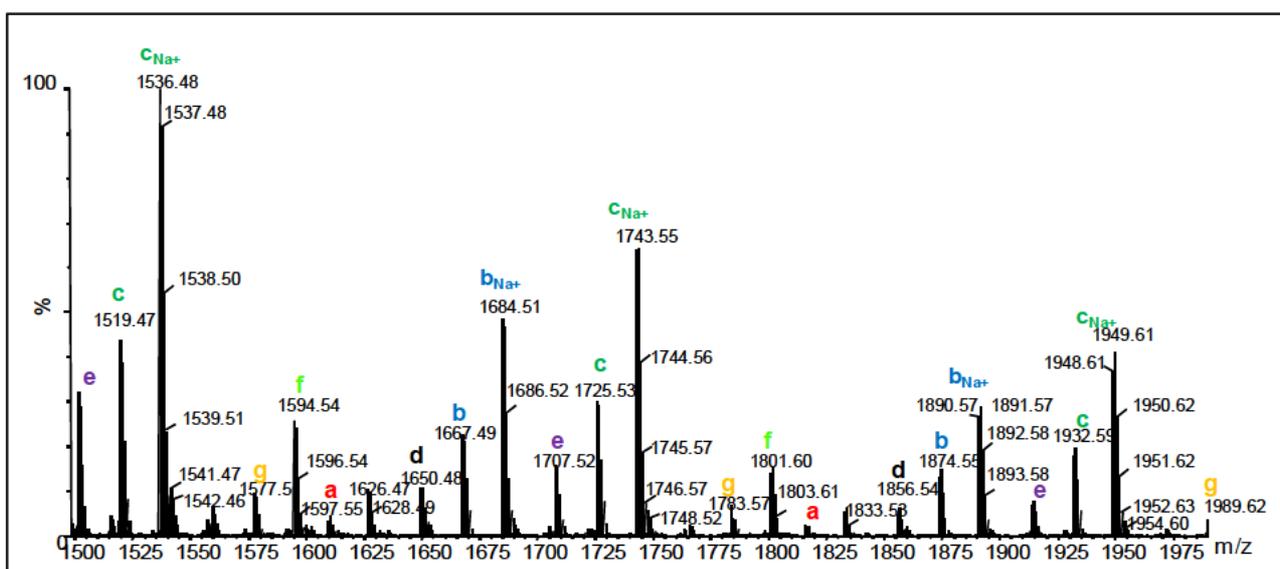
Figure 25. Zoomed spectrum in the range of m/z 1500 – 1990 for the structural identification of the different endgroups present in the final sample s28 of the PA-PG batch with positive mode ionization

The structures which could be correlated back to that of the MALDI-TOF were found at m/z 1607, 1667 and 1725, which were assigned **a**, **b** and **c**, respectively, and are summarized along with the corresponding linear structures in Table 7. Subsequently, the cyclic structures **d** and **e** were assigned at m/z 1650 and 1707. The peaks with the highest intensities were due to sodium cationized $Na^+/PG-[PA-PG]_n-H$ species labeled **[c]Na$^+$**, followed by the sodium cationized $Na^+/HO-[PA-PG]_n-H$ species labeled **[b]Na$^+$**. Although Na^+ adduct peaks were also found for the rest of the assigned structures, they were much less in intensity and tended to overlap with the proton related adduct peak distributions. Moreover, the presence of potassium ionized

58

Results and Discussion

peaks could also be accounted for but their intensities were also negligible for the same reasons. The m/z values listed in Table 9 therefore refer to the protonated adducts in order to simplify assignments. Furthermore, two additional sets of peak distributions were found at m/z 1590 and 1577, the first of which was calculated to suggest a cyclic of the type ([PA-PG]$_n$-PA) labeled **f**. The second oligomeric peak distribution also differed in the repeating unit [PA-PG] mass 206Da, but the final combined endgroup mass came to a value of 135Da. This could possibly indicate a linear structure similar to PG-[PA-PG]$_n$-H labeled **c**, but with the inclusion of another propylene glycol unit, suggesting either the insertion of the glycol on the other side of the repeating unit resembling PG-[PA-PG]$_n$-PG or PG-PG-[PA-PG]$_n$. It could be argued that the starting diol suffered from impurities at the onset of the esterification reaction whereby the dimeric glycol units were taken up into the esterification reaction. On the other hand, the excess molar diol present compared to the diacid could allow the possibility of diols reacting with each other to form an ether product. The dehydration procedure is, however, known not to be as simple and require catalysis from a strong acid. The various structures identified from ESI-QTOF MS with their corresponding labels and m/z values related to the degree of oligomerization can be referred to in Table 9.

Table 9. Proposed structures identified from the ESI-QTOF MS analysis of sample s28 in the PA-PG batch with positive mode ionization. The m/z values correspond to H+ related adducts.

Structures	Label		Values of n			
HO-[PA-PG-]$_n$-PA	a	n	6	7	8	-
		m/z$_{(exp)}$	1402	1608	1814	-
HO-[PA-PG]$_n$-H	b	n	6	7	8	9
		m/z$_{(exp)}$	1255	1461	1667	1873
PG-[PA-PG]$_n$-H	c	n	6	7	8	9
		m/z$_{(exp)}$	1313	1519	1725	1931
cyclic of [PA-PG]$_n$	d	n	6	7	8	9
		m/z$_{(exp)}$	1238	1444	1650	1856
cyclic of PG-[PA-PG]$_n$	e	n	6	7	8	9
		m/z$_{(exp)}$	1295	1501	1707	1913
cyclic of [PA-PG]$_n$-PA	f	n	6	7	8	-
		m/z$_{(exp)}$	1388	1594	1800	-

59

Results and Discussion

unknown 1 (+)	g	n	6	7	8	9
		$m/z_{(exp)}$	1371	1577	1783	1989

Due to the fact that it has been established that a combination of hydroxyl and carboxyl terminal groups were present in the polyester samples, the additional feature of ESI to do negative mode ionization was employed. The result of the PA-PG sample s28 is illustrated in Figure 26 and a much less complicated spectrum was obtained showing only a few distributions. The base peak was found at m/z 429, supporting the theory that the dominating structure in the sample was HO-[PA-PG]$_n$-H, with an increasing repeat unit value ending at n = 9.
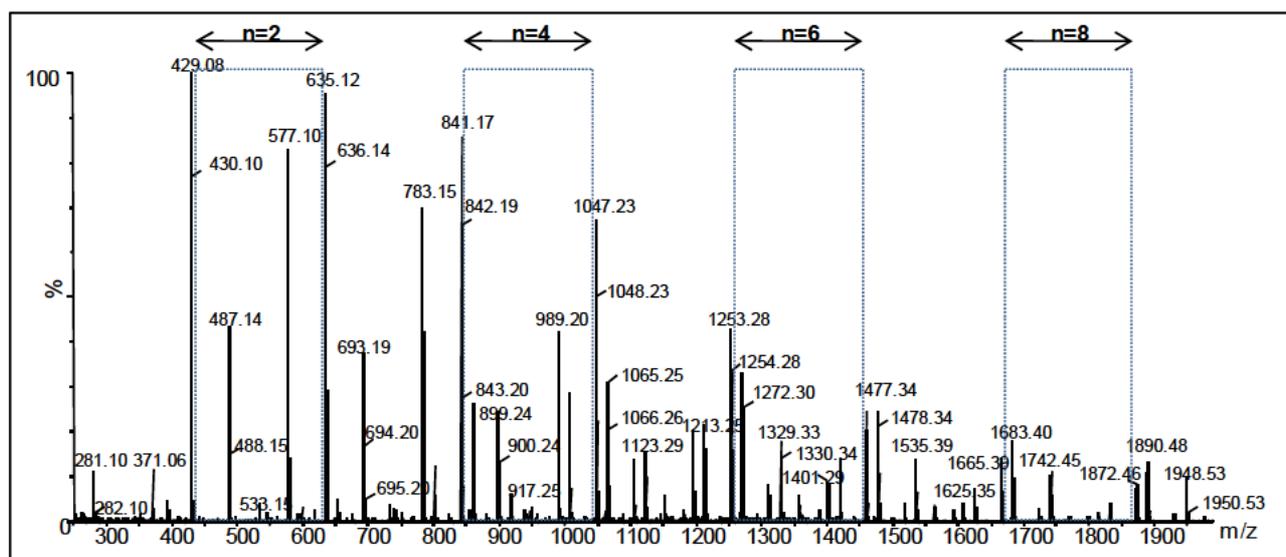

Figure 26. ESI-QTOF MS spectrum of sample s28 in the PA-PG batch with negative mode ionization. The different degrees of polyesterification are identified with series n = 1 to n = 9

In Figure 27, the magnified spectra of the range m/z 1100 to 1900 clearly shows the distribution of peaks related to the three linear structures given in Table 9 labeled **a** to **c**. These structures all possess either a carboxyl and/or hydroxyl endgroup. Based on the differences in peak intensity between **a**, **b** and **c** structures it appears as though the –OH on the carboxyl group is more readily deprotonated as **b** has the highest intensity followed by **a** and with **c** having the smallest intensity. More importantly, four additional distributions at m/z 1123, 1151, 1213 and 1273 were obtained (u_1 to u_4), each representing an oligomeric structure consisting of a different endgroup combination.

Results and Discussion
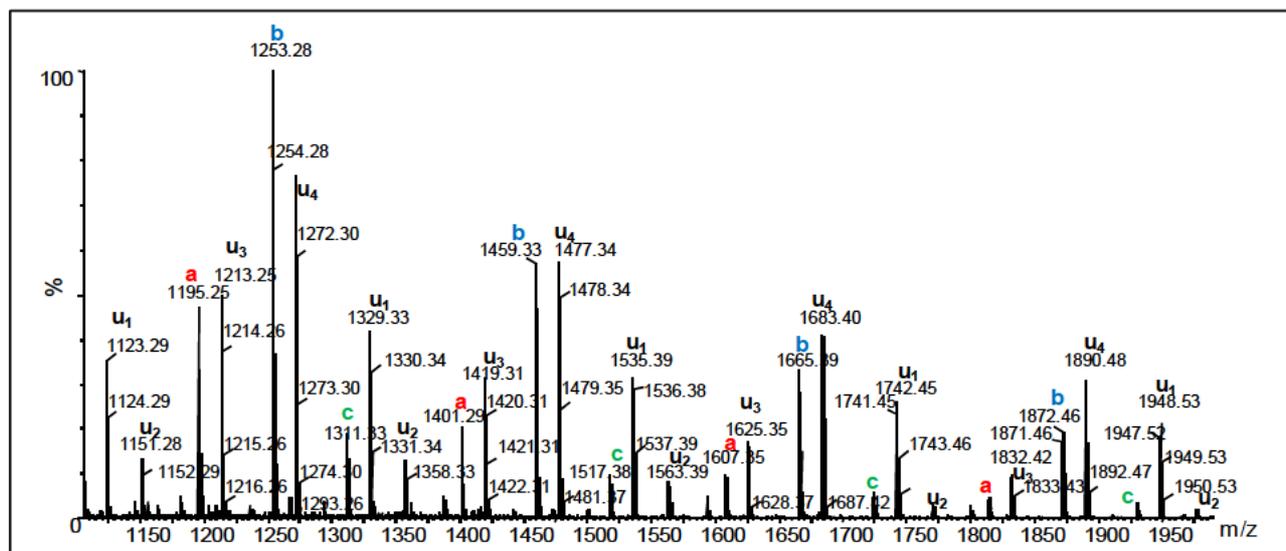
Figure 27. Magnified spectrum in the range of m/z 1100 – 1900 for the structural identification of the different endgroups present in the final sample s28 of the PA-PG batch with negative mode ionization. The labels u1-u4 refer to the unidentified structures also present in the sample.

The total terminal group mass values were 113Da, 85Da, 183Da, and 35Da respectively, which cannot be resolved from the possibilities of the starting materials used for the polycondensation. From the intensity of the peaks, their contribution to the total spectrum is significant which suggests that they would most likely consist of carboxylic groups and that these unidentified species should be considered when the extent of side reaction formation in the PA-PG system is evaluated.

The exact same sample preparation and analysis conditions were used for the analysis of the final sample in the MA-PG polyester batch, s16. The impetus for conducting ESI-QTOF MS analysis on this particular batch was due to the limited information that could be acquired from MALDI-TOF MS. The increased sensitivity and more efficient ionization were proven by the ESI-QTOF MS spectrum obtained in the scanning range of 200 to 2000 amu as much higher molecular weight distributions were obtained in the positive ionization mode as compared to MALDI-TOF MS. The results are given in Figure 28 where degrees of polyesterification were obtained up to a value of n = 11, with the tailing and number of the peaks suggesting that even higher molecular weight oligomers do in fact exist.

Results and Discussion
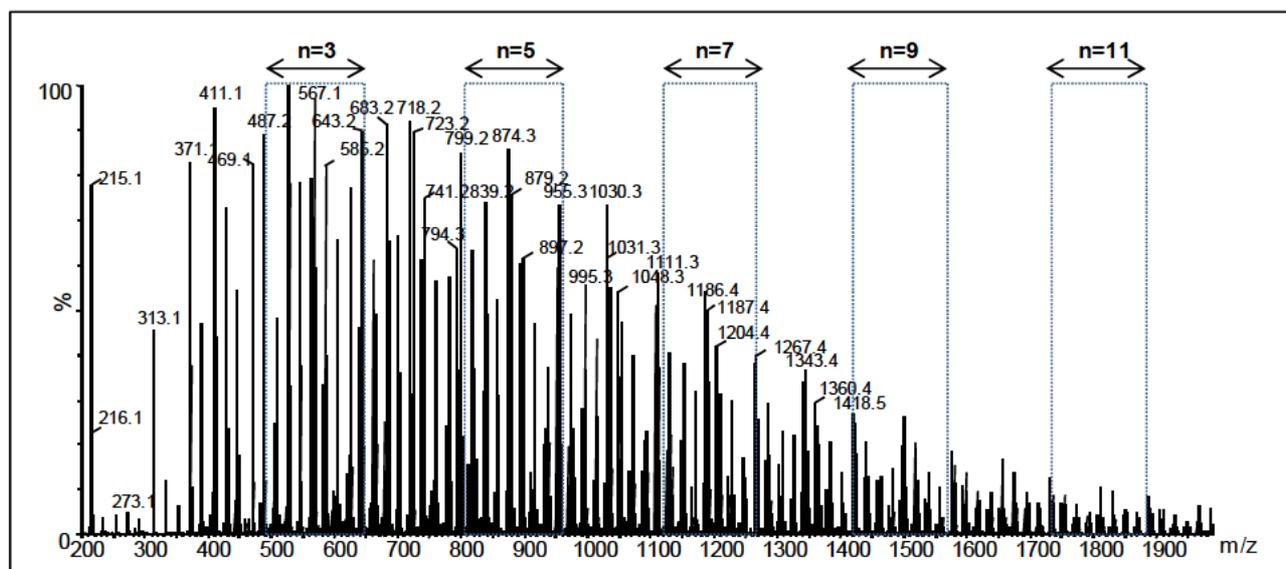
Figure 28. ESI-QTOF MS spectrum of sample s16 in the MA-PG batch with positive mode ionization. The different degrees of polyesterification are identified with series n = 2 to n = 11

The ion peak with the highest intensity of m/z 567 is associated with the cyclic oligomer series of **b** ([MA-PG]$_n$-MA). Similar to the previous batch, this structure was already identified in the MALDI-TOF analysis and along with the mass values obtained for the expected linear counterparts it was used as a reference to assist in assigning subsequent possible endgroup combinations. The extent of variations occurring in the backbone or repeating unit of the oligomer chains was also investigated. The higher molecular weight range m/z 1050 to 2000 was selected to investigate the various distributions, the result of which is shown in Figure 29. At least nine different structure possibilities were elucidated, all of which included oligomers having the ideal repeat unit mass of 156Da as well as an additional oligomeric species consisting of a different chemical composition by showcasing a repeat unit with the mass value of 214Da. In order to avoid confusion, the labeling of the structures was adjusted by the addition of an MA (maleic anhydride) subscript. The first new assignment differing by 156Da suggested a cyclic with an additional PG insertion (PG-[MA-PG]$_n$) labeled **g**$_{MA}$. Based on a terminal group value of 40Da, the second new assignment propose a linear structure of the PG-[MA-PG]$_n$-OH type where the repeat unit differs from previous in that the –OH endgroup constituent is part of the glycol and the –H part of the carboxylic acid; followed by a dehydration mechanism at both endgroups to give CH$_3$CH=CH-[MA-PG]$_n$$^+$ labeled **f**$_{MA}$. Although fragmentation involving certain functionalities is also known to occur during the ionization process (which could also possibly explain the formation of the cation at the glycol end) it should be noted that this phenomenon and the subsequent structural assignment is highly speculative.
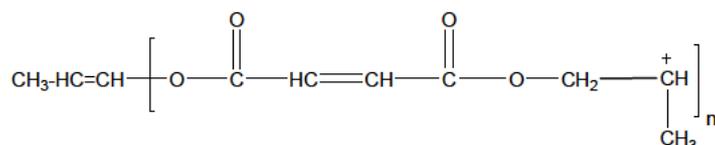
Results and Discussion

The peaks separated by 214Da suggested the inclusion of an extra PG unit, in this instance within the distribution of the repeating unit.
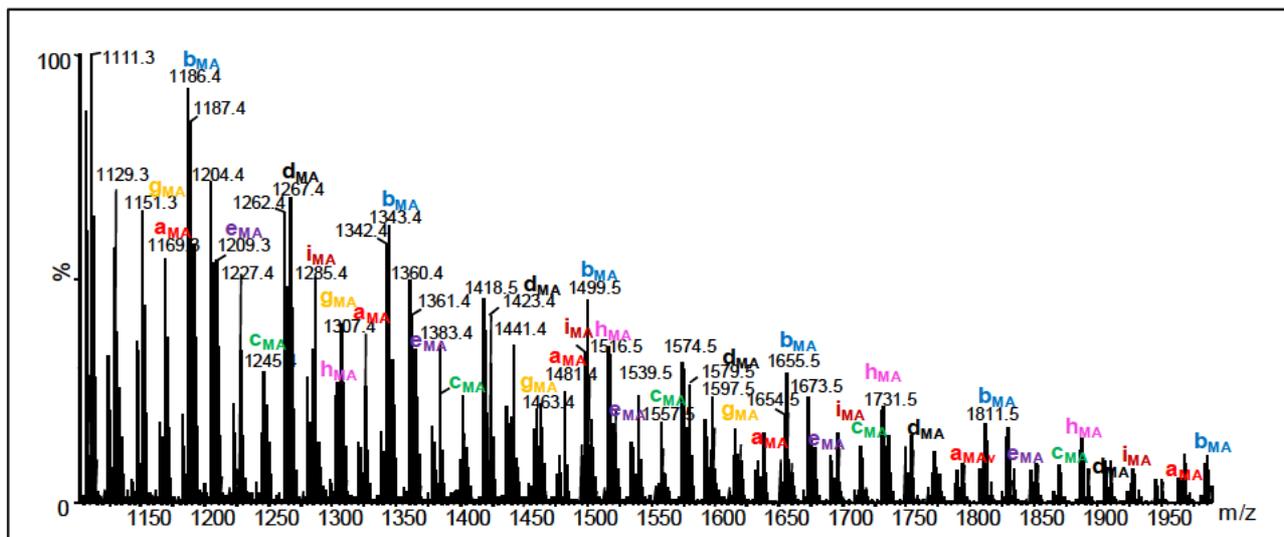
Figure 29. Magnified spectrum in the range of m/z 1050 to 1900 for the structural identification of the different endgroups present in the final sample s16 of the MA-PG batch with positive mode ionization

Therefore, structures labeled h_{MA} for H-[PG-PG-MA]$_n$-H and i_{MA}, a cyclic of [PG-PG-MA]$_n$ are proposed. Subsequently, the different repeat units, along with their possible endgroup combinations and the corresponding m/z values found for the values of n within the mass range are summarized in Table 10. For all the above mentioned distributions, corresponding adducts of sodium and potassium were found, which complicated the assignments of peaks to their related structures. In addition to several metal-ion adduct peaks overlapping with the protonated adducts, the isotopic resolution found in ESI added to the complexity.

Results and Discussion

Table 10. Proposed structures identified from the ESI-QTOF MS analysis of sample s16 in the MA-PG batch with positive mode of ionization. The m/z values correspond to H+ related adducts.

Structures	Label	Values for n			
PG-[MA-PG]$_n$-H	a_{MA}	n	7	8	9	10
		$m/z_{(exp)}$	1170	1326	1482	1638
cyclic of [MA-PG]$_n$-MA	b_{MA}	n	7	8	9	10
		$m/z_{(exp)}$	1191	1347	1503	1659
cyclic of [MA-PG]$_n$	c_{MA}	n	7	8	9	10
		$m/z_{(exp)}$	1093	1249	1405	1561
HO-[MA-PG]$_n$-H	d_{MA}	n	7	8	9	10
		$m/z_{(exp)}$	1111	1267	1423	1579
HO-[MA-PG]$_n$-MA	e_{MA}	n	8	9	10	11
		$m/z_{(exp)}$	1365	1521	1677	1833
CH$_3$CH=CH-[MA-PG$^+$]$_n$	f_{MA}	n	7	8	9	10
		$m/z_{(exp)}$	1289	1445	1601	1757
cyclic of PG-[MA-PG]$_n$	g_{MA}	n	7	8	9	10
		$m/z_{(exp)}$	1151	1307	1463	1619
H-[PG-PG-MA]$_n$-OH	h_{MA}	n	6	7	8	9
		$m/z_{(exp)}$	1303	1517	1731	1944
cyclic of [PG-PG-MA]$_n$	i_{MA}	n	6	7	8	9
		$m/z_{(exp)}$	1285	1499	1713	1927

The negative mode ionization results in Figure 30 were dominated by the peaks associated with the linear structures due to the fact that their freely available functional endgroups are more susceptible to de-protonation. Again, the peaks related to structures having carboxylic endgroups showed a stronger affinity to negative mode ionization as their corresponding intensities were found to be the highest. The molecular weight range of the distributions appeared much lower as compared to that of the positive mode of ionization suggesting that as the oligomeric species increase in mass, the ionization becomes less efficient. It is also possible that as the polyesterification reaction proceeds, the intermolecular chain transfer increases leading

Results and Discussion

to a larger amount of chains consisting of randomized chemical compositions. In turn, the intra-molecular transfer, leading to cyclic formation becomes less relevant.
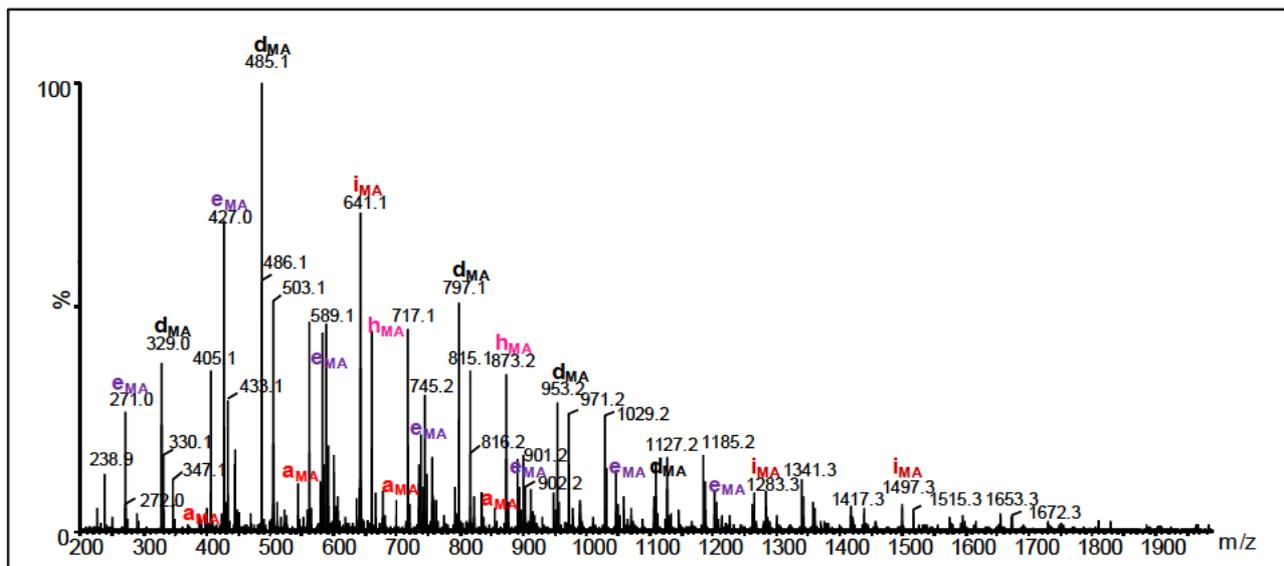
Figure 30. ESI-QTOF MS spectrum of the final sample s16 in the MA-PG batch with negative mode ionization.

Although the ESI results for the MA-PG sample are much improved over that of MALDI-TOF, it is clear that compared to the PA-PG batch sample, this polyester type appears to be more challenging in attaining the desired final product due to the complicated manner in which the main polyesterification proceed alongside numerous side reactions. Regardless, compared to the MALDI-TOF results, more detailed information was obtained and the higher complexity of the MA-PG over that of the PA-PG polyester system in terms of chemical composition distribution is clearly demonstrated by the identification of additional oligomeric species.

Results and Discussion

---

4. Hyphenation of Liquid Chromatography Analysis with Mass Spectrometric Techniques

Following the successful method development of both liquid chromatography and mass spectrometry for the characterization of the PA-PG and MA-PG model polyester sample batches, the two methodologies were combined to essentially overcome the limitations experienced during their respective analyses. In each case, the main objective of the investigation regarding the complex heterogeneity of the polyesters was to achieve separation and enable identification of the separated species. The SEC analysis shed light on the molecular weight and molecular weight distribution properties of the samples produced during polyesterification, which was in turn supported by both mass spectrometry processes. Due to the broad dispersity and chemical composition distributions obtained from the subsequent mass spectrometry analysis of the bulk samples, the need for obtaining simplified fractions by separation and isolation was emphasized as identification and evaluation of the large amount of resultant peaks proved to be a challenging task. Equally important is the fact that even though separation of the bulk samples was achieved by means of gradient elution HPLC, further characterization strategies had to be taken to establish the mechanism behind the elution behaviour of the separated species, especially since the obtained chromatograms of the two polyester batches showed very different results. The advantage of the subsequent MS analysis of the more homogeneous fractions means that structural details regarding the oligomer chains can be obtained in combination with an improved analysis determining molecular weight and/or molecular weight distributions.

In order to isolate fractions of sufficient concentration, the final samples in each of the batches were repeatedly subjected to gradient HPLC fractionation under their respective optimized gradient conditions (section 2.2). Initially, the samples were prepared at different concentrations to determine the highest concentration that can be injected before overloading of the stationary phase occurs and the separation selectivity is lost. For both polyesters the highest attainable concentration was found to be 20mg/ml, with an injection volume of 20μl. Fraction collection was set to be time-based and was carried out continuously until sufficient concentration of each fraction was isolated. Once the isolated fractions were sufficiently dried they were immediately prepared for mass spectrometry analysis under the conditions optimized and discussed in section 3. Although LC coupled offline to MALDI-TOF MS is prone to difficulties in reproducibility, best efforts were made to overcome sample preparation variations. Originally, the online coupling of LC-ESI MS was attempted but due to the solvent combination of THF and hexane, baseline drift in the produced chromatogram created interpretation problems. In addition, the continued increase in back-pressure on the LC system made offline ESI-QTOF MS the preferred choice.

Results and Discussion

4.1 Gradient HPLC fractionation of the PA-PG polyester s28 with off-line coupling to MALDI-TOF and ESI-QTOF mass spectrometry

The fractionation profile of s28 is presented in Figure 31 where the ELSD signal is compared to the UV signal at 254nm. Even though the fractionation time scales were set to the UV response signal, the ELSD provided the advantage of a regular baseline as compared to the baseline drift found in the former detection method due to the continuously increasing THF concentration of the mobile phase[249]. It, thereby, simplified and assisted in determining the boundaries of the individual oligomer peaks needed from fractionation.
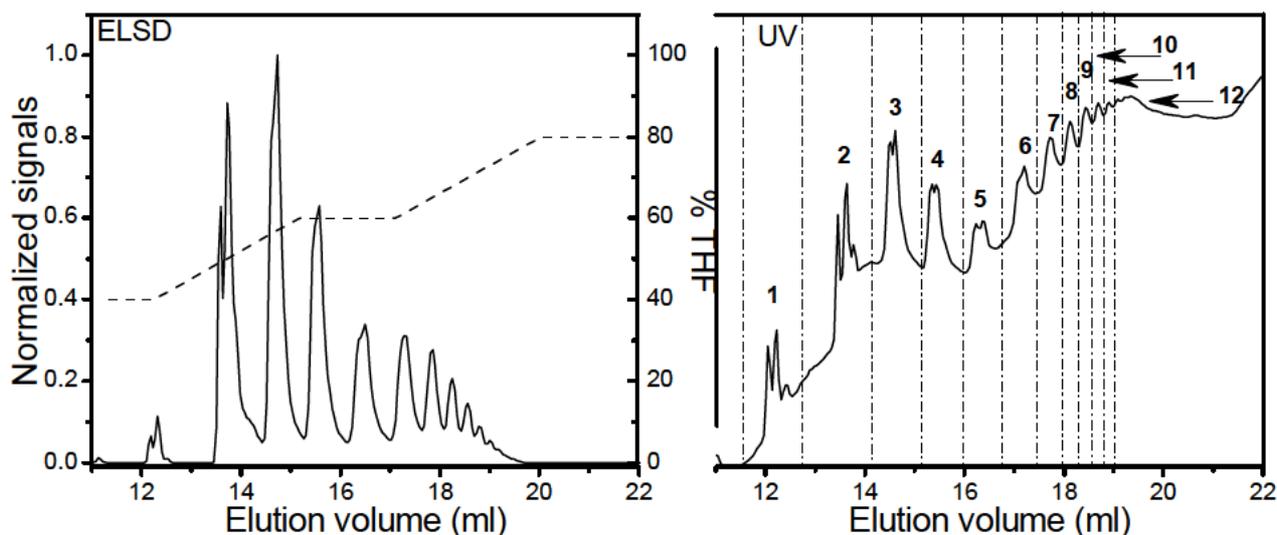
Figure 31. ELSD and UV (254nm) chromatograms of the gradient elution HPLC of sample s28 of the PA-PG batch with fractionation increments used for off-line mass spectrometry. The gradient profile is illustrated by the dashed lines in the ELSD chromatogram. Gradient separation conditions are given in section 2.2.1 with gradient profile nr.8 in Table 4. The sample concentration was 20mg/ml of which 20µl was injected.

The quality of solvent could have largely played a role in the base-line drift exhibited in the UV detection. Despite the fact that the samples were dried off before further sample preparation for MS measurements, the effects of impurities can still be considerable as they can include peroxides and THF oligomers which remain present even after evaporation.

The fractionation area spanned from 12 to 22ml elution volume and in total, twelve separate fractions were collected and submitted for MALDI-TOF MS and ESI-QTOF MS, respectively, where they were analyzed by order of elution volume. The time delay between the UV detector and the fraction collector was determined via the injection of a dye sample provided by Agilent technologies. As the dye elutes through the system it is detected by a sensor at the depositing arm unit of the fraction collector. The accurate difference in elution volume (time) between the detector and fraction collector is calculated automatically.

4.1.1 MALDI-TOF MS as off-line detection

The resulting spectra of fractions 2 to 5 consisted of similar low molecular weight peak distributions from m/z 220 to m/z 1100 and are presented in Figure 32. The results of fraction 1 have been omitted as the corresponding range proved to be of lower molecular weight where the peaks obtained were mostly due to starting materials, overlapping with matrix and metal-ion adducts. All the species **A** to **E** obtained during the

Results and Discussion

bulk analysis of sample s28 (Table 7, section 3.1), were readily identified with the degree of oligomerization increasing from n = 2 to n = 4 in all four fractions. In a similar fashion as the bulk analysis, the Na^+ related adducts showed the most intense peaks for the linear structures of **A** to **C**, while the cyclic of $[PA-PG]_n$ **D** had a higher affinity for H^+ ionization.
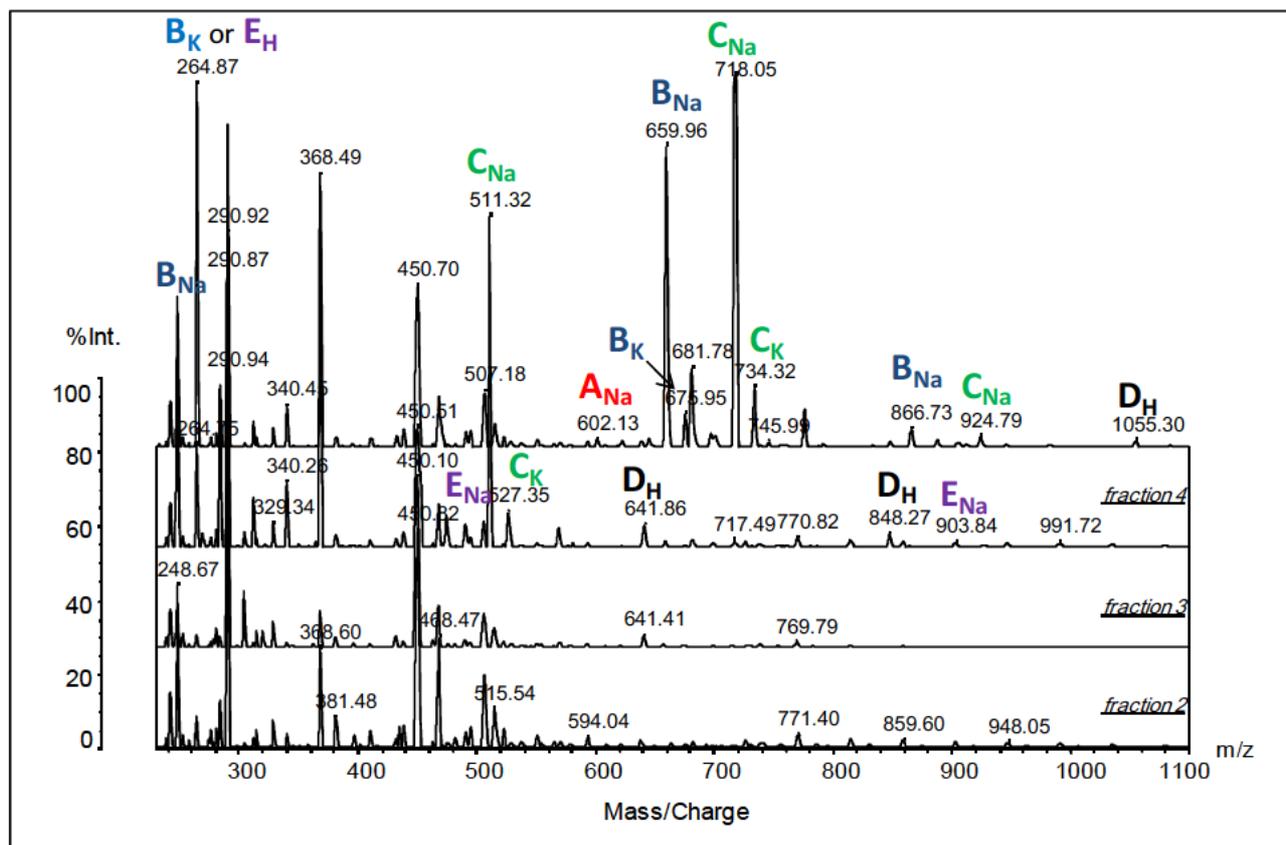
Figure 32. MALDI-TOF spectra of the respective fractions 2 to 5 collected after the gradient elution HPLC separation of sample s28 in the PA-PG batch. The subscripts of each label refer to the metal-ion and/or protonated adduct.

It could be argued that the high intensity of the peak found at m/z 264 could perhaps be due to the fact that the mass corresponds to both K^+/ $HO-[PA-PG]_n-H$ (structure **B**) and the cyclic of H^+/ $PG-[PA-PG]_n$ (structure **E**), although in contrast, the next peak in the same series at m/z 675 is much smaller. A more reasonable explanation would rather be that the mass corresponds to the potassium adduct of structure **B**, since in the MALDI TOF analysis of the bulk sample only sodium adducts of structure **E** were found, which in turn is supported by the presence of m/z 903 and m/z 491 even though at very weak intensities compared to the other distributions. The most important finding, however, was that based on the difference in m/z shift from fraction 2 to 5, it could be concluded that the gradient elution HPLC analysis was an oligomeric separation dominated by chemical composition distribution of the main chain and that the elution order was based on increasing degree of oligomerization. When the sample is injected in the non-solvent conditions of 100% hexane, the 2 minute residence time is required to allow the chains to align themselves along the stationary phase in a manner that is determined by their chemical composition. As the percentage of good solvent is increased, the distinct oligomer sets are re-dissolved, whereby interaction between the chains and the packing material is systematically being disrupted. The shorter oligomers are therefore eluted first, followed by increasingly larger counterparts.

68

Results and Discussion

This phenomenon was more pronounced in the results of the subsequent fractions 6 to 11 as illustrated in Figure 33. The molecular weight distribution ranged from m/z 600 to 2600, after which no further peaks could be resolved. The spectrum of fraction 12 was omitted as it showed baseline noise only, suggesting that the final fraction consisted only of solvent based molecules. Results showed that for the higher molecular weight fractions, essentially only 3 structural distributions dominated and could be identified, with peaks having an increasing m/z distribution value. The first two were easily distinguishable as structure **B** (HO-[PA-PG]$_n$-H) and **C** (PG-[PA-PG]$_n$-H), with both Na$^+$ and K$^+$ adducts present. Besides the fact that fraction 5 to 7 still had lower molecular weight constituents present, it became clear that the cyclic structures found previously were absent or at least became negligible with respect to the core distributions as the molecular weight increased. Mass values corresponding to structure **A** (HO-[PA-PG]$_n$-PA) were also absent in the higher fractions.
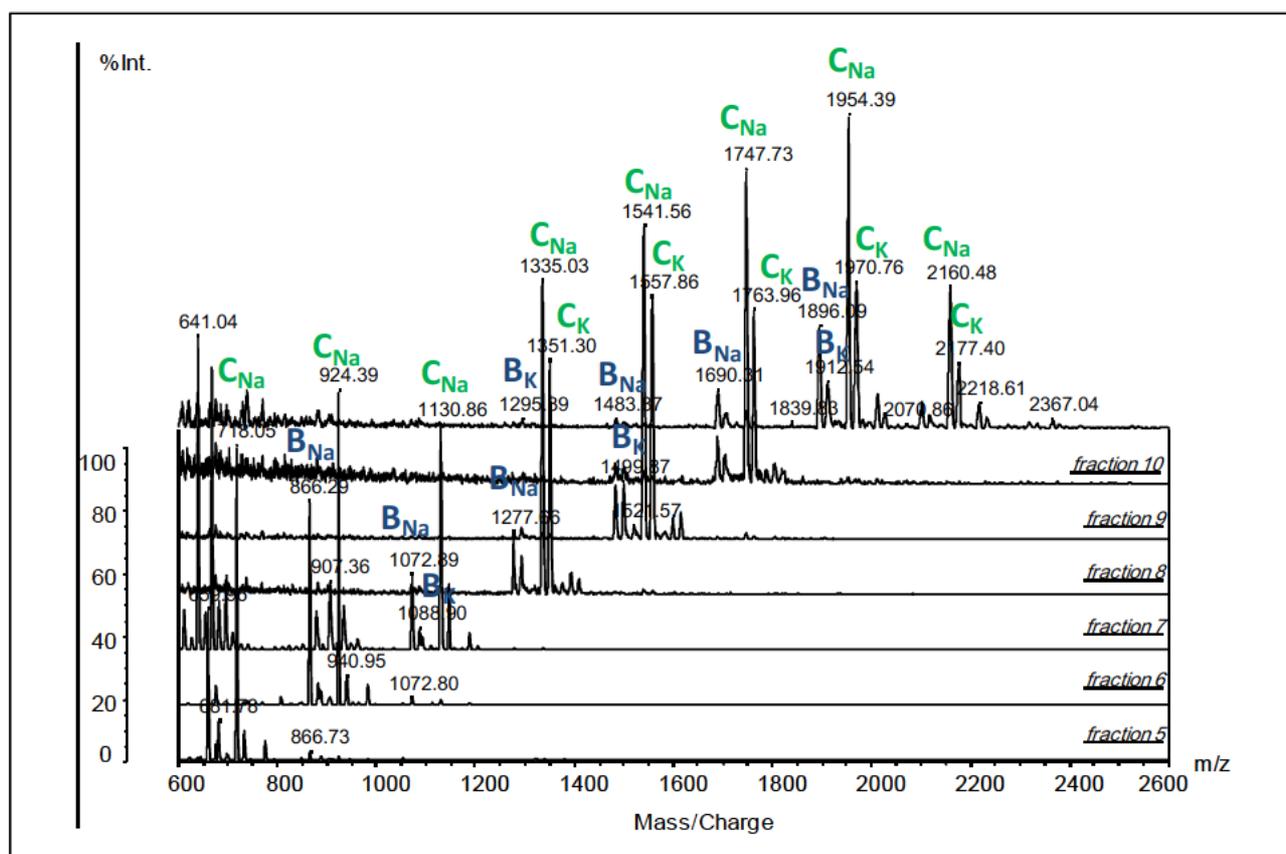
Figure 33. MALDI-TOF spectra of the respective fractions 5 to 11 collected from the gradient elution HPLC separation of sample s28 in the PA-PG batch.

For the structural assignment of the third distribution, magnified spectra of fractions 9 to 11 are given in Figure 34. The calculations established that the distribution of interest also differed in 206Da but that it was 58Da larger than its linear sodium ionized structure **C** (Na$^+$/PG-[PA-PG]$_n$-H) counterpart. This in fact corresponded to the unknown protonated adduct structure found previously in the ESI analysis of the bulk sample s28, labeled **g** in Table 9. The difference in endgroup indicated the insertion of another PG unit (minus the -OH), either as di-propylene glycol or the presence of a dehydrated glycol unit -CH=CH-CH$_3$ at the other end of the linear chain. The third possibility could be the formation of -CH$_2$-CH=CH$_2$ as propylene glycol is known to isomerize to allyl alcohol. The onset of the formation of this particular structure could, however, not be established during the bulk analysis. Through the use of gradient elution HPLC to obtain narrowly distributed fractions having well-defined entities, it was possible not only to identify the structure but

Results and Discussion

also to determine at which point does its formation occur and start to become significant during the later stages of the oligomerization.
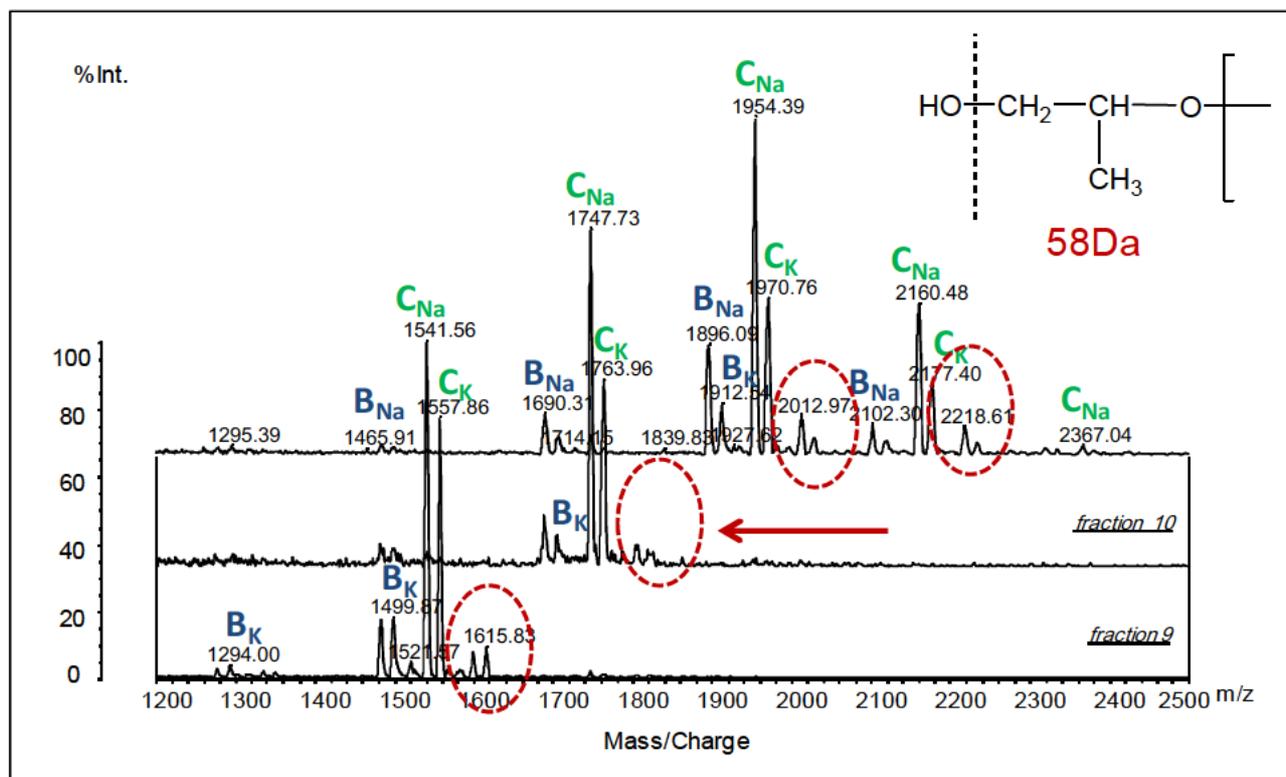
Figure 34. Magnified MALDI-TOF MS spectra from m/z 1200 to 2500 of fractions 9 to 11 to indicate the presence of an additional oligomeric structure.

Finally, the spectra of the fractions corresponded with that of the bulk analysis in that the same structural entities dominated with increasing molecular weight.

4.1.2 ESI-QTOF MS as Off-line detection

Due to the higher sensitivity found with the ESI MS technique, the required concentration of the individual fractions were not as high as for MALDI-TOF MS. Although all the fractions obtained were investigated in order to illustrate a sensible comparison between the two MS techniques, the spectra of three of the higher molecular weight fractions were analyzed and presented in Figure 35. In contrast with the ESI analysis of the bulk sample, peak identification and structure elucidation was simplified since only the isolated fractions had to be considered. Although all three spectra indicated that the resultant peaks with the highest intensities were mostly metal cationized species, an attempt was made to do a detailed assignment and in turn Na^+, K^+ and H^+ related ions were identified. The first agreement with the MALDI-TOF MS was the increase in molecular weight distribution from fraction 5 to fraction 7. In addition, the mass range of each was identical to that of their corresponding fraction analyzed by the previous MS technique. Secondly, structures **b** (HO-[PA-PG]$_n$-H) and **c** (PG-[PA-PG]$_n$-H) were found to yet again be the two main structures in all three fractions, with both sodium and potassium adducts present. Furthermore, only low intensity peaks were found for structure **g** (PG-PG-[PA-PG]$_n$-H) in all fractions, even though the MALDI-TOF MS spectra indicated that the peak intensity of the related species increased with increasing value of n.

Results and Discussion
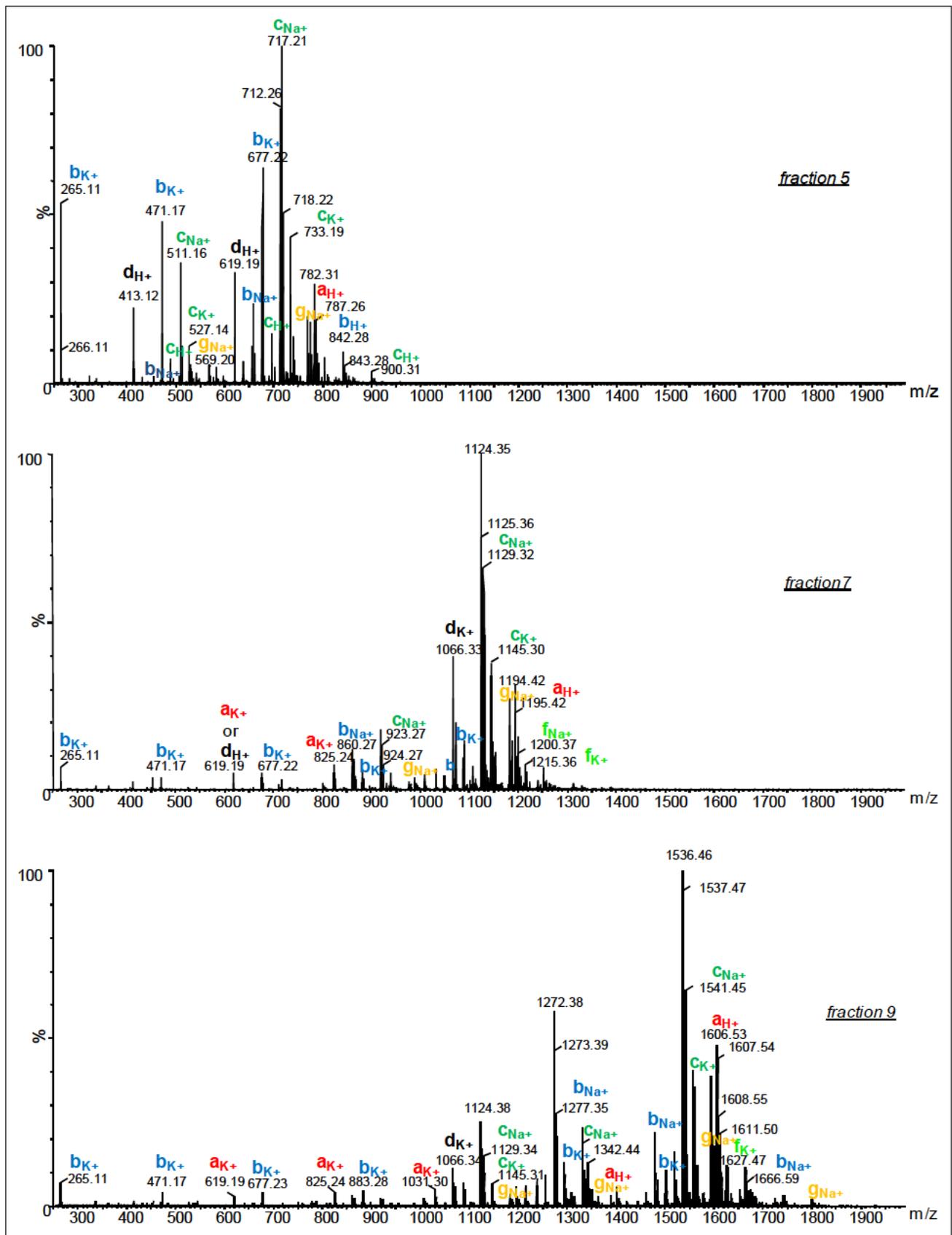
Figure 35. ESI-QTOF MS spectra of fractions 5, 7 and 9 of sample s28 in PA-PG batch with positive mode ionization. The fractions show the variety of metal-ion adduct distributions obtained for the dominating oligomeric structures

Results and Discussion

In contrast to the MALDI-TOF MS, structures **a** (HO-[PA-PG]$_n$-PA) and **d** (cyclic of [PA-PG]$_n$) could also be identified. The fact that they were obtained at much lower peak intensities in comparison with the assignments of the two previous structures, suggest that their concentration is much lower and explains why they were not found during the previous MS analysis.

The difference between the particular linear (**a**) and cyclic structures (**d**) were their variation in the degree of polymerization and type of adduct formation from fraction 5 to 7. Lower molecular weight constituents of the protonated cyclic **d** is present in fraction 5 and 7 at m/z 413 and m/z 619, which is substituted with a potassium adduct at m/z 1066. This also proved to be the highest degree of oligomerization at which **d** is present in fraction 9 as no higher species could be found. Alternatively, the protonated structure **a** only had one value of n present in fraction 5 at m/z 784, while fraction 7 and 9 had several peak distributions related to protonated and potassium adducts. Due to the fact that baseline separation could not be achieved in the HPLC for the bulk sample s28 in general, the spectra of fraction 9 in particular also contained traces of lower degrees of oligomerization for structure **b**. This is possibly due to co-elution of oligomeric species belonging to adjacent peaks. This is supported by the fact that the earlier fraction 5 which had improved separation during the HPLC exhibited very narrow peak distributions, with the later fractions consisting of a broader range of n values. The results of all the structures obtained in the fractions are summarized in Table 11 which shows the different endgroup combinations as well as their degrees of oligomerization n for each structure present.

Results and Discussion

Table 11. Structures identified from ESI-QTOF MS analysis of fractions 5, 7 and 9 of sample s28 in the PA-PG batch with positive mode ionization. The m/z values correspond to the metal-ion adducts found at different degrees oligomerization in each fraction.

Structures	Label		Values for n		
HO-[PA-PG]$_n$-PA	a_{H+}	n	3	5	7
		m/z$_{(exp)}$	785	1197	1609
	a_{K+}		2	3	4
			619	825	1031
HO-[PA-PG]$_n$-H	b_{H+}	n	4	5	6
		m/z$_{(exp)}$	842	1048	1254
	b_{Na+}		2	4	7
			453	865	1483
	b_{K+}		1	4	7
			265	883	1500
PG-[PA-PG]$_n$-H	c_{H+}	n	2	3	4
		m/z$_{(exp)}$	488	694	900
	c_{Na+}		2	5	7
			511	1129	1541
	c_{K+}		2	5	7
			528	1145	1558
cyclic of [PA-PG]$_n$	d_{H+}	n	2	3	-
		m/z$_{(exp)}$	413	619	-
	d_{K+}		-	-	5
			-	-	1069
cyclic of [PA-PG]$_n$-PA	f_{Na+}	n	-	5	7
		m/z$_{(exp)}$	-	1201	1613
	f_{K+}		-	5	7
			-	1218	1630
PG-PG-[PA-PG]$_n$-H	g_{Na+}	n	2	5	8
		m/z$_{(exp)}$	570	1187	1805

Subsequently, negative mode ESI was conducted on all the fractions of s28. For the sake of continuity, results of fractions 5, 7 and 9 are discussed and presented in Figure 36. Coinciding with the negative mode spectra of the bulk sample analysis in section 3.2, structures **a**, **b** and **c** were easily identified. Notably, an additional distribution of peaks indicating structures with inconclusive endgroup combinations can clearly be

Results and Discussion

seen in fraction 5 ranging from m/z 1000 to 1350. These structures could be traced back to identical m/z values of unknown species found in the bulk sample analysis and was subsequently labeled **u1** to **u4**.

Results and Discussion
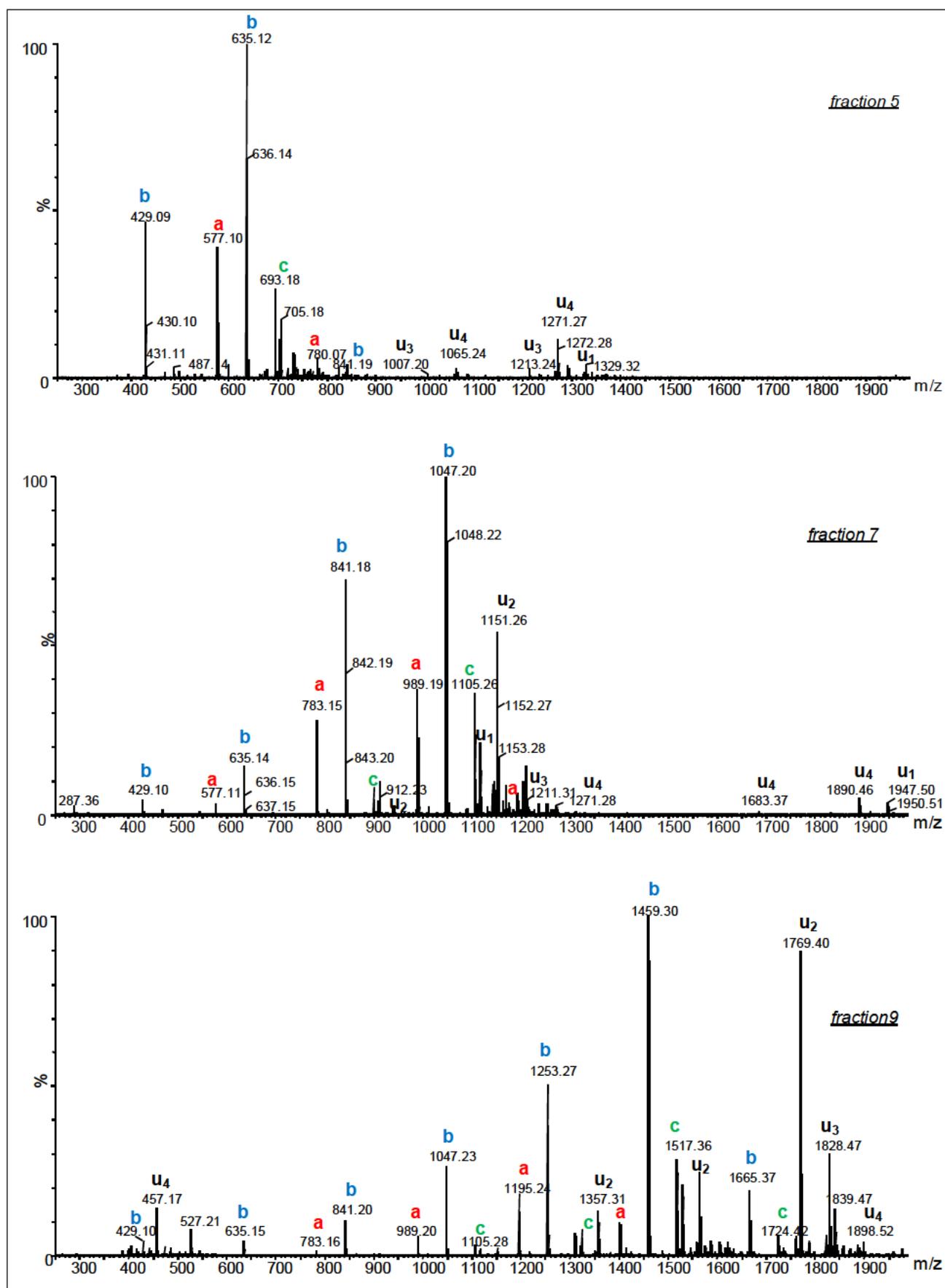
Figure 36. ESI-QTOF MS spectra of fractions 5, 7 and 9 of sample s28 in PA-PG batch with negative mode ionization. The fractions show the deprotonated structures and their corresponding oligomeric distributions

75

Results and Discussion

Peaks having an increase in degree of oligomerization in the following fractions 7 and 9 suggested the increasing importance of the formation and presence of the related structures during the polyesterification procedure. The fact that they were not found during positive mode analysis of the fractions support the hypothesis made earlier that they are likely to consist of carboxylic endgroups which are more susceptible towards deprotonation. It also highlights the increasing randomization and altering of endgroup combinations occurring at later stages of the reaction. Concomitantly, the m/z values and intensity of the peaks obtained for structures **a**, **b** and **c** showed similar trends in terms of mass range and width of distribution with their associated counterparts found in the positive mode analysis of the isolated fractions. The deprotonation of structure **b** appeared to be favored over that of structure **a**, with structure **c** having the smallest peak intensity. The m/z values along with their degree of oligomerization of each of the structures found are summarized in Table 12. It can be seen that the values for n are increasing in nature and that the unknown structures are selective towards higher molecular weight species which elute during the later stages of the gradient HPLC separation.

Table 12. Structures identified from ESI-QTOF MS analysis of fractions 5, 7 and 9 from sample s28 in the PA-PG batch with negative mode ionization. The m/z values correspond to the deprotonated structures and their oligomeric distributions

Structures	Label		Values for n		
		n	2	4	6
HO-[PA-PG]$_n$-PA	**a**	m/z$_{(exp)}$	577	989	1401
		n	2	5	8
HO-[PA-PG]$_n$-H	**b**	m/z$_{(exp)}$	429	1047	1665
		n	3	5	8
PG-[PA-PG]$_n$-H	**c**	m/z$_{(exp)}$	693	1105	1724
		n	5	6	9
Unknown 1	u$_1$	m/z$_{(exp)}$	1123	1329	1947
		n	5	6	8
Unknown 2	u$_2$	m/z$_{(exp)}$	1151	1357	1769
		n	4	5	8
Unknown 3	u$_3$	m/z$_{(exp)}$	1007	1213	1769
		n	5	6	9
Unknown 4	u$_4$	m/z$_{(exp)}$	1065	1271	1889

Results and Discussion

4.2 Gradient HPLC fractionation of the MA-PG polyester s16 with off-line coupling to MALDI-TOF and ESI- mass spectrometry

Based on the fact that the gradient HPLC of the MA-PG polyester batch proved to be a more challenging task than in the case of the previous polyester batch, the purpose of employing mass spectrometry as detection method was to assist in determining the driving force behind the chromatographic behavior of the samples. Seeing that the HPLC separation was less efficient, the UV detection signal played a critical role in that the selected gradient demonstrated a reproducible step-wise profile which was utilized in assigning the boundaries of the individual fractions. Essentially the fractionation area spanned over a much larger elution volume (time) with no real individual peaks to collect. Instead the fractionation time was stipulated by the UV drift exhibited during each mobile phase altering step in the gradient. This roughly correlated with each of the weakly resolved peaks in the ELSD response. The selected fractionation profile of sample s16, along with the ELSD and UV signal (254nm) is given in Figure 37.
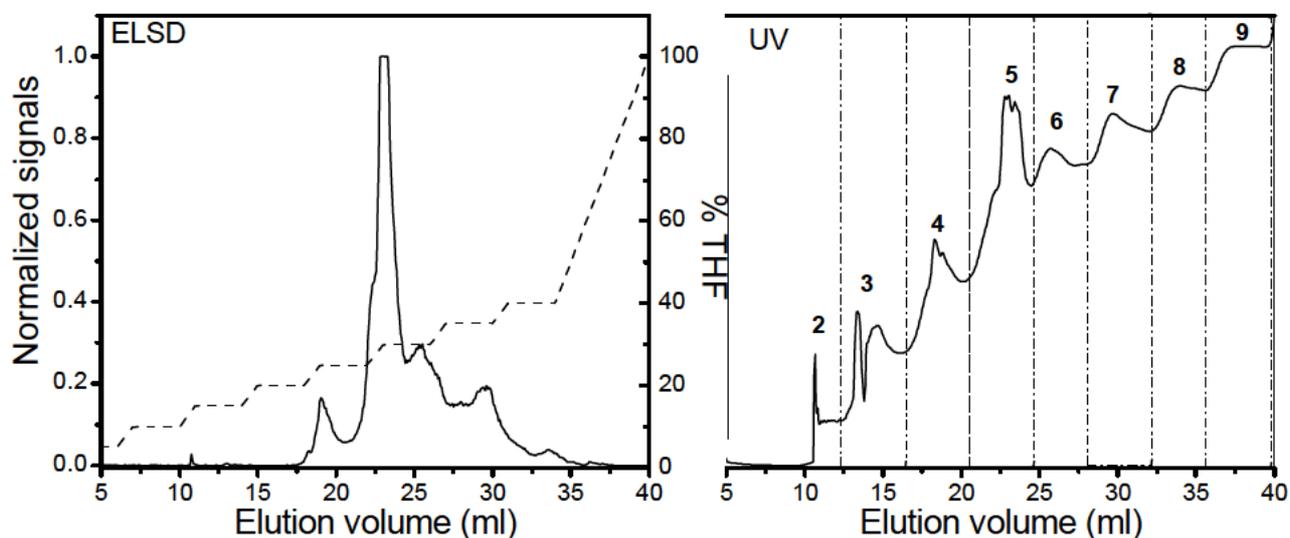
Figure 37. The ELSD and UV chromatograms of the reversed phase gradient HPLC of sample s16 of the MA-PG batch with the fractionation increments used for off-line mass spectrometry. The gradient profile is illustrated by the dashed lines in the ELSD chromatogram. Gradient separation conditions are given in section 2.2.2 with gradient profile nr 14 in Table 4. The sample concentration was 20mg/ml of which 20μl was injected.

Nine fractions were repetitively collected, dried and submitted for MALDI-TOF and ESI-QTOF MS analysis in the order of elution. The elution volume of fraction 1 is omitted as the peak found at 3.5ml in the UV signal was essentially due to mobile phase changes in the dead volume range and not sample constituents.

4.2.1 MALDI-TOF MS as off-line detection

As predicted, very different results were obtained from the fractionation set of the current sample as compared to the PA-PG system. Although a number of peaks with similar m/z values to that of the bulk sample MALDI-TOF analysis were found, several other distributions, which were previously only possible to identify from ESI bulk analysis, were present from the early fractions. Since fraction 2 had no sample related peaks, consisting mostly of solvent molecules entailing noisy baseline, the spectra of fractions 3 to 5 are given in Figure 38. Although the mass range from m/z 200 to 750 was of very low molecular weight species,

Results and Discussion

no definitive trend could be identified between the three fractions as peak intensities appeared to be very similar and present in basically all the spectra. Only a very slight shift in molecular weight distribution, increasing from fraction 3 to 5 was obtained. The LiCl added as cationizing agent during the sample preparation procedure also allowed the formation of Li^+ adducts in combination with the protonated ones so that an obvious preferred method of ionization for individual structures could not be determined. Fraction 3 had very few peaks, having the interesting combination of the protonated cyclic structures of **C** ($H^+/[MA-PG]_n$) and **I** ($H^+/[PG-PG-MA]_n$) and the linear structures of **F** ($H^+/CH_3-HC=CH-[MA-PG]_n-H$) and **H** ($H^+/H-[PG-PG-MA]_n-H$). In all cases, the corresponding lithium adducts were also present, although at negligible intensity.
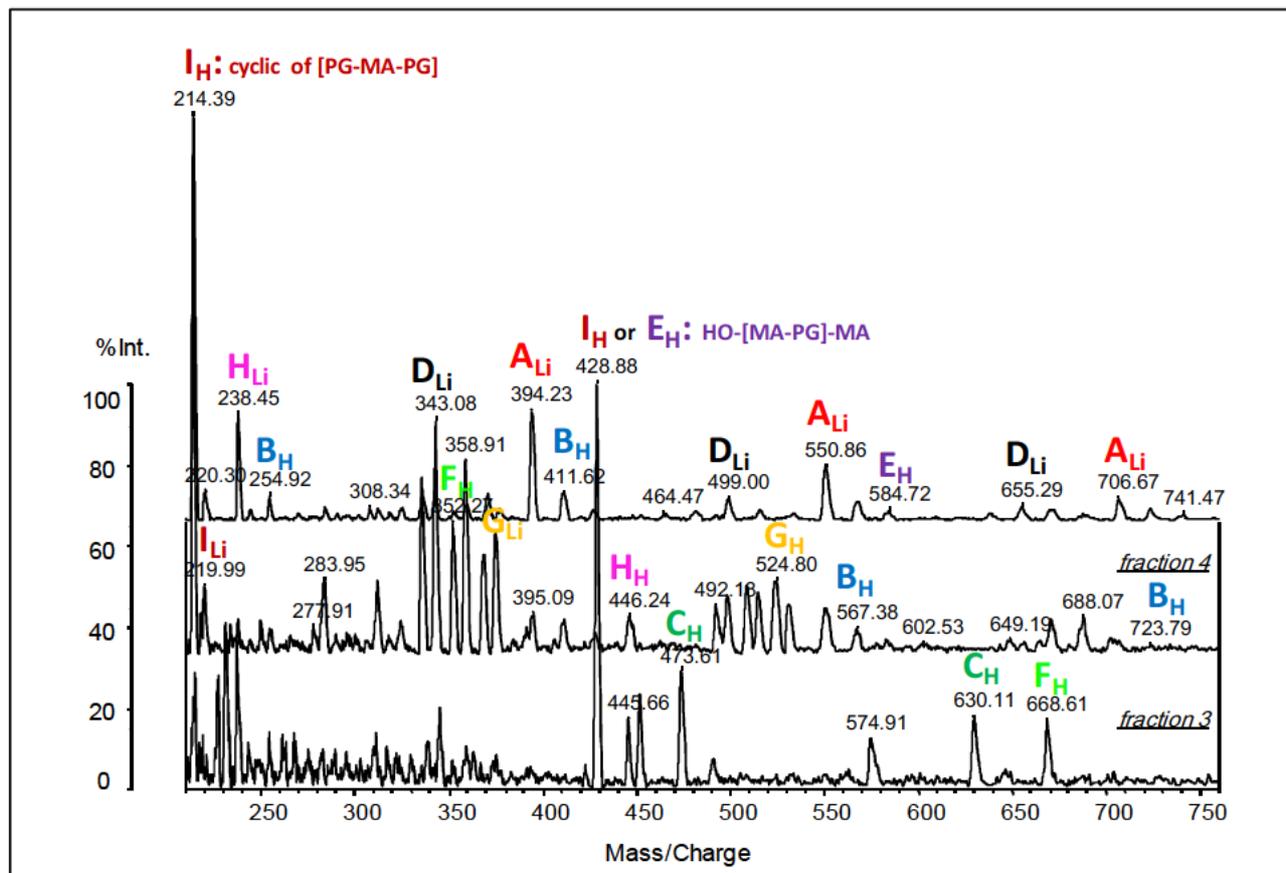
Figure 38. MALDI-TOF spectra of the respective fractions 3 to 5 collected after the gradient HPLC separation of sample s16 in the MA-PG batch. The subscripts of each label refer to the metal-ion and/or protonated adduct.

This could be due to the fact that the concentration of these species in comparison with the rest of the sample constituents is extremely low as can be seen from the ELSD signal in Figure 37, where no peaks were detected at that particular fraction of the chromatogram. The spectra of fraction 4 and 5 had the addition of structures **G** (cyclic of PG-$[MA-PG]_n$), **B** (cyclic of $[MA-PG]_n-MA$) and **A** ($PG-[MA-PG]_n-H$), **D** (HO-$[MA-PG]_n-H$) and **E** (HO-$[MA-PG]_n-MA$) respectively. This clearly supports the poor separation selectivity obtained in the HPLC separation as several lithium and proton related adducts of the structures overlapped, which made definitive structural assignments extremely difficult. It does, however, suggest that even at very low molecular weight a complex heterogeneous system already exists and that the variety of oligomer chains being formed continue to participate later in the esterification process. In Figure 39 the MALDI-TOF spectra

Results and Discussion

of fractions 6 and 7 illustrate a larger molecular weight distribution ranging from m/z 400 to 1800, with very little difference between the two respective fractions. More importantly, the increase in mass distribution from the previous set of fractions 3 to 5, imply that the gradient HPLC separation was partial towards a molecular weight effect and that the different distributions, although weakly resolved are eluting in the order of increasing oligomer size. Thus an increase in the degree of polymerization leads to the formation of more hydrophobic units which experience stronger interactions with the hydrophobic stationary phase than their smaller counterparts. However, due to the complex nature of the MA-PG system, additional effects from the large variation of endgroups present should also be considered during the HPLC separation. Initially, it was thought that the peaks having the highest intensities are predominantly imparted by the H^+ related adducts of structure **B**, **C** and **D** but from the zoomed-in part of the spectra from m/z 750 to 1300 it can be seen that structures **A** and **E** could also be identified with considerable intensities. Furthermore, weak intensity peaks related to structures **F** and **I** confirmed their presence in fraction 6, although they appeared to be negligible in fraction 7. Traces of structure **G** was found up until m/z 840, while structure **H** proved to be absent.
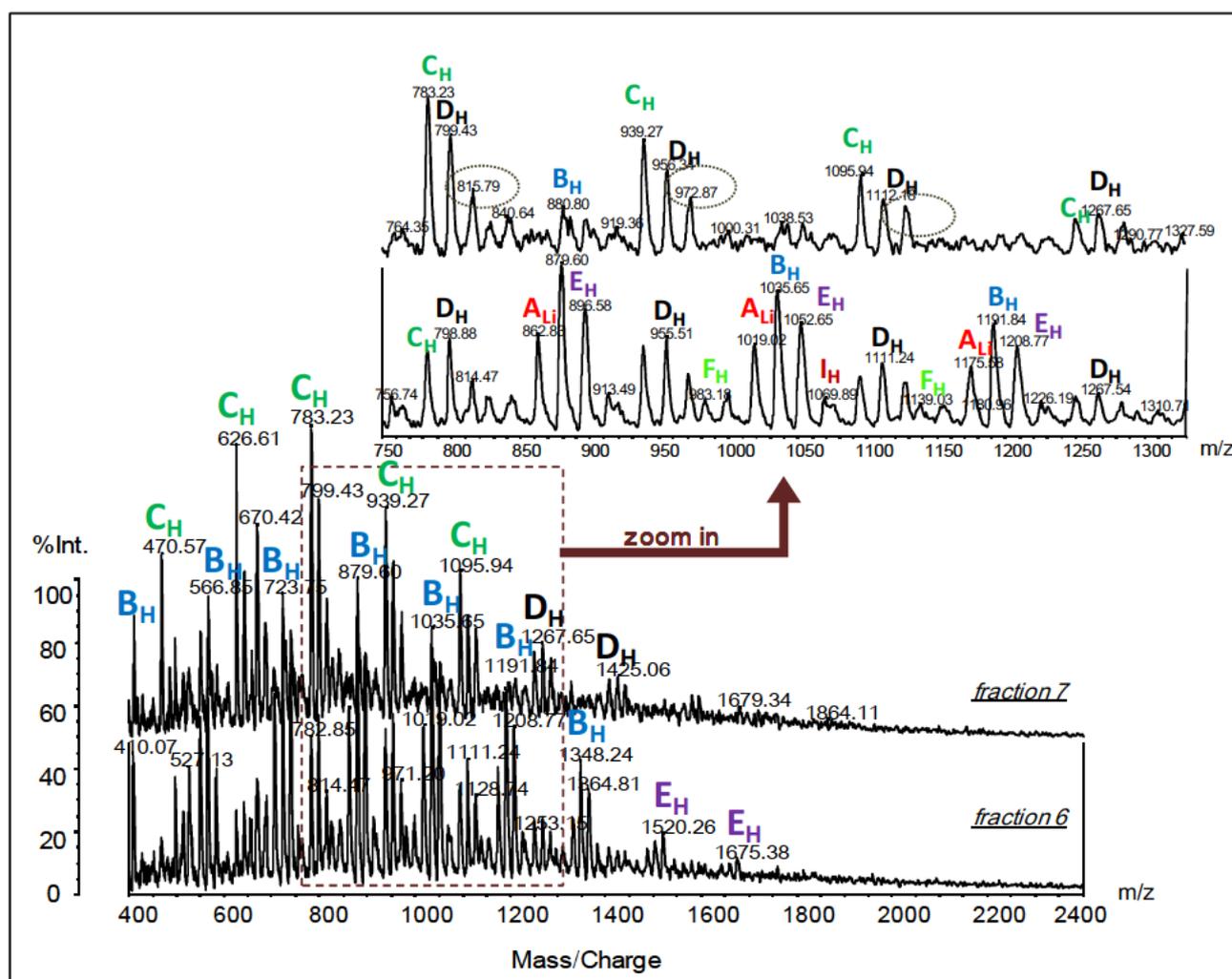
Figure 39. MALDI-TOF MS spectra of fractions 6 and 7 in the range m/z 400 to m/z 2400. A more detailed assignment is given in the zoomed-in range of m/z 750 to m/z 1300. All labels refer to the structural assignments made from bulk MS analysis with the subscripts donating the specific cationizing adduct

However, since both aforementioned structures had peaks of reasonable intensity in the bulk sample ESI spectra conducted previously it would be false to assume that they don't have molecular weight distributions

Results and Discussion

within this range. A better proposal would rather be that their ionization in the MALDI-TOF technique is insufficient in comparison to ESI MS, thus explaining their absence. The variation in ionization efficiency could also be the reasoning behind the fact that different structural species appear to dominate in the two different fractions. Importantly, an unknown structural distribution was found at m/z 815, m/z 972 and m/z 1128 which has a repeating unit mass of 156Da. Due to the fact that this peak distribution was found in both positive and negative mode ESI of the bulk sample analysis, it can be concluded that it cannot be a Li^+ related adduct. In addition, it has a mass difference of 16Da when compared to the most simplified structure of the MA-PG batch namely **D** (HO-[MA-PG]$_n$-H).

The MALDI-TOF MS spectrum of fraction 8 presented in Figure 40 serves as the final fraction in the investigation, since fraction 9 proved to be baseline noise only, indicating that the majority of the sample has in fact been eluted from the stationary phase. Even though the mass range from m/z 1000 to 6000 overlaps with the range illustrated in fractions 6 and 7 at the lower molecular weight side, the oligomeric distribution reaches a value of approximately m/z 3500, which is much higher than the average distribution obtained from the MALDI-TOF analysis of the bulk sample s16. The zoomed insert shows that only four peak distributions dominated which included m/z values for structures **A** to **D**. The assignment of this particular fraction is identical to that of the initial MS analysis conducted on the bulk samples of the MA-PG batch, s11 to s16.
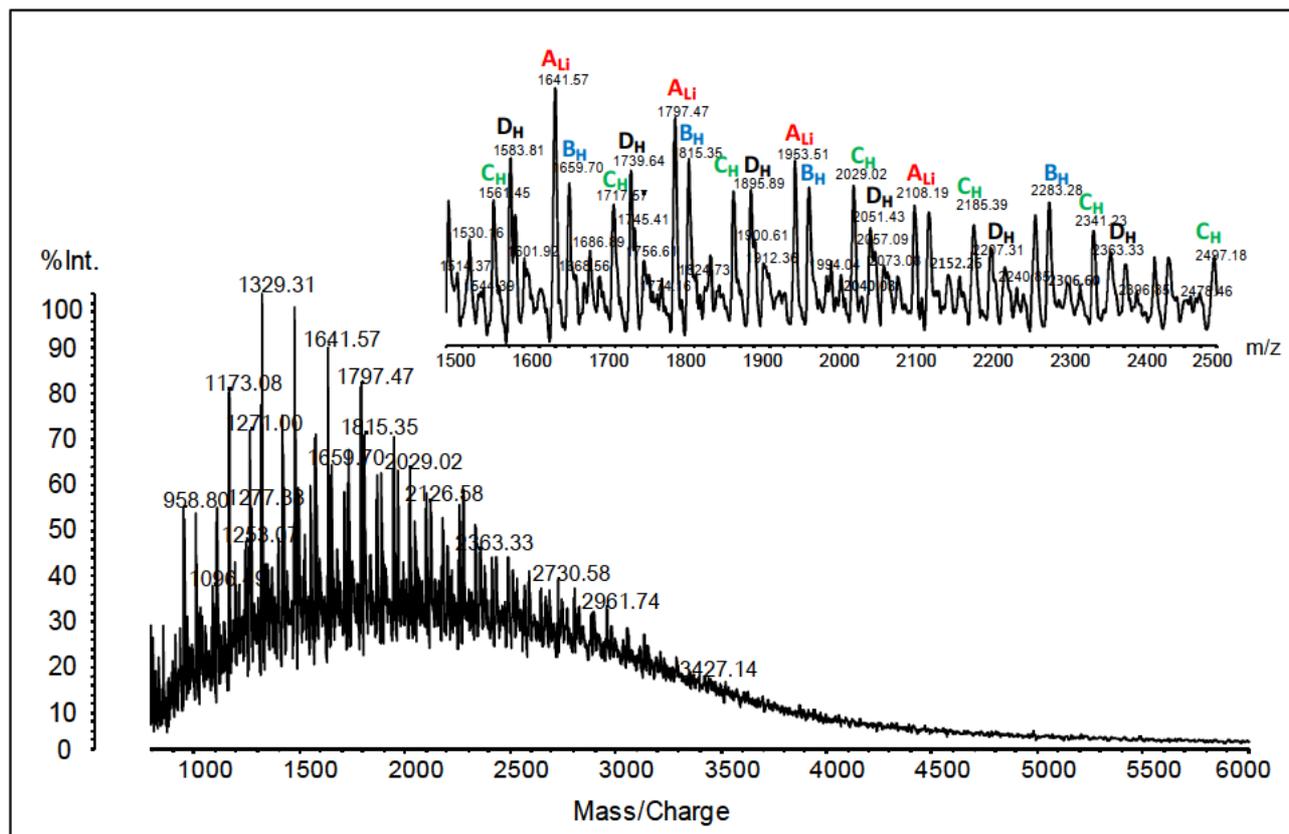
Figure 40. MALDI-TOF spectra of fraction 8 from m/z 1000 to m/z 6000. The structural assignments are presented in the zoomed insert.

It is most likely that these structures constitute the bulk of the structural composition of the polyester throughout the polyesterification reaction and mask the presence of the additional, secondary structures. The

Results and Discussion

only difference here is that besides structure A which is lithium cationized, all the other distribution values are H$^+$ related adducts.

4.2.2 ESI-QTOF MS as off-line detection

Owing to the fact that during the gradient HPLC analysis of the bulk sample s16, most of the sample constituents appear to be separated and eluted from the stationary phase between the elution volume of 20-35ml, the ESI-QTOF MS spectra of fractions 5 to 7 are presented and discussed. In similarity to the MALDI-TOF analysis, the positive mode ESI results obtained molecular weight distributions that spanned from approximately m/z 400 to 1500 for all three fractions. Surprisingly, the spectra were somewhat simplified in comparison with the PA-PG batch since, in all the fractions clearly defined oligomeric distributions were found for what seemed to be the major structural constituents. In addition, the m/z values for all the peaks appeared to be proton related adducts only, thus enabling a much more basic assignment. In Figure 41, the molecular weight distribution of fraction 5 is slightly lower than those of fraction 6 and 7, but very little difference was found between the two latter spectra in terms of mass. The most obvious variation was the change in intensity of the assigned peaks from the earlier to later fraction. In fraction 5, the dominating distributions were cyclic structures of **b** ([MA-PG]$_n$-MA), **c** ([MA-PG]$_n$) and **g** (PG-[MA-PG]$_n$) with the latter starting with as low a value of n=1 at m/z 215. Clearly, the rest of the structures which have been assigned in the previously discussed MALDI-TOF analysis are also present but due to their much weaker intensities they make part of the highly dense smaller distribution envelope. The difference between the two techniques can be ascribed to the fact that the addition of Li salt, although affording and/or aiding ionization in the MALDI-TOF, also lead to the drowning of peaks related to structures which are not as favorable to lithium cationization. Concomitantly, fraction 6 shows the increasing peak intensity of the oligomeric distributions associated with the linear structures **d** (HO-[MA-PG]$_\mathbf{n}$-H) and **e** (HO-[MA-PG]$_\mathbf{n}$-MA) with both starting at n=2 degrees of oligomerization. Peaks related to structure **b**, however, remain the dominating distribution reaching a value of m/z 1503, while the distribution of structure **c** start to become smaller in intensity.

In contrast to the MALDI-TOF analysis of the associated fraction, the positive mode ESI spectra of fraction 7 presented structures **d** and **e** as the main entities, with the oligomeric distributions of **b** and **g** having much decreased intensity compared to the previous two fractions and structure **c** related peaks masked in the smaller intensity distribution envelope. In addition, fraction 7 also indicated the increasing value of n for structure **f** (CH$_3$-HC=CH-[MA-PG]$_n$-H), suggesting that its presence becomes increasingly significant at higher molecular weights.

Results and Discussion
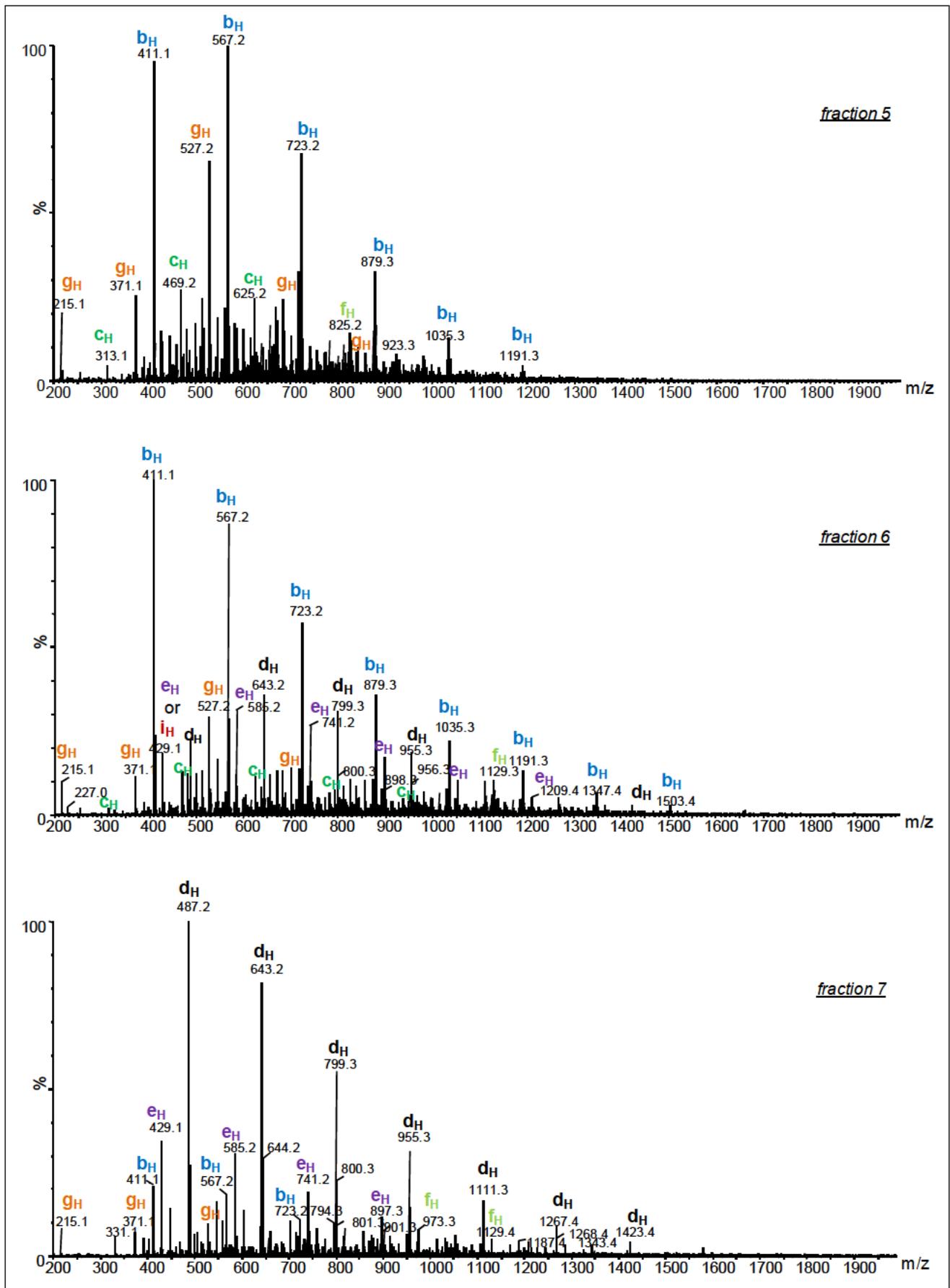
Figure 41. ESI-QTOF MS spectra of fractions 5, 6 and 7 of sample s16 in the MA-PG batch with positive mode ionization. The fractions show the H+ related adduct distributions obtained for the dominating oligomeric structures

82

Results and Discussion

In order to evaluate the variation in peak intensity of the different distributions assigned in the previous spectra with increasing molecular weight, the relative intensity values are plotted against the elution volume of each fraction in Figure 42. The goal was to investigate whether a qualitative trend could be determined with regards to the abundance of the linear structures versus that of the cyclics. The graph shows the relationship between the total relative concentrations of the peaks in the most abundant structural distributions in relation to each other. It can be seen that the cyclic structures **b**, **c** and **g** initially dominate in presence and percentage intensity but as the molecular weight increase, the presence of linear structures become more apparent.

b cyclic of $[MA-PG]_n$-MA
c cyclic of $[MA-PG]_n$
d $HO-[MA-PG]_n$-H
e $HO-[MA-PG]_n$-MA
f $CH3-HC=CH-[MA-PG]_n$-H
g cyclic of $PG-[MA-PG]_n$
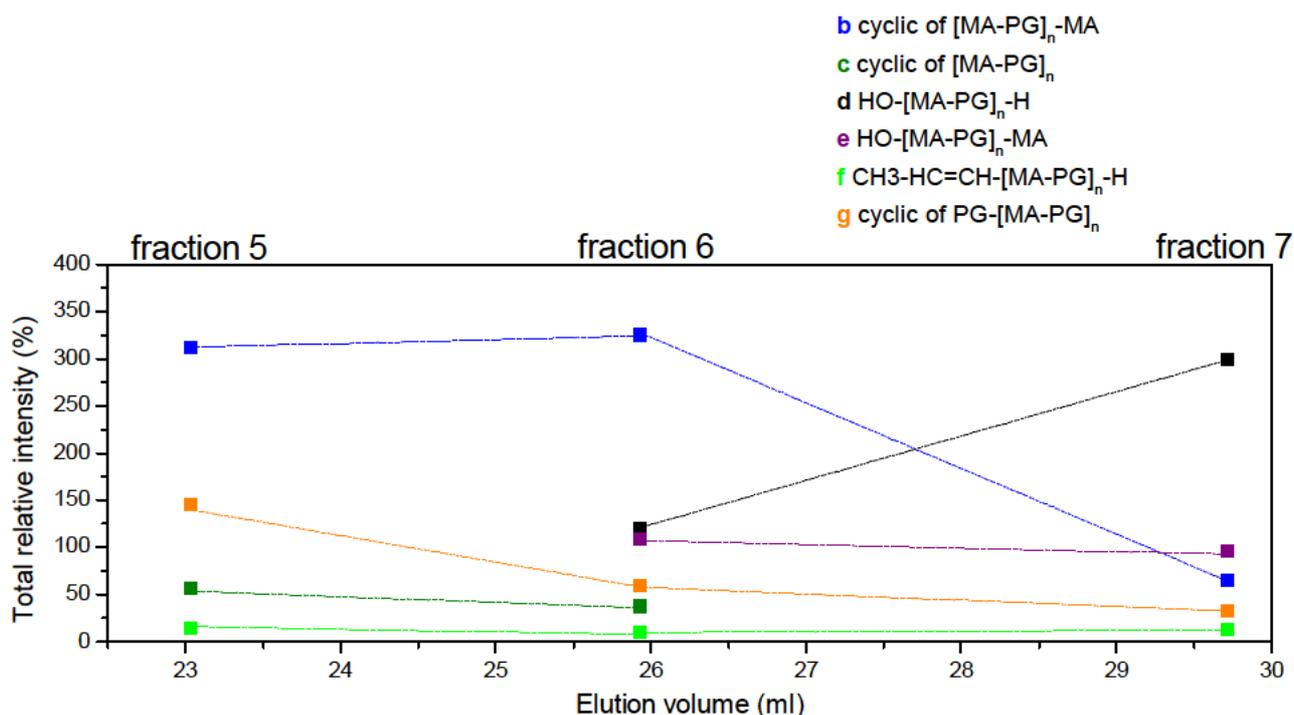
Figure 42. The relative peak intensities of the most abundant peaks representing the different structural distributions obtained in positive mode ESI-QTOF MS ionization in relation with their fractionation elution volume.

The m/z values corresponding with the structural assignments of the main peak distributions in the three fractions along with their values of n are summarized in Table 13. With the exception of **g**, which only had peaks up to a value of n=3, all the other structural entities are present at several values of n, ranging from n=2 to n=9. Moreover, the unknown structural assignment indicated in the MALDI-TOF analysis of fraction 7 in the previous section, was not found as a noteworthy distribution but rather was part of the smaller dense envelope. Due to the isotopic resolution found in ESI MS, the corresponding m/z values were also in close proximity of the peaks related to structure **f**, which made an unambiguous assignment difficult.

Results and Discussion

Table 13. Structures identified from ESI-QTOF MS analysis of fractions 5, 6 and 7 of sample s16 in the MA-PG batch with positive mode ionization. The m/z values correspond to the H^+/ related adducts found at different degrees oligomerization in each fraction

Structures	Label		Values for n		
cyclic of $[MA\text{-}PG]_n\text{-}MA$	b	n	2	6	9
		$m/z_{(exp)}$	411	1035	1503
cyclic of $[MA\text{-}PG]_n$	c	n	2	4	6
		$m/z_{(exp)}$	313	624	936
$HO\text{-}[MA\text{-}PG]_n\text{-}H$	d	n	2	3	9
		$m/z_{(exp)}$	330	486	1422
$HO\text{-}[MA\text{-}PG]_n\text{-}MA$	e	n	2	5	7
		$m/z_{(exp)}$	428	895	1207
$CH_3HC=CH\text{-}[MA\text{-}PG^+]_n$	f	n	5	6	7
		$m/z_{(exp)}$	825	981	1129
cyclic of $PG\text{-}[MA\text{-}PG]_n$	g	n	1	2	3
		$m/z_{(exp)}$	215	371	527

The negative mode ESI analysis of the fractions conferred the same molecular weight distributions as found in the positive mode ionization. Due to the presence of a large variety of endgroup combinations consisting of carboxylic acid functionalities which are more susceptible towards deprotonation, the corresponding spectra in Figure 43 illustrate densely populated distributions. Even though fraction 6 and 7 appear to be virtually identical in terms of a larger number of structures dominating, the variation in peak intensities also appeared to be more pronounced. In fraction 5, the mean distributions could be correlated back to structures **b**, **d**, **e** and **a,** with **d** having the most defined distribution starting at m/z 329. Even though **a** and **e** could be identified from m/z 388 and 271 respectively, they were mostly confined to the crowded distributions showing much lesser intensities. Fraction 6 and 7 had the addition of clearly defined distributions of structure **f** and **h** although their peak intensities are reversed going from the aforementioned fraction to the last. In addition, peaks from the unknown entity mentioned in the positive mode ionization were also present in fraction 7 from m/z 825 onwards, yet for the same reasons could not be assigned conclusively.

Results and Discussion
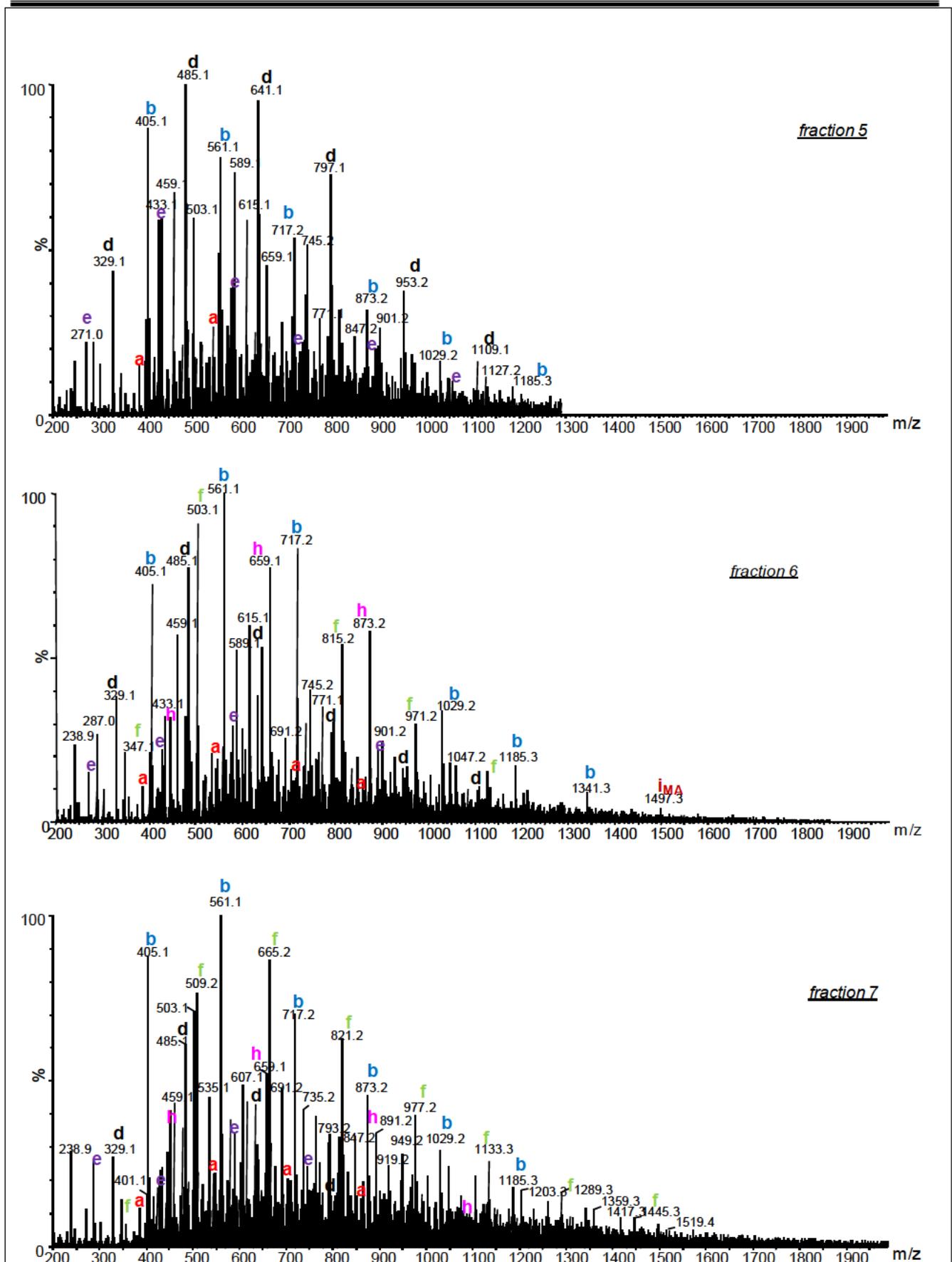
Figure 43. ESI-QTOF MS spectra of fractions 5, 6 and 7 of sample s16 in MA-PG batch with negative mode ionization. The fractions show the deprotonated structures and their corresponding oligomeric distributions

85

Results and Discussion

The relative peak intensity relationship between the different structural distributions obtained with negative mode ESI-QTOF MS is given in Figure 44. In general, the negative mode trend corresponds well to that found with positive mode in that peaks having the highest relative percentage are still due to **b** and **d**. Interestingly, opposite trends are found going from fraction 5 to 7 for the two structural distributions in the present case but that is most likely due to deprotonation affinity. More importantly, the peak distributions of secondary structures compared to the expected linear structures become more significant towards higher elution volume.

a PG-[MA-PG]$_n$-H
b cyclic of [MA-PG]$_n$-MA
d HO-[MA-PG]$_n$-H
e HO-[MA-PG]$_n$-MA
f CH3HC=CH-[MA-PG]$_n$-H
h H-[PG-MA-PG]$_n$-H
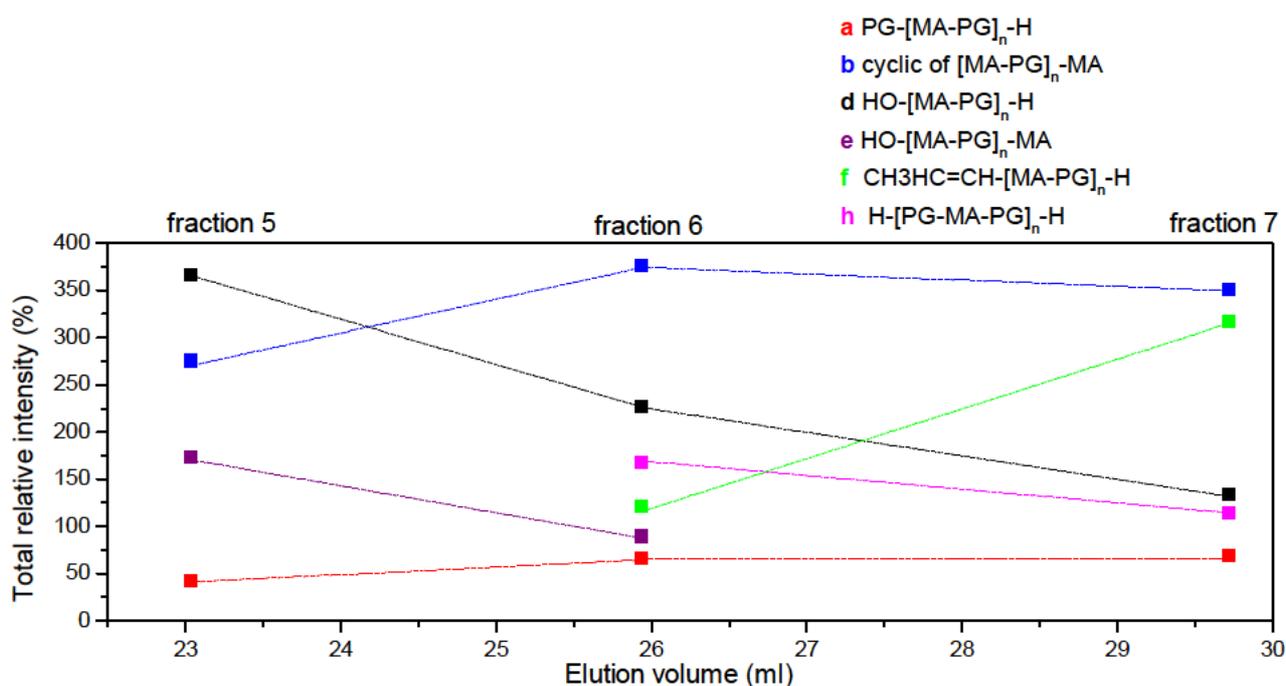
Figure 44. The relative peak intensities of the most abundant peaks representing the different structural distributions obtained in negative mode ESI-QTOF MS ionization in relation with their fractionation elution volume.

The assignments of all the structures and their corresponding degrees of oligomerization are compiled in Table 14. With the exception of structure **i**, the values of n span over a large range from n=2 to n=8, especially in the case of structures **b** and **f**. In fact, structure **i** was found only at m/z 1497, supporting the theory that these secondary structural distributions become increasingly important towards higher molecular weights and later stages of the polyesterification reaction. Furthermore, the presence of chains having the structural conformation of **c** and/or **g** should not be ignored as they could possibly have less affinity towards deprotonation or be masked in the smaller intensity distribution envelope.

Results and Discussion

Table 14. Structures identified from ESI-QTOF MS analysis of fractions 5, 6 and 7 from sample s16 in the MA-PG batch with negative mode ionization. The m/z values correspond to the deprotonated structures and their oligomeric distributions

Structures	Label		Values for n		
PG-[MA-PG]$_n$-H	a	n	2	4	5
		m/z$_{(exp)}$	387	699	855
cyclic of [MA-PG]$_n$-MA	b	n	2	5	8
		m/z$_{(exp)}$	409	877	1345
HO-[MA-PG]$_n$-H	d	n	2	5	7
		m/z$_{(exp)}$	329	797	1109
HO-[MA-PG]$_n$-MA	e	n	2	4	6
		m/z$_{(exp)}$	427	740	1052
CH$_3$HC=CH-[MA-PG$^+$]$_n$	f	n	2	6	9
		m/z$_{(exp)}$	353	977	1445
H-[PG-PG-MA]$_n$-H	h	n	2	4	5
		m/z$_{(exp)}$	429	857	1071
cyclic of [PG-PG-MA]$_n$	i	n	-	-	4
		m/z$_{(exp)}$	-	-	856

In essence, utilizing both modes of ionization available in ESI-QTOF MS in combination with the results obtained from MALDI-TOF made it possible to give detailed insight into the extent of structural variation present within isolated, narrowly distributed fractions collected from gradient elution HPLC. From the mass spectrometry techniques, it was possible to conclude that even though the LC separation behavior for both of the polyesters was based on the elution of oligomers with increasing degree of n, their separation efficiency was very different. The PA-PG bulk sample s28 was fractionated into well-defined distributions, of which the MS data corresponded extremely well in terms of ionization efficiency and dominating structures and could be correlated back to the bulk sample analysis. The formation and importance of cyclic structures in conjunction with their linear counterparts at early eluting peaks was established.

In the same manner, the complexity of the MA-PG polyesterification reaction was highlighted. The mass spectrometry provided the evidence that increasingly more structural entities are being produced throughout the synthesis. In turn, the extent to which they are present ensures that a dominating principle behind the basis of separation is difficult to achieve. Nevertheless, the fractionation results proved to be invaluable as structures present in lesser quantities could be identified whereas they are normally masked by the main distributions in the bulk analysis. Subsequently, the importance of HPLC separation and fractionation methods is, therefore accentuated. Employing the additional feature of negative mode ESI MS in both polyester batches, ensured the identification of additional structures whose presence would otherwise would not have been known. Even though conclusive assignments could not be made, their deprotonation behavior suggests that they are likely to consist over carboxylic acid related functional groups.

Part IV. Experimental

1. Chromatography

1.1 Chromatographic equipment

Separations were achieved on an Agilent 1260 Infinity series (Agilent Technologies) consisting of a 1260 degasser and quaternary pump, 1260 ALS auto-sampler and 1260 variable wavelength UV detector operating at a wavelength of 254nm. A Polymer Labs PL-ELS 1200 series evaporative light scattering detector was also used. A flow rate of 1ml/min was applied with a column oven temperature of 30°C.The injection volumes varied from 20µl to 100µl depending on the type of chromatography conducted. The sample concentrations varied from 5-20mg/ml depending on the LC technique being employed. In the case of two-dimensional chromatography the chromatographs were connected via an electronically driven eight-port injection valve (Valco) and two storage loops of 100µl each was used. The flow rate in the first dimension was reduced to 0.05ml/min with an injection volume of 50µl while the flow rate in the second dimension was set to 4ml/min. Chromatograph 1 represents the liquid adsorption separation and chromatograph 2 the size exclusion separation. Data collection was done by the "PSS WinGPC Unity" (Polymer Standards Service, Mainz, Germany) software.

1.2 Stationary phases

1.2.1 SEC

Set of three columns, PLgel 3µm Guard (50 x 7.5mm) and 2 PLgel 3µm Mixed-E (300 x 7.5mm) (Polymer Laboratories, Varian Inc. Shropshire, UK).

PL-Rapide L, 100 x 10mm I.D. (Polymer Laboratories, Varian Inc. Shropshire, UK)

1.2.2 Gradient HPLC

Silica 100Å, 5µm, 250 x 4.6mm I.D (Machery-Nagel, Düren, Germany)

Discovery® CN 100 Å 5µm, 250 x 4.6mm I.D. (Supelco Bellefonte, USA)

Nucleosil® 100-5 C18, 100 Å 5µm, 250 x 4.6mm I.D. (Machery-Nagel, Düren, Germany)

1.3 Solvents

Solvents used were acetonitrile (ACN), dichloromethane (DCM), hexane (Hex), tetrahydrofuran (THF), and water, all of HPLC-grade (Sigma-Aldrich, South Africa).

Experimental

1.4 Polymer standards for calibration:

All narrow distributed polymer standards of polystyrene (PS) were purchased from Polymer Laboratories (Varian Inc. Amherst, USA)

2. Mass spectrometry

2.1 MALDI-TOF MS

MALDI-TOF spectra were recorded on a Shimadzu Biotech Axima ToF2 in linear mode. The phthalic anhydride/propylene glycol (PA-PG) batch samples were dissolved in THF (4mg/ml), with dithranol in dioxane (10mg/ml) as matrix and the best results obtained were in the absence of salt. The maleic anhydride/propylene glycol (MA-PG) batch samples were dissolved in THF (4mg/ml), with LiCl as cationizing agent and no matrix.

2.2 ESI-MS

ESI spectra were recorded on a Waters API quadrupole time –of-flight (Q-TOF) Ultima mass spectrometer. The injection volume was 3 µl. The mass spectrometer was operated in positive ionization mode with a capillary voltage of 3.5kV and a cone voltage of 35V, RF1:40. The source temperature was 100 ºC. Masses were scanned from 200 to 2000 amu and data were collected and processed using MassLynx v.4.0 software (Waters). A NaF solution was used for calibration. A desolvation temperature of 350 ºC was applied, whereas the desolvation and cone gas flows (N_2) were 350 l/h and 50 l/h respectively.

3. Samples

All the polyester samples were synthesized on a laboratory scale and supplied courtesy of Freeworld Coatings Research Centre (Stellenbosch, South Africa).

Polyester synthesis

The propylene glycol (PG) and maleic anhydride (MA) or phthalic anhydride (PA) is charged to a 4-neck 1l reactor fitted with a condenser, temperature probe and stirrer. N_2 is blown into the reactor before heating starts for approximately 15 minutes to displace any oxygen, after which it is blown throughout the whole process. The mixture is heated using a heating mantle from room temperature to 220ºC. Sampling from the reactor commenced once the first drops of water distilled off (usually at ±180°C), and thereafter at the predetermined levels of extracted water, subsequently at different molecular weights. Reactant quantities for the two different batch types can be found in Table 13.

Experimental

Table 15: Reactant quantities of the respective MA-PG and PA-PG batches.

Batch	Propylene Glycol (PG) (g)	Maleic Anhydride (MA) (g)	Phthalic Anhydride (PA) (g)
30% more PG than MA	495.88	491.54	-
30% more PG than PA	353.16	-	528.78

Part V. Summary and Conclusions

The application of several polymer characterization techniques to successfully achieve the aims of the current dissertation was demonstrated. Liquid chromatography, mass spectrometry and their respective coupling methodologies allowed detailed information regarding two inherently different model anhydride polyester batches synthesized with a 30% molar excess of glycol. Investigations of the kinetic sample sets entailed the elucidation of a variety of aspects which included the subsequent differences at various stages of the polyesterification reaction in terms of distributive properties, as well as possible structural conformations associated with each polyester batch. The study indicated that all of these aspects related to each of the anhydride systems, should be considered in the case of utilizing both in copolyester synthesis to produce industrial type polyester resins.

The results for the current dissertation are summarized as follow:

I. Different modes of LC were developed and successfully employed to investigate two polyester batches consisting of phthalic anhydride- and maleic anhydride-1,2-propylene glycol, respectively. From SEC, an oligomeric separation was achieved in all samples, with average molecular weight values ranging between approximately 100-6000mg/ml based on polystyrene calibrations. In order to investigate the differences obtained between calculated and experimental values, efforts were made to achieve more absolute values in terms of molecular weight distribution by conducting fractionation on the last sample in the polyester batch. As a complimentary technique, MALDI-TOF MS results of the fractions corresponded well with that of SEC up to a degree of oligomerization of n=7. With increasing molecular weight, an increasing deviation was found between the values obtained from the two analyses techniques in that the average molecular weight from MALDI-TOF MS was considerably lower. In addition, the mass spectrometry gave the first indication towards the presence of species consisting of different endgroup functionalities and structural conformations. In LAC investigations, the elution behavior of the two batches differed to such an extent that a single stationary phase-mobile phase combination optimized for both systems could not be developed. Normal-phase gradient HPLC, with a CN- functionalized stationary phase and THF/hexane as mobile phase composition was used to achieve successful separation of the PA-PG polyester samples. Several steps were followed to achieve an optimized gradient profile and although base-line separation was not achieved, the samples were fractionated into several peak distributions. The early eluted peaks demonstrated peak-splitting behaviour, which suggested that the separation was affected by a combination of factors and not solely based on chemical composition, functionality type or degree of polymerization. Analysis on samples taken during different stages of the esterification reaction illustrated the formation and continuation of an increasing number of peak distributions, signifying that lower species associated with the onset of the reaction need to be considered in the final product. In contrast, the reversed-phase gradient HPLC analysis of the MA-PG polyester samples showed poor reproducibility, long elution times and weak selectivity. The C18-functionalized stationary phase with a THF/hexane mobile phase combination produced only slight variations in separation between the different kinetic samples. Finally, the link between chemical composition and molecular weight distribution was determined via the on-line coupling of the two LC techniques. The 2D gradient HPLC x SEC results of the last sample in each batch highlighted the differences in separation efficiency of the gradient HPLC conditions used for the two polyesters. From the PA-PG sample contour plot

Summary and Conclusions

several entities could be identified compared to only two distributions found in the MA-PG sample. The contour plots of the kinetic samples in the PA-PG polyester batch were a visual confirmation that the first dimension gradient HPLC separation was based on chemical composition with increasing degree of oligomerization in the second dimension. Following the PS calibration of the SEC separation, the two polyesters exhibited similar values in molecular weight distribution as obtained from the one dimensional analysis.

II. MALDI-TOF and ESI-QTOF mass spectrometry were utilized as complimentary techniques to LC in order to investigate the accurate molecular weight distributions of the bulk samples in each of the polyester batches. More importantly, the obtained spectra allowed the determination of repeat unit values, endgroup combinations as well as identify linear and cyclic structures in both cases. In turn, the complex heterogeneity with regards to chemical composition between the polyesters was confirmed.

MALDI-TOF MS: In order to achieve optimized reproducible results, different methodologies for the PA-PG and MA-PG samples involving different sample preparation procedures were successfully developed. In each case, the kinetic samples were analyzed to determine their molecular weight distributions in comparison to the SEC values found previously as well as to investigate their variation from sample to sample. Very different ionization patterns were found for the two batches in that Na^+ and K^+ adducts dominated for the phthalic polyesters while H^+ and Li^+ adducts were predominantly found for the maleic polyesters. The PA-PG results illustrated the presence of higher species up to $n = 14$ which were previously unresolved in SEC, while much lower distributions of $n = 5$ were found for the MA-PG samples. In both instances, linear and cyclic structures were identified consisting of different endgroup functionality combinations, most of which correlated well with the excess glycol present during the synthesis procedure. The peak intensities of the linear structures were the most intense, suggesting that they are the main distributions being formed. In the PA-PG bulk sample analysis, m/z values corresponded to the following three linear structures: HO-[PA-PG]$_n$-PA, HO-[PA-PG]$_n$-H and PG-[PA-PG]$_n$-H. The cyclic structures of ([PA-PG]$_n$) and (PG-[PA-PG]$_n$) were also identified. Importantly, a decrease in peak intensity of the cyclics with increasing molecular weight of the kinetic sample set was shown, suggesting that they are confined to the early stages of esterification. In contrast, peak intensities related to the cyclic structures found in the bulk sample analysis of the MA-PG batch had equal intensity to that of the linear counterparts throughout the sample set. The structural conformations assigned in the MA-PG set were as follows: PG-[MA-PG]$_n$-H, HO-[MA-PG]$_n$-H as well as cyclics of [MA-PG]$_n$ and ([MA-PG]$_n$-MA). Cyclic formation is believed to be increased based on the several side reactions that are possible in the MA system.

ESI-QTOF MS: The importance of attaining ESI results of the final sample in each of the polyester batches was two-fold. With positive and negative mode of ionization, it served to support the results obtained from MALDI-TOF as well as provide invaluable additional information which highlighted the higher complexity of the MA-PG polyester over that of the PA-PG batch. On the other hand, due to the higher sensitivity at hand, higher peak distributions showcasing isotopic resolution were obtained which were independent of matrix effects. As a result, the m/z values of several metal-ionized adduct structures overlapped, thus complicating the assignments. However, in agreement with MALDI-TOF, the five major structures could be identified for the PA-PG batch with positive mode ionization. Furthermore, the structural distributions illustrating the highest peak intensities for PG-[PA-PG]$_n$-H and HO-[PA-PG]$_n$-H which supports the theory that their

Summary and Conclusions

likelihood of formation is based on the excess glycol participating in the synthesis reaction. The advantage of the higher sensitivity in ESI allowed the identification of two additional structures which included a cyclic of ([PA-PG]$_n$-PA) and a linear conformation consisting of two glycol units PG-[PA-PG]$_n$-PG or PG-PG-[PA-PG]$_n$-H. More importantly, besides supporting the positive mode interpretations, negative mode ionization ensured the identification of four unknown structural conformations which otherwise would have been overlooked. The positive mode spectra of the last sample in MA-PG polyester batch allowed a more detailed elucidation compared to the MALDI-TOF analysis. Higher molecular weight distributions in conjunction with several additional structures were obtained. Two new cyclic structures ([MA-PG]$_n$-MA) and (PG-[MA-PG]$_n$), the first of which was found to have the highest peak intensity distribution were illustrated, while a new repeat unit of 214Da was also identified. The latter implicates an insertion of an extra PG unit in the original repeat unit of 156Da. Finally, m/z values corresponding to the linear structure CH$_3$-CH=CH-[MA-PG] completed the amount of 9 structural assignments in total for the MA-PG polyester sample. The negative mode analysis was dominated by the linear assignments, although consisting of lower molecular weight distributions. Overall, the mass spectrometry analysis shed light on the extent of complexity of the MA-PG system in that the linear, main structural conformations are difficult to achieve as the amount of side reactions increases with increasing degree of oligomerization. The results are supportive of the LC techniques in illustrating the variety of distributions present in both polyesters.

III. The off-line coupling of LAC with MS methodologies successfully achieved separation and identification of the separated species, essentially overcoming the limitations found during respective bulk sample analyses. Structural details in combination with improved determination of molecular weight and molecular weight distributions of the more homogeneous fractions from gradient HPLC were obtained. In employing MALDI-TOF along with both modes of ionization in ESI-QTOF MS proved that the fractionation methodology is invaluable as structures present in lesser quantities could be identified whereas they are normally masked by the main distributions in the bulk analysis and essentially overlooked.

MALDI- TOF MS of the 12 fractions from the final PA-PG sample s28 made it possible to conclude that the HPLC separation was an oligomeric separation dominated by the CCD of the main chain and that the elution order was by increasing degree of oligomerization. The low molecular weight fractions imitated peak distributions found in the bulk sample analysis, while the higher molecular weight proved to have three linear structures dominating, one of which corresponded to the same species obtained in bulk ESI which was proposed to be either dipropylene glycol, -CH=CH-CH$_3$ or –CH$_2$-CH=CH$_2$. The cyclics appeared to become negligible with increasing molecular weight fractions. Although the positive mode ESI spectra were prone to metal adduct distributions, the relative intensities of the dominating peak distributions correlated well and the increase in molecular weight ranges of the fractions were identical to the MALDI TOF results. The 4 unknown structural distributions found previously in the negative mode bulk analysis proved to have increasing importance with an increase in molecular weight.

For the MA-PG system, the hyphenation of the techniques was essential in determining the driving force behind the chromatographic behaviour. The slight shift in molecular weight distribution in the SEC separation of the subsequent fractions towards higher values suggests that the gradient HPLC separation is partial to molecular weight effect with the different distributions eluting in increasing chemical composition. In general, very different results were obtained as compared to the previous polyester batch. Both MS techniques

Summary and Conclusions

confirmed the extent of chemical heterogeneity, which is already present at the lower molecular weight fractions and continues to show considerable relative peak intensities towards higher molecular weight fractions. The MALDI-TOF spectra specifically showed equal preference to cyclic and linear structures as peak distributions didn't exhibit any dominating intensities in the lower molecular weight fractions. Due to the fact that the gradient HPLC showed weak separation efficiency, the higher species were virtually identical in that the dominating structural distributions mirrored that of the bulk sample analysis. One advantage of the fraction analysis over that of the bulk was the identification of an additional unknown structure. Another was the fact that the average molecular weight distribution of the final structure was higher than that found for the bulk sample. With the positive mode ESI results clearly defined oligomeric distributions for major constituents were obtained. The most obvious variation was the change in relative peak intensities of the major constituents present in the higher species. Mass spectrometry results were proof that increasingly more structural entities are being produced throughout the MA-PG synthesis. As a result, their participation in further randomizing the chemical composition distribution ensures that a dominating principle behind the basis of separation is difficult to achieve.

IV. The chemical structures identified during the characterization techniques employed in the current dissertation are summarized as follow:

1. Side reactions involving the starting materials at high temperature polyesterification:

Dimerization of the diol
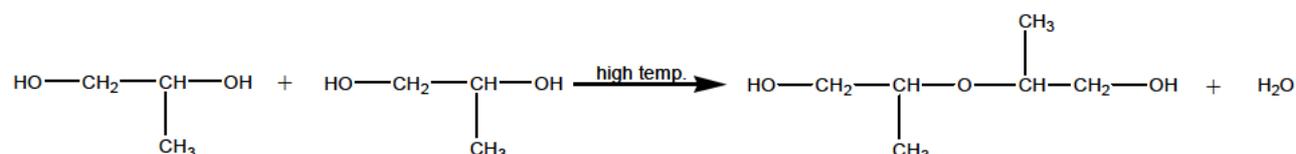
Decarboxylation of the diacid
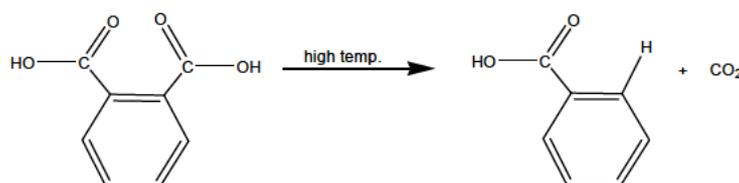
PA:
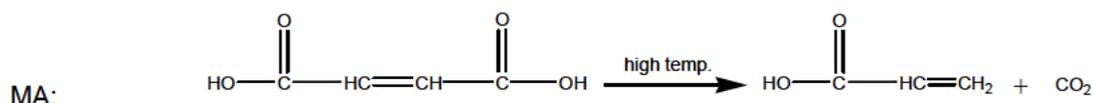
MA:

Summary and Conclusions

2. Formation of the proposed structures for the PA-PG system

(i) Monoester formation
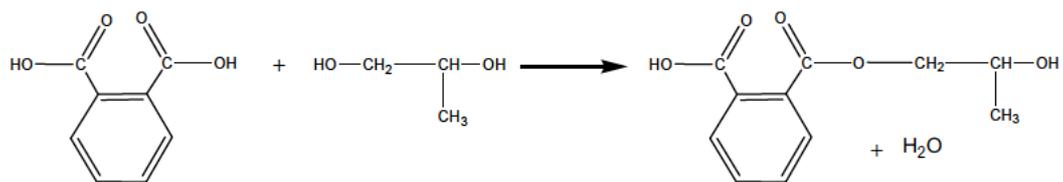
or

(ii) Polycondensation from monoester

Structure **B**

or

Structure **G**

95
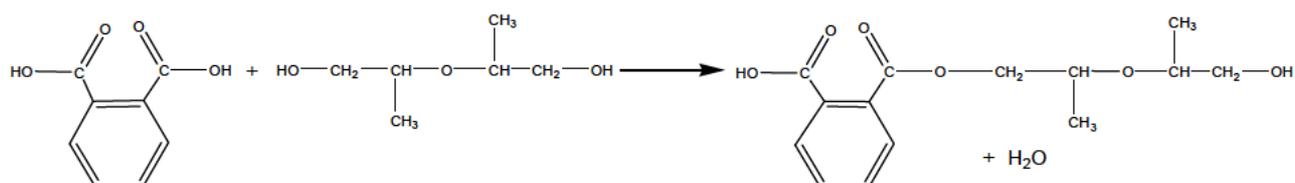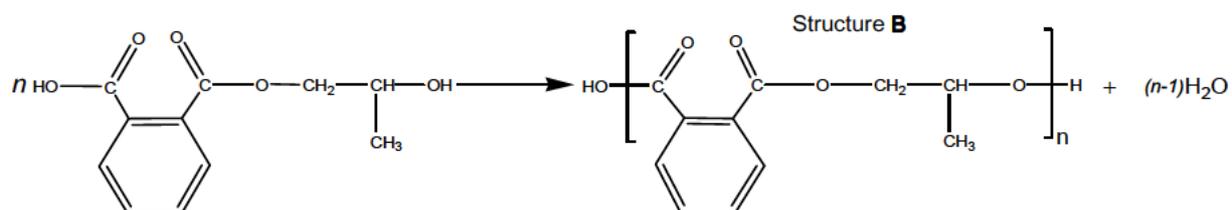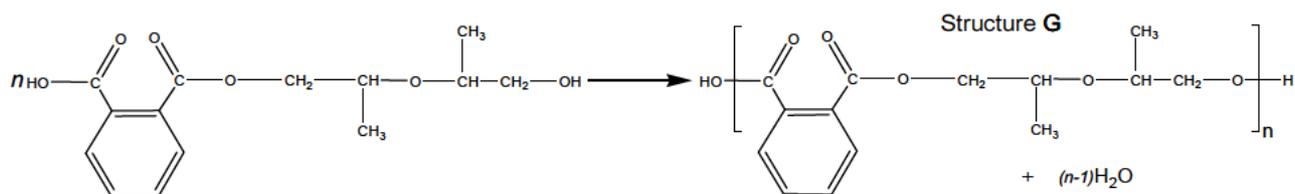
Summary and Conclusions

(iii) Endgroup variations

(iv) Cyclic formation

Summary and Conclusions

Structure **E**

+ H$_2$O

Structure **F**

+ H$_2$O
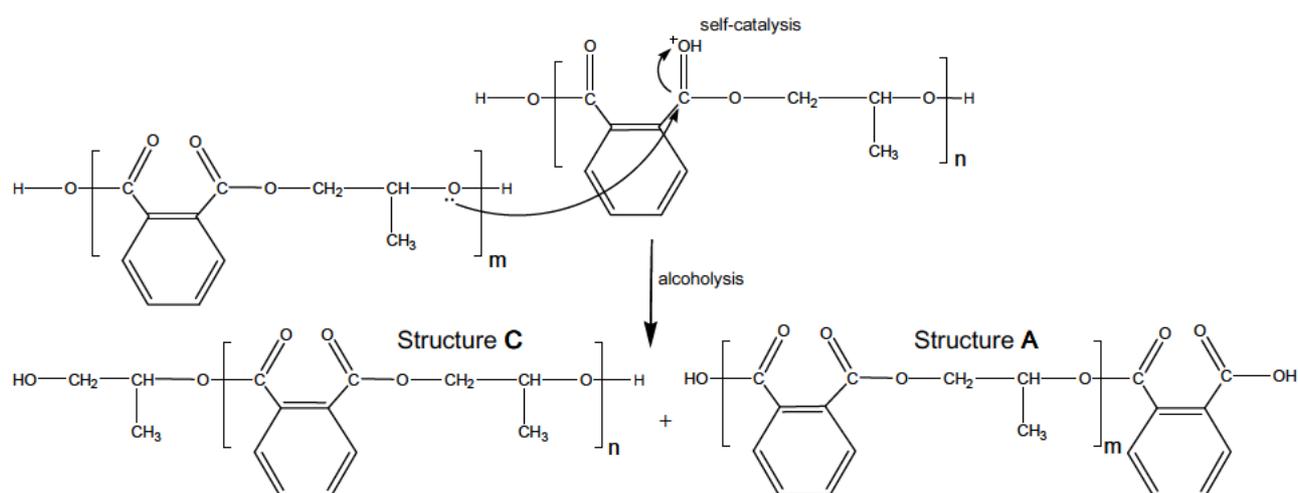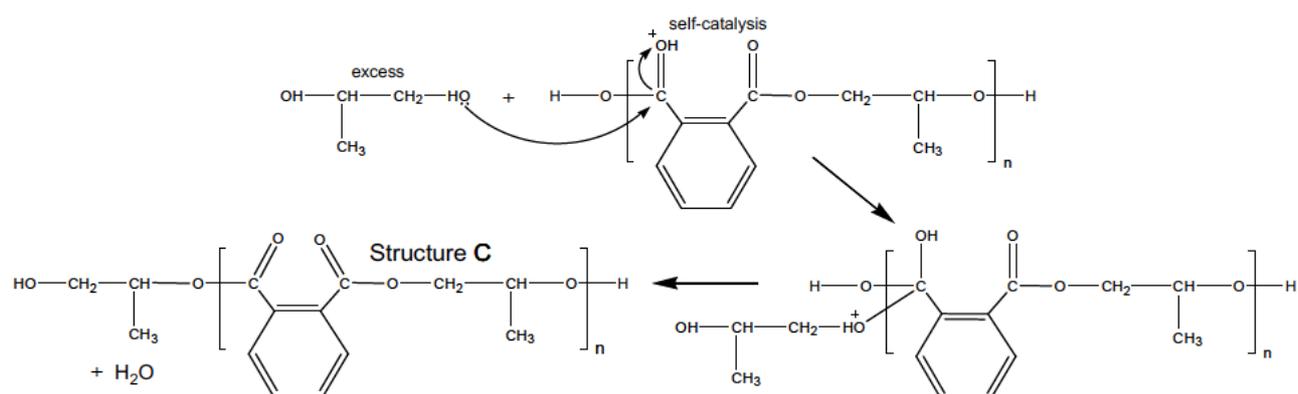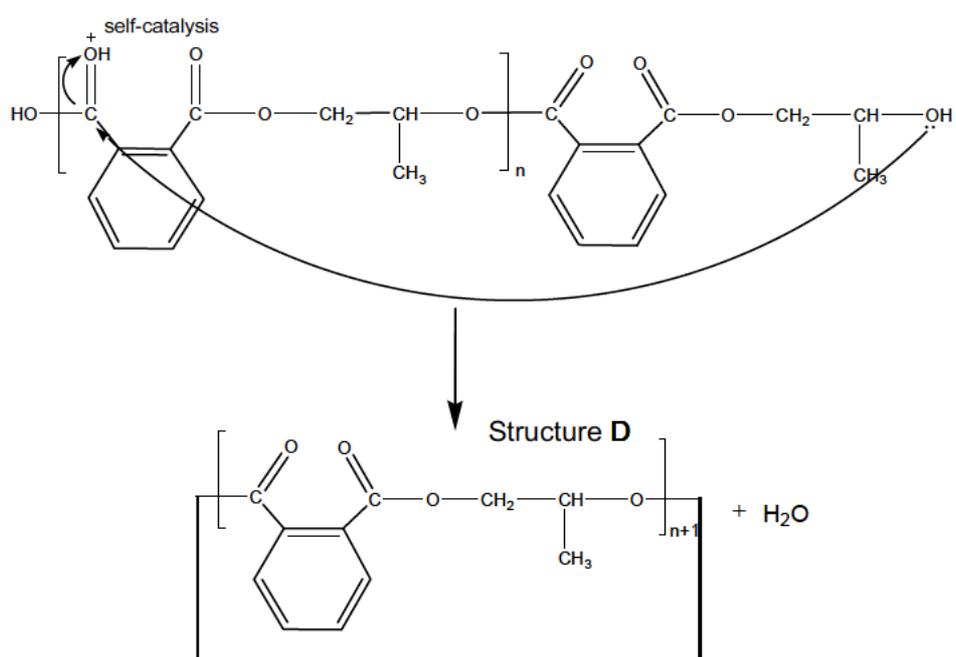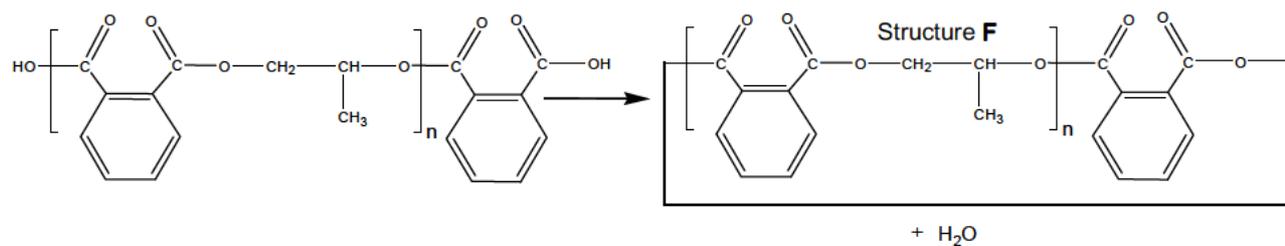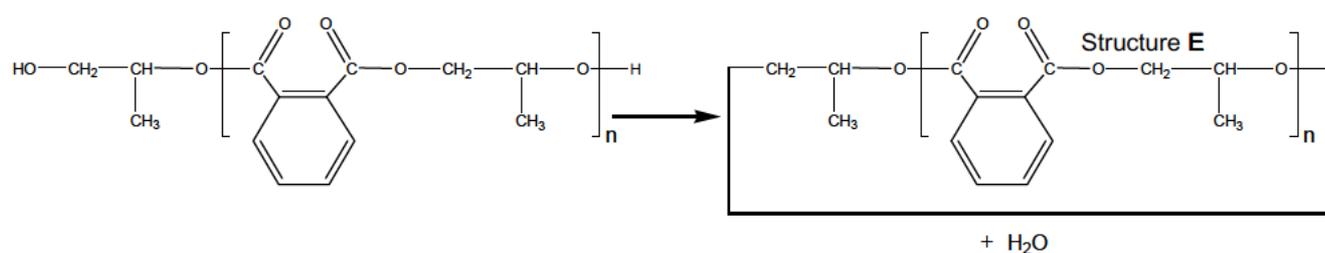
3. Formation of the proposed structures for the MA-PG system

(i) Monoester formation
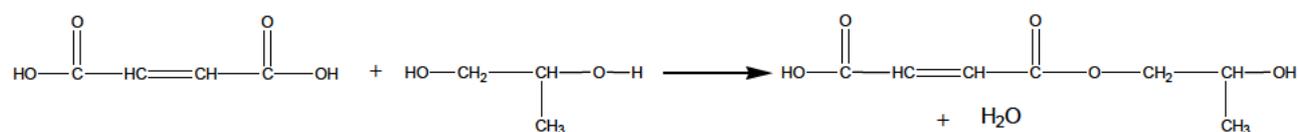
+ H$_2$O

or

+ H$_2$O

(ii) Polycondensation from monoester

Structure **D**

+

(n-1) H$_2$O

or

97
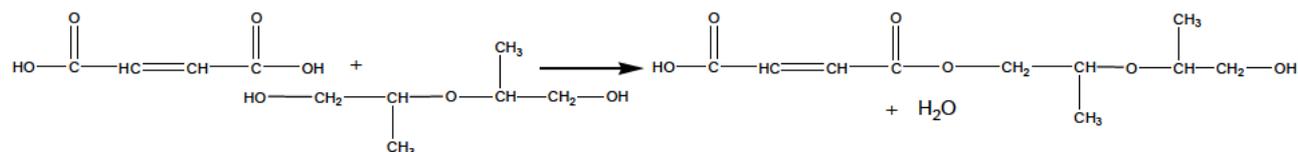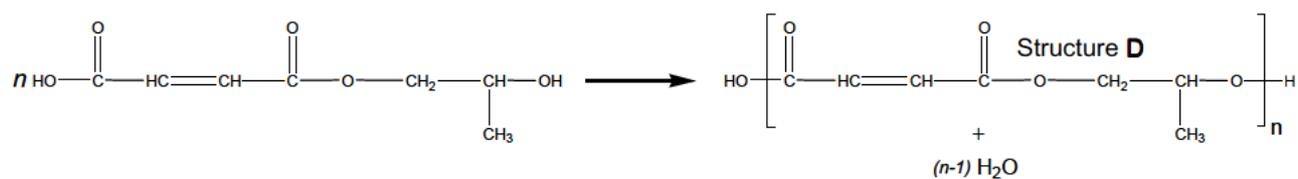
Summary and Conclusions
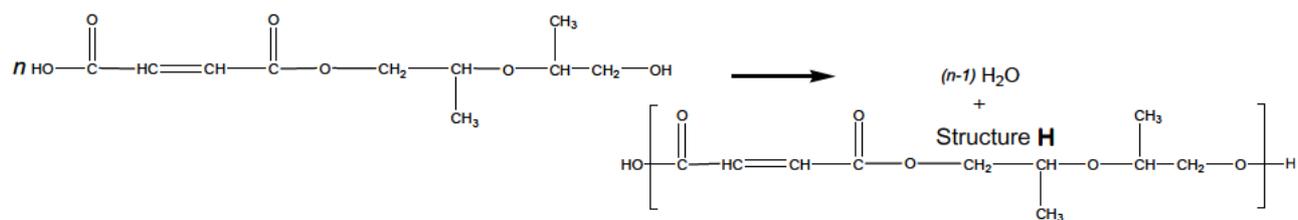
(iii) Endgroup variations
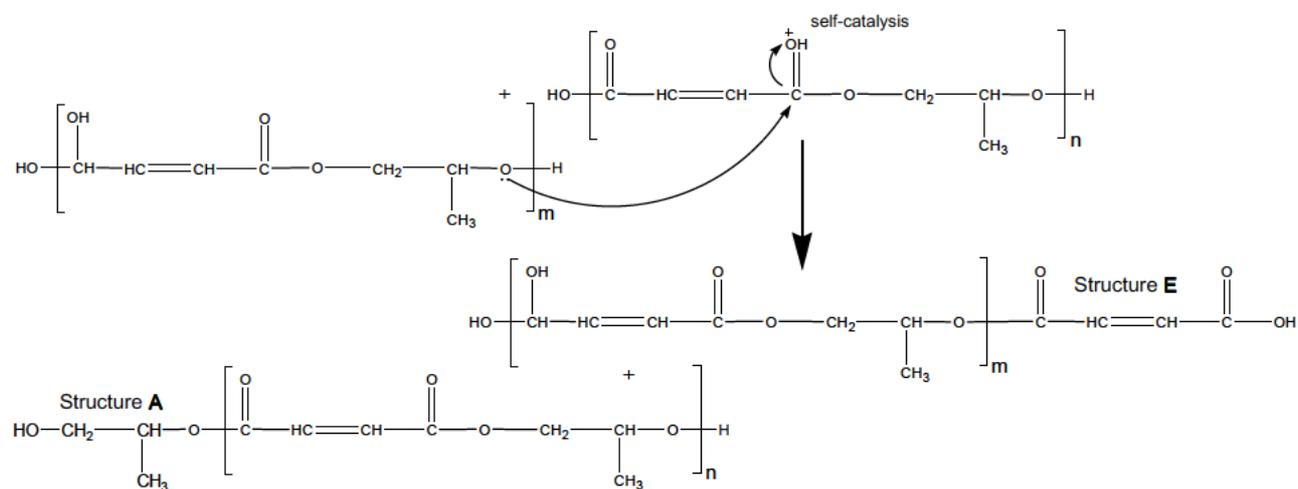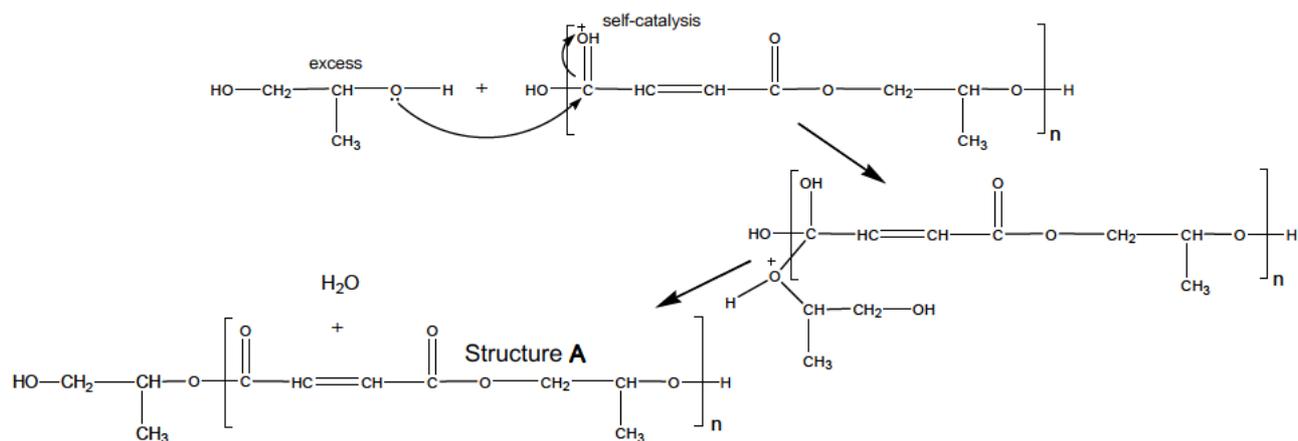
Summary and Conclusions

(iv) Cyclic formation

## *Summary and Conclusions*

Structure I
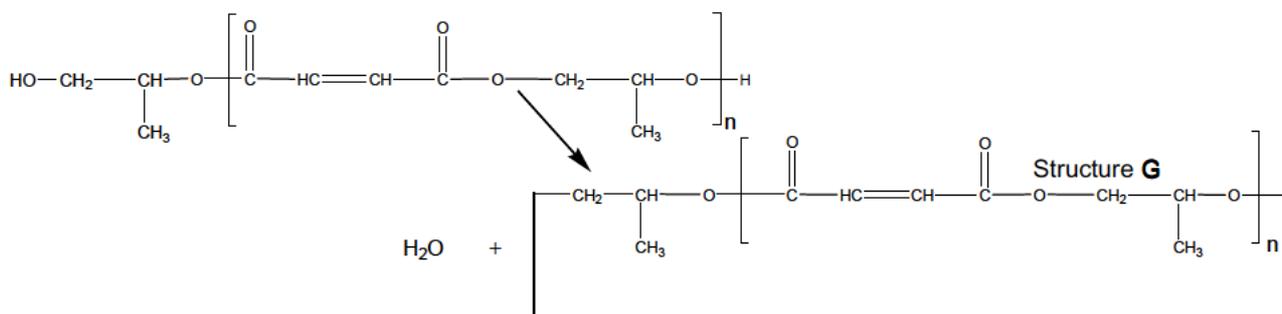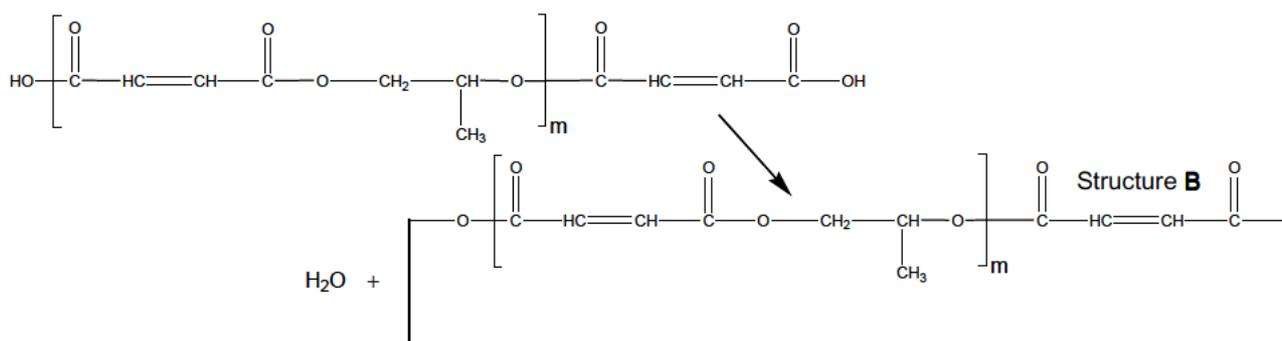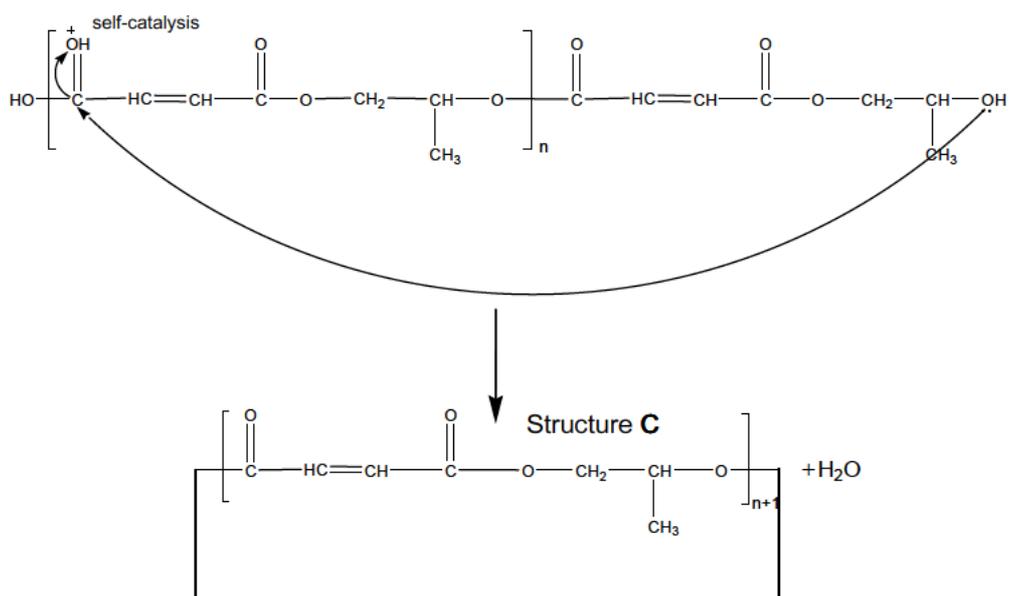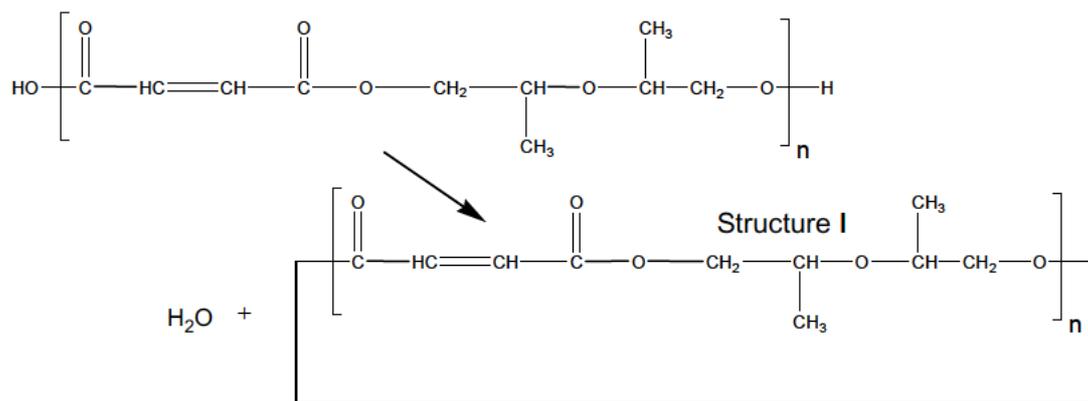
Part VI. Bibliographic References

1.   A. Pizzi, in *Handbook of Adhesive Technology, Revised and Expanded*, CRC Press, 2003.

2.   W.H. Carothers and J.A. Arvin, *Journal of the American Chemical Society*, **51**, 2560-2570 (1929).

3.   P.J. Flory, *Journal of the American Chemical Society*, **61**, 3334-3340 (1939).

4.   E.E. Parker and E.W. Moffett, *Industrial & Engineering Chemistry*, **46**, 1615-1618 (1954).

5.   E.E. Parker, *Reinforced Plastics Symposium*, **58**, 53-58 (1966).

6.   E. Makay-Bodi and I. Vancso-Szmercsanyi, *European Polymer Journal*, **5**, 145-153 (1969).

7.   G.J. Pietsch, *Ind. Eng. Chem. Prod. Res. Dev*, **9**, 149-154 (1970).

8.   A. Kaštánek, J. Zelenka, and K. Hájek, *Journal of Applied Polymer Science*, **26**, 4117-4124 (1981).

9.   B. Cherian and E.T. Thachil, *International Journal of Polymeric Materials*, **53**, 829-845 (2004).

10.   B. Cherian and E.T. Thachil, *Polymer-Plastics Technology and Engineering*, **44**, 931-938 (2005).

11.   J.F. Engelbrecht, et al., U.S. Patent, Ed., Freeworld Coatings Capital, South Africa, 2009, Vol. PCT/ZA03/00140.

12.   L.V. Cristobal and G.A. Perdomo Mendoza, *Polymer Bulletin*, **23**, 577-581 (1990).

13.   T. Salmi, et al., *Chemical Engineering Science*, **49**, 5053-5070 (1994).

14.   R. Jedlovčnik, et al., *Polymer Engineering & Science*, **35**, 1413-1417 (1995).

15.   M. Malik, V. Choudhary, and I.K. Varma, *Polymer Reviews*, **40**, 139-165 (2000).

16.   M. Shah, E. Zondervan, and A.B. de Haan, *Journal of Applied Science*, **10**, 2551-2557 (2010).

17.   I.V. Szmercsányi, L.K. Maros, and A.A. Zahran, *Journal of Applied Polymer Science*, **10**, 513-522 (1966).

18.   J. Lehtonen, et al., *Chemical Engineering Science*, **51**, 2799-2804 (1996).

19.   E. Paatero, et al., *Chemical Engineering Science*, **49**, 3601-3616 (1994).

20.   T.R. Felthouse, et al., in *Kirk-Othmer Encyclopedia of Chemical Technology*, John Wiley & Sons, Inc., 2000.

21.   A. Fradet and E. Maréchal, in *Polymerizations and Polymer Properties*, Springer Berlin / Heidelberg, 1982, Vol. 43, pp 51-142.

22.   A. Fradet and E. Maréchal, *Die Makromolekulare Chemie*, **183**, 319-329 (1982).

23.   V.Z. Ordelt, *Die Makromolekulare Chemie*, **63**, 153-161 (1963).

24.   M. Paci and F. Campana, *European Polymer Journal*, **21**, 717-721 (1985).

25.   G.L. Marshall and S.J. Wilson, *European Polymer Journal*, **24**, 933-937 (1988).

26.   J. Simitzis, L. Zoumpoulakis, and S. Soulis, *Polymer International*, **51**, 308-318 (2002).

27.   S. Podzimek, *Chromatographia*, **33**, 377-384 (1992).

Bibliographic References

28. Vanscó-Szmercsányi, K. Maros-Gréger, and E. Makay-Bödi, *Journal of Polymer Science*, **53**, 241-248 (1961).

29. M. Felici, et al., *Chim. Ind. (Milan)*, **45**, 169-172 (1963).

30. M. Gordon, B.M. Grieverson, and I.D. McMillan, *Journal of Polymer Science*, **18**, 497-514 (1955).

31. M. Paci, et al., *Die Makromolekulare Chemie*, **183**, 377-387 (1982).

32. J. Grobelny and A. Kotas, *Polymer*, **36**, 1363-1374 (1995).

33. T. Matynia, M. Worzakowska, and W. Tarnawski, *Journal of Applied Polymer Science*, **101**, 3143-3150 (2006).

34. L.G. Curtis, et al., *I&EC Product Research and Development*, **3**, 218-221 (1964).

35. P.B. Zetterlund, et al., *Polymer International*, **52**, 749-756 (2003).

36. U. Schulze, et al., *Journal of Applied Polymer Science*, **64**, 527-537 (1997).

37. S. Podzimek and J. Hyršl, *Journal of Applied Polymer Science*, **53**, 1351-1356 (1994).

38. F. Codari, et al., *Macromolecular Materials and Engineering*, **295**, 58-66 (2010).

39. L. Ahjopalo, et al., *Polymer*, **41**, 8283-8290 (2000).

40. W.H. Carothers, *Journal of the American Chemical Society*, **51**, 2548-2559 (1929).

41. J. Brandrup, E.H. Immergut, and E.A. Grulke, *Polymer Handbook*, John Wiley and Sons, Inc, New York, 1999.

42. J.J. Berzelius, *Rapport annuel sur les progres des sciences physiques et chimiques*, Fortin, Masson, 1841.

43. J.J. Berzelius, S. Academie Royale des, and M. Plantamour, *Rapport annuel sur les progres des sciences physiques et chimiques: presente... a L'Academie Royale des Sciences de Stockholm*, Fortin, Masson et cie, 1847.

44. M.M. Berthelot, *Comptes Rendus*, **37**, 398-405 (1853).

45. A.V. Lorenzo, *Annales De Chimie Et De Physique*, **67**, 293 (1863).

46. W.H. Carothers and J.W. Hill, *Journal of the American Chemical Society*, **54**, 1566-1569 (1932).

47. W.H. Carothers, Du Pont, United States, 1938, Vol. 2130947.

48. W.H. Carothers, Du Pont, United States, 1938, Vol. 2130948.

49. J.H. Saunders and F. Dobinson, in *Comprehensive Chemical Kinetics*, R.W. Carr, Ed., Elsevier, 1976, Vol. 15, pp 473-581.

50. A. Rudin, in *Elements of Polymer Science and Engineering (Second Edition)*, Academic Press, San Diego, 1999, pp 155-188.

51. T.E. Long, et al., in *Applied Polymer Science: 21st Century*, Pergamon, Oxford, 2000, pp 979-997.

52. R.C. Hayward and D.J. Pochan, *Macromolecules*, **43**, 3577-3584 (2010).

53. J. Grobelny, *Polymer Reviews*, **39**, 405-444 (1999).

54. J.J. Hernández, et al., *Langmuir*, **26**, 10731-10737 (2010).

Bibliographic References

55.   I. Tanis and K. Karatasos, *Macromolecules*, **42**, 9581-9591 (2009).

56.   W. Brügel and K. Demmler, *Journal of Polymer Science Part C: Polymer Symposia*, **22**, 1117-1137 (1969).

57.   L. Turunen, *I&EC Product Research and Development*, **1**, 40-45 (1962).

58.   G.L. Marshall and S.J. Wilson, *European Polymer Journal*, **24**, 939-945 (1988).

59.   A. Piras, PhD thesis, Universite Pierre et Marie Curie, Paris (VI), France, 1988.

60.   K. Pang, R. Kotek, and A. Tonelli, *Progress in Polymer Science*, **31**, 1009-1037 (2006).

61.   Y.S. Yang and J.P. Pascault, *Journal of Applied Polymer Science*, **64**, 133-145 (1997).

62.   Y.S. Yang and J.P. Pascault, *Journal of Applied Polymer Science*, **64**, 147-156 (1997).

63.   M. JanÄ o, T. Prudskova, and D. Berek, *International Journal of Polymer Analysis and Characterization*, **3**, 319-332 (1997).

64.   H. Pasch, *Advances in Polymer Science*, **128**, 1-45 (1997).

65.   H. Pasch and B. Trathnigg, *HPLC of Polymers*, Springer, Berlin, 1997.

66.   H. Pasch, *Macromolecular Symposia*, **178**, 25-37 (2002).

67.   G. Du, et al., *Journal of Applied Polymer Science*, **110**, 1182–1194 (2008).

68.   H.J.A. Philipsen, et al., *Journal of Chromatography A*, **790**, 101-116 (1997).

69.   G. Glöckner, *Gradient HPLC of copolymers and chromatographic cross-fractionation*, Springer, Berlin Heidelberg New York, 1991.

70.   E.F. Casassa, *Journal of Polymer Science B*, **5**, 773-778 (1967).

71.   E.F. Casassa, *Macromolecules*, **9**, 182-185 (1976).

72.   A.V. Gorshkov, et al., *Journal of Chromatography*, **523**, 91-102 (1990).

73.   A.M. Skvortsov and A. Gorbunov, *Polymer Science U.S.S.R.*, **21**, 371-380 (1979).

74.   H.J.A. Philipsen, et al., *Journal of Chromatography A*, **727**, 13-25 (1996).

75.   S.G. Entelis, V.V. Evreinov, and A. Gorschkov, *Advances in Polymer Science*, **76**, 129-175 (1986).

76.   S. Entelis, et al., in *Pharmacy/Thermomechanics/Elastomers/Telechelics (Advances in Polymer Science)*, Springer Berlin / Heidelberg, 1986, Vol. 76, pp 129-175.

77.   M.B. Tennikov, et al., *Vysokomol Soedin*, **A19**, 657-660 (1977).

78.   B.G. Belenkii, et al., *Dokl Acad Nauk U.S.S.R*, **231**, 1147 (1976).

79.   T. Macko and D. Hunkeler, *Advances in Polymer Science*, **163**, 61-136 (2003).

80.   D. Berek, *Macromolecular Chemistry and Physics*, **209**, 695-706 (2010).

81.   W. Lee, et al., *Macromolecules*, **35**, 529-538 (2002).

82.   W. Lee, S. Park, and T. Chang, *Analytical Chemistry*, **73**, 3884-3889 (2001).

83.   W. Lee, et al., *Macromolecules*, **34**, 2353-2358 (2001).

Bibliographic References

84. D. Berek, *Progress in Polymer Science*, **25**, 873-908 (2000).

85. D. Berek, *Macromolecular Chemistry and Physics*, **209**, 695–706 (2008).

86. T. Macko and D. Hunkeler, *Advances in Polymer Science*, **163**, 61-136 (2006).

87. W. Hiller, et al., *Macromolecules*, **43**, 4853-4863 (2010).

88. H. Pasch, *Polymer*, **34**, 4095-4099 (1993).

89. H. Pasch, C. Brinkmann, and Y. Gallot, *Polymer*, **34**, 4100-4104 (1993).

90. H. Pasch, Y. Gallot, and B. Trathnigg, *Polymer*, **34**, 4986-4989 (1993).

91. E. Heftmann, *Chromatography Part A: Fundamentals and Techniques*, Elsevier, Amsterdam, 1992.

92. J.C. Moore, *Journal of Polymer Science, A-2*, **2**, 285 (1964).

93. T. Provder, *Detection and Data Analysis in Size Exclusion Chromatography*, American Chemical Society, 1987.

94. C.-Y. Kuo and T. Provder, in *Detection and Data Analysis in Size Exclusion Chromatography*, American Chemical Society, 1987, Vol. 352, pp 2-28.

95. H.G. Barth, B.E. Boyes, and C. Jackson, *Analytical Chemistry*, **68**, 445R-466R (1996).

96. S.R. Sandler, et al., in *Polymer Synthesis and Characterization*, Academic Press, San Diego, 1998, pp 140-151.

97. A. Rudin, in *Elements of Polymer Science and Engineering (Second Edition)*, Academic Press, San Diego, 1999, pp 73-120.

98. J. Silberring, et al., in *Journal of Chromatography Library*, Elsevier, 2004, Vol. Volume 69, pp 213-251.

99. M. Cantow, *Polymer Fractionation*, Acedemic Press, New York, 1967.

100. F. Francuskiewicz, *Polymer Fractionation*, Springer, Berlin, 1994.

101. J.C. Moore, *Journal of Polymer Science: Part A*, **2**, 835-843 (1964).

102. C.M. Serban and D. Victor, in *Journal of Chromatography Library*, Elsevier, 2002, Vol. Volume 65, pp 165-211.

103. C.-S. Wu, *Handbook of Size Exclusion Chromatography*, Dekker, M., New York, 1995.

104. U.D. Neue, *HPLC Columns. Theory, Technology and Practice*, Wiley- VCH, New York, 1997.

105. C.-S. Wu, *Column Handbook for Size Exclusion Chromatography*, Academic Press, San Diego, CA, 1999.

106. T.H. Mourey and T.G. Bryan, *Journal of Chromatography A*, **964**, 169-178 (2002).

107. E.F. Casassa and Y. Tamami, *Macromolecules*, **2**, 14-26 (1969).

108. E.F. Casassa, *Separation Science*, **6**, 305-319 (1971).

109. E.F. Casassa, *Journal of Physical Chemistry*, **75**, 3929-3939 (1971).

110. J.C. Giddings, et al., *Journal of Physical Chemistry*, **72**, 4397-4408 (1968).

Bibliographic References

111.   W.W. Yau, C.P. Malone, and S.W. Fleming, *Journal of Polymer Science: Part B*, **6**, 803-807 (1968).

112.   W.W. Yau and C.P. Malone, *Polymer Preprints, American Chemical Society, Division Polymer Chemistry*, **12(2)**, 797-803 (1971).

113.   Y.C. Guillaume, J.F. Robert, and C. Guinchard, *Analytical Chemistry*, **73**, 3059-3064 (2001).

114.   Y. Vander Heyden, S.T. Popovici, and P.J. Schoenmakers, *Journal of Chromatography A* **957**, 127-137 (2002).

115.   R.M. Smith and E. Heftmann, in *Journal of Chromatography Library*, Elsevier, 2004, Vol. Volume 69, pp 95-138.

116.   C.F. Poole, in *The Essence of Chromatography*, Elsevier Science, Amsterdam, 2003, pp 267-429.

117.   H.G. Barth, B.E. Boyes, and C. Jackson, *Analytical Chemistry*, **70**, 251R-278R (1998).

118.   H. Pasch, *Advances in Polymer Science*, **150**, 1-66 (2000).

119.   N.V. Cuong and B. Trathnigg, *Journal of Separation Science*, **33**, 1052-1057 (2010).

120.   G. Glöckner, *Chromatographia*, **37**, 7-12 (1993).

121.   G. Glöckner, D. Wolf, and H. Engelhardt, *Chromatographia*, **39**, 170-174 (1994).

122.   G. Glöckner, D. Wolf, and H. Engelhardt, *Chromatographia*, **38**, 559-565 (1994).

123.   G. Glöckner, D. Wolf, and H. Engelhardt, *Chromatographia*, **39**, 557-563 (1994).

124.   G. Glöckner, D. Wolf, and H. Engelhardt, *Chromatographia*, **38**, 749-755 (1994).

125.   A.J.P. Martin, *Biochemistry Society Symposia* **3**, 4-20 (1949).

126.   M. Wang, J. Mallette, and J.F. Parcher, *Journal of Chromatography A*, **1218**, 2995-3001 (2011).

127.   R.S. Alm, R.J.P. Williams, and A. Tiselius, *Acta Chemica Scandinavica*, **6**, 826-836 (1952).

128.   L.R. Snyder and H.D. Warren, *Journal of Chromatography*, **15**, 344-360 (1964).

129.   P. Jandera and J. Churacek, *Journal of Chromatography*, **91**, 207-221 (1974).

130.   P. Jandera and J. Churacek, *Journal of Chromatography*, **93**, 17-39 (1974).

131.   F.P.B. van der Maeden, M.E.F. Biemond, and P.C.G.M. Janssen, *Journal of Chromatography A*, **149**, 539-552 (1978).

132.   M.A. Bashir and W. Radke, *Journal of Chromatography A*, **1163**, 86-95 (2007).

133.   H.J.A. Philipsen, B. Klumperman, and A.L. German, *Journal of Chromatography A*, **746**, 211-224 (1996).

134.   P. Jandera, *Journal of Chromatography A*, **797**, 11-22 (1998).

135.   H.J.A. Philipsen, et al., *Chromatographia*, **55**, 533-540 (2002).

136.   P. Nikitas, et al., *Analytical Chemistry*, **80**, 5508-5514 (2008).

137.   J. Ståhlberg, *Journal of Chromatography A*, **1217**, 2172-3179 (2010).

138.   Y. Brun and P. Alden, *Journal of Chromatography A*, **966**, 25-40 (2002).

Bibliographic References

139.   T. Kotaka, et al., *Makromolekular Chemie*, **176**, 1273-1288 (1975).

140.   S. Mori, *Macromolecular Symposia*, **110**, 87-95 (1996).

141.   S. Teramachi, *Macromolecular Symposia*, **110**, 217-229 (1996).

142.   S. Mori, *Journal of Chromatography*, **541**, 375-382 (1991).

143.   H. Sato, M. Sasaki, and K. Ogino, *Polymer Journal*, **21**, 965 (1989).

144.   D.W. Armstrong and R.E. Boehm, *Journal of Chromatographic Science*, **22**, 378-385 (1984).

145.   T.H. Mourey, *Journal of Chromatography*, **357**, 101-106 (1986).

146.   T.C. Schunk, *Journal of Chromatography A*, **661**, 215-226 (1994).

147.   H.J.A. Philipsen, et al., *Journal of Chromatography A*, **775**, 157-177 (1997).

148.   T. Chang, *Advances in Polymer Science*, **163**, 1-60 (2003).

149.   W.M.A. Niessen and E. Heftmann, in *Journal of Chromatography Library*, Elsevier, 2004, Vol. Volume 69, pp 403-430.

150.   D. Berek and A. SÌŒEisÌŒkovaÌ, *Macromolecules*, **43**, 9627-9634 (2010).

151.   J.-A. Raust, et al., *Macromolecules*, **43**, 8755-8765 (2010).

152.   F. Erni and R.W. Frei, *Journal of Chromatography A*, **149**, 561-569 (1978).

153.   J. Gerber and W. Radke, *Polymer*, **46**, 9224-9229 (2005).

154.   J. Adrian, et al., *Polymer*, **41**, 2439-2449 (2000).

155.   T. Ikegami, et al., *Journal of Chromatography A*, **1106**, 112-117 (2006).

156.   K. Im, et al., *Journal of Chromatography A*, **1103**, 235-242 (2006).

157.   A. van der Horst and P.J. Schoenmakers, *Journal of Chromatography A*, **1000**, 693-709 (2003).

158.   B. Trathnigg, *Progress in Polymer Science*, **20**, 615-650 (1995).

159.   H. Pasch and P. Kilz, *Macromolecular Rapid Communications*, **24**, 104–108 (2003).

160.   P. Dugoa, et al., *Journal of Chromatography A*, **1189**, 196-206 (2008).

161.   L.W. Pottsa, et al., *Journal of Chromatography A*, **1217**, 5700-5709 (2010).

162.   W.R. LaCourse and C.O. Dasenbrock, *Analytical Chemistry*, **70**, 37R-52R (1998).

163.   L.D. Rothman, *Analytical Chemistry*, **68**, 587-598 (1996).

164.   A.J. Anderson, *Analytical Chemistry*, **71**, 314 (1999).

165.   G. Patonay, *HPLC Detection. Newer Methods*, VCH, New York, 1992.

166.   D. Parriott, *A Practical Guide to HPLC Detection*, Academic, San Diego, 1993.

167.   R.P.W. Scott, *Chromatographic Detectors*, Dekker, New York, 1996.

168.   P.J. Wyatt, D.N. Villalpando, and P. Alden, *Journal of Liquid Chromatography and Related Technology*, **20**, 2169-2180 (1997).

Bibliographic References

169.   S.T. Balke, T.H. Mourey, and T.C. Schunk, *Polymer Reaction Engineering*, **7**, 429-452 (1999).

170.   Y. Brun, *Journal of Liquid Chromatography and Related Technology*, **21**, 1979-2015 (1998).

171.   R. Murgasova, et al., *European Polymer Journal*, **34**, 659-663 (1998).

172.   R.A. Kee and M. Gauthier, *Journal of Polymer Science: Part A: Polymer Chemistry*, **46**, 2335-2346 (2008).

173.   N.M. Tukur, et al., *Macromolecular Symposia*, **263**, 121-129 (2008).

174.   Y. Xu, *Journal of Chromatography A*, **1191**, 40-56 (2008).

175.   M. Netopil´ık, et al., *Polymer International*, **57**, 1152-1158 (2008).

176.   T.H. Mourey, *International Journal of Polymer Analysis and Characterization*, **9**, 97 - 135 (2004).

177.   M. Gaborieau, et al., *Journal of Chromatography A*, **1190**, 215-223 (2008).

178.   J.B. McLeary, et al., *Chemical Communications*, 1950-1951 (2004).

179.   J.B. McLeary and B. Klumperman, *Soft Matter*, **2**, 45-53 (2006).

180.   J.B. McLeary, et al., *Polymer Preprints*, **44**, 781-782 (2003).

181.   B. Trathnigg, *Chromatography of Polymers: Hyphenated and Multidimension Techniques*, American Chemical Society, Washington DC, 1999.

182.   B. Trathnigg, et al., *Polymer Material Science Engineering*, **77**, 48-49 (1997).

183.   B. Trathnigg, et al., *Journal of Chromatography A*, **791**, 21-35 (1997).

184.   W. Hiller, et al., *Analytical Chemistry*, **82**, 8244-8250 (2010).

185.   W. Hiller, et al., *Macromolecules*, **43**, 4853-4863 (2010).

186.   W. Hiller, P. Sinha, and H. Pasch, *Macromolecular Chemistry and Physics*, **210**, 605-613 (2009).

187.   T. Kitayama, et al., *Analytical Chemistry*, **72**, 1518-1522 (2000).

188.   G. Schlotterbeck, H. Pasch, and K. Albert, *Polymer Bulletin*, **38**, 673-679 (1997).

189.   S.H. Smallcombe, S.L. Patt, and P.A. Keifer, *Journal of Magnetic Resonance Serie A*, **117**, 295-303 (1995).

190.   A.S. Kulkami and G. Beaucage, *Journal of Polymer Science Polymer Physics*, **44**, 1395-1405 (2006).

191.   N. Fandrich, et al., *Macromolecular Chemistry and Physics*, **211**, 1678-1688 (2010).

192.   C.A. Jackson and W.J. Simonsick, *Current Opinion in Solid State and Materials Science*, **2**, 661-667 (1997).

193.   M.W.F. Nielen, *Mass Spectrometry Reviews*, **18**, 309-344 (1999).

194.   H. Pasch, *Physical Chemistry Chemical Physics*, **1**, 3879-3890 (1999).

195.   G. Montaudo, F. Samperi, and M.S. Montaudo, *Progress in Polymer Science*, **31**, 277-357 (2006).

196.   L. Chikh, M. Tessier, and A. Fradet, *Macromolecules* **41**, 9044-9050 (2008).

Bibliographic References

197. T. Gruendling, et al., *Polymer Chemistry*, **1**, 599-617 (2010).

198. J.L. Koenig, in *Spectroscopy of Polymers (Second Edition)*, Elsevier Science, New York, 1999, pp 441-480.

199. Á. Somogyi, et al., in *Medical Applications of Mass Spectrometry*, Elsevier, Amsterdam, 2008, pp 93-140.

200. H. Pasch and F. Gores, *Polymer*, **36**, 1999-2005 (1995).

201. S.D. Hanton, *Chemical Reviews*, **101**, 527-569 (2001).

202. P.M. Peacock and C.N. McEwen, *Analytical Chemistry*, **76**, 3417-3428 (2004).

203. S.M. Weidner and S. Trimpin, *Analytical Chemistry*, **80**, 4349-4361 (2008).

204. S.M. Weidner and S. Trimpin, *Analytical Chemistry*, **82**, 4811-4829 (2010).

205. L. Prokai, *International Journal of Polymer Analysis and Characterization*, **6**, 379-391 (2001).

206. S.M.A.B. Batoy, et al., *Applied Spectroscopic Review*, **43**, 485-550 (2008).

207. K. Tanaka, et al., *Rapid Communications in Mass Spectrometry*, **2**, 151-153 (1988).

208. M. Karas and F. Hillenkamp, *Analytical Chemistry*, **60**, 2299-2301 (1988).

209. K. Mauritz, Mauritz Research Group, http://www.psrc.usm.edu/mauritz/maldi.html, 2004.

210. H. Pasch and W. Schrepp, *MALDI-TOF Mass Spectrometry of synthetic polymers*, Springer, Berlin, 2003.

211. A. Lee, et al., *Bulletin of Korean Chemical Society*, **30**, 1127-1130 (2009).

212. D.C. Schriemer and L. Li, *Analytical Chemistry*, **68**, 2721-2725 (1996).

213. X. Lou and J.L.J. van Dongen, *Journal of Mass Spectrometry*, **35**, 1308-1312 (2000).

214. X. Lou, et al., *Journal of Chromatography A*, **976**, 145-154 (2002).

215. R.D. Deegan, et al., *Nature*, **389**, 827-829 (1997).

216. A. Hortal, et al., *Applied Physics A: Material Science Process*, **92**, 859-863 (2008).

217. M. Mazarin, T.N.T. Phan, and L. Charles, *Rapid Communications in Mass Spectrometry*, **22**, 3776-3782 (2008).

218. S.D. Hanton and J.R. Stets, *Journal of American Society Mass Spectrometry*, **20**, 1115-1118 (2009).

219. S.T. Ellison, et al., *Macromolecules*, **42**, 5526-5533 (2009).

220. W.J. Erb and K.G. Owens, *Rapid Communications in Mass Spectrometry*, **22**, 1168-1174 (2008).

221. S.M. Weidner and J. Falkenhagen, *Rapid Communications in Mass Spectrometry*, **23**, 653-660 (2009).

222. W.C. Wiley and I.H. McLaren, *Review Scientific Instruments*, **26**, 1150-1157 (1955).

223. A.J. Kearsley, http://www.ima.umn.edu/2007-2008/MM8.6-15.08/abstracts.html, 2008.

224. U. Bahr, et al., *Analytical Chemistry*, **64**, 2866-2869 (1992).

Bibliographic References

225.   M. Dole, et al., *Journal of Physical Chemistry*, **49**, 2240-2249 (1968).

226.   S.F. Wong, C.K. Meng, and J.B. Fenn, *Journal of Physical Chemistry*, **92**, 546-550 (1988).

227.   T. Nohmi and J.B. Fenn, *Journal of American Chemical Society*, **114**, 3241-3246 (1992).

228.   Y. Lin, et al., http://www.springerimages.com/Images/MedicineAndPublicHealth/1-10.1007_s10620-008-0656-5-2, 2009.

229.   S.M. Hunt, et al., *Analytical Chemistry*, **70**, 1812-1822 (1998).

230.   M.W.F. Nielen, *Rapid Communications in Mass Spectrometry*, **13**, 826-827 (1999).

231.   G. Hart-Smith and C. Barner-Kowollik, *Macromolecular Chemistry and Physics*, **211**, 1507-1529 (2010).

232.   S. Koster, et al., *Macromolecules*, **35**, 4919-4928 (2002).

233.   S.M. Hunt, M.M. Sheil, and P.J. Derrick, *European Mass Spectrometry*, **4**, 475-486 (1998).

234.   S.M. Hunt, et al., *Analytical Chemistry*, **70**, 1812-1822 (1998).

235.   Q. Zhan, A. Guesev, and D.M. Hercules, *Rapid Communications in Mass Spectrometry*, **13**, 2278 (1999).

236.   E. Esser, et al., *Polymer*, **41**, 4039-4046 (2000).

237.   M.W.F. Nielen and F.A. Buijtenhuijs, *Analytical Chemistry*, **71**, 1808 (1999).

238.   C. Keil, E. Esser, and H. Pasch, *Macromolecular Materials and Engineering*, **286**, 161-167 (2001).

239.   D.J. Aaserud, L. Prokai, and W.J. Simonsick Jr., *Analytical Chemistry*, **71**, 4793-4799 (1999).

240.   H.J.A. Philipsen, B. Klumperman, and A.L. German, *Journal of Chromatography A*, **746**, 211-224 (1996).

241.   H.J.A. Philipsen, et al., *Journal of Chromatography A*, **761**, 147-162 (1997).

242.   M. Al Samman, et al., *Macromolecules*, **43**, 3215-3220 (2010).

243.   H.J.A. Philipsen, et al., *Chromatographia*, **52**, 325-333 (2000).

244.   H.J.A. Philipsen, et al., *Chromatographia* **48**, 623-630 (1998).

245.   P. Jandera, *Journal of Chromatography*, **314**, 13-36 (1984).

246.   P. Jandera and J. Rozkosna, *Journal of Chromatography*, **362**, 325-343 (1986).

247.   P. Jandera, *Journal of Chromatography*, **449**, 361-389 (1988).

248.   F.A.M. Leermakers, H.J.A. Philipsen, and B. Klumperman, *Journal of Chromatography A*, **959**, 37-47 (2002).

249.   K. Rissler, *Journal of Chromatography A*, **786** 85-98 (1997).

250.   P. Jandera, *Chromatographia*, **26**, 417-422 (1988).

251.   Waksmundzka-Hajnos Monika, Petruczynik Anna, and H. Anna, *Journal of Chromatography A*, **919** 39-50 (2001).

252.   K. Rissler, *Journal of Chromatography A*, **871**, 243-258 (2000).

Bibliographic References

253. E. Beaudoin, et al., *European Polymer Journal*, **44**, 514-522 (2008).

254. G. Montaudo, et al., *Journal of Polymer Science Part A: Polymer Chemistry*, **34**, 439-447 (1996).

255. H. Pasch, et al., *Die Angewandte Makromolekulare Chemie*, **241**, 95-111 (1996).

256. T. Gruendling, et al., *Macromolecular Chemistry and Physics*, **211**, 520-528 (2010).

257. G. Hart-Smith, et al., *Polymer*, **50**, 1986-2000 (2009).

258. J.B. Williams, A.I. Gusev, and D.M. Hercules, *Macromolecules*, **30**, 3781-3787 (1997).

259. J. Guittard, et al., *Journal of Mass Spectrometry*, **31**, 1409-1421 (1996).

260. R.M. Whittal, et al., *Macromolecular Rapid Communications*, **17**, 59-64 (1996).

261. A.J. Hoteling, et al., *Analytical Chemistry*, **76**, 5157-5164 (2004).

262. M.A.R. Meier, N. Adams, and U.S. Schubert, *Analytical Chemistry*, **79**, 863-869 (2007).

263. C. Puglisi, et al., *Macromolecules*, **35**, 3000-3007 (2002).

264. S. Lorenz, E.P. Maziarz, and T. Wood, *Appl. Spectrosc.*, **53**, 18A-36A (1999).

265. A.C. Crecelius, A. Baumgaertela, and U.S. Schubert, *Journal of Mass Spectrometry*, **44**, 1277-1286 (2009).

Acknowledgements

I would like to thank my supervisor, Prof Harald Pasch for his time and efforts throughout the duration of my PhD research. His contribution is greatly appreciated and will never be forgotten. I greatly appreciate all the support, collaboration opportunities and tons of motivation to help me achieve my biggest goal thus far.

To my co-supervisor, Dr James McLeary, thank you for taking a chance on a third year student all those years ago. I could write books regarding your part in my post grad journey. All the lessons are much appreciated.

A big gratitude towards Jaylin Simpson for synthesizing all the polyester samples of the respective batches. Without your hard work, dedication and delivering the samples on schedule, the characterization of all the samples would not have been possible.

The following individuals are acknowledged for analytical contributions to the work presented here:

Dr Marietjie Stander at Central Analytical Facility (CAF) at Stellenbosch University for all the ESI-QTOF MS analysis.

Dr Wolfgang Radke, Dr Robert Brüll and the whole team in Darmstadt (formerly known as Deutsches Kunststoff Institute DKI), especially the Analytik group for the opportunity to collaborate with their institute and students.

A special thank you has to go to Karsten Rhode for his assistance with the MALDI-TOF MS analysis. Your input was invaluable and much appreciated.

To Christoph Brinkmann, for all the guidance and help with my LC analysis by teaching me all the inner workings of instruments and detectors. These are skills I take with me forever.

I am grateful to the staff at Polymer Science, for making life a little easier in Polymer Science building in terms of administration and technical assistance.

Thanks all the members of the Polymer Analytics group in the Polymer Science Division, Department of Chemistry and Polymer Science.

On a personal note:

All my friends in Germany, especially Jacques Raust, Michael Al Samman, Melanie Stein and Tino Otte. Thank you very much for making Darmstadt my home away from home. I cannot say how much all you did mean to me, the work stuffs, the party stuffs, the admin stuffs. I will never forget it and I hope we'll see each other soon!

Acknowledgments

A million thanks to my "inner onion layer": Morné Swart, Pritish Sinha, Liesl Keulder, William Cloete and Corinna Bazelet. You guys always knew just what to say and do to bring laughter and sunshine on the cloudy days. It wouldn't have been as much fun without all the tastings, festivals and brazen time. Yay!!

My two polybesties Gareth Bayley and Jacques Rinquest. How many years has it been?! From Honours until beyond…Unfortunately we don't get to see each other and all that comes with it that often anymore but how epic are we still? LOL!!

My very big extended family: all the Makans, Cornelissens and Pretorius', you are way too many to mention but thank you from the bottom of my heart for every message, every call, understanding when I had to disappear or couldn't join in.

To my guy Ashwell Makan, for being there through all my ups and downs. For holding my hand when I needed and just knowing without me saying when the going got tough. Thanks for all the brainstorming, cups of tea, cooked meals, venting and total silence when I had to work crazy hours of the day, week and months. This would have been an empty victory without you.

Most importantly to my mother Marechia and brother Vincent Pretorius, I have no words to describe the gratitude I feel. I decided to take on this journey a long time ago, when we were still four. Over time, life threw its punches by taking Dad away from us but because our foundation was solid, we stood together strong. The love and support I felt all these years made this moment possible. This would not be if it wasn't for you... I hope I made all of your proud.

"I don't know how I got here,

I knew it wouldn't be easy

But your faith in me was so clear

It didn't matter how many times I got knocked on the floor

But you knew one day I would be standing tall,

Just look at me now

Everything starts from something, but something would be nothing

If your heart didn't dream with me,

Where would I be?

If you didn't believe" Believe- JB